

ABSTRACT

Title of dissertation: LOCAL MOLECULAR FIELD THEORY
FOR NONEQUILIBRIUM SYSTEMS

Edward B. Baker III, Doctor of Philosophy, 2019

Dissertation directed by: Professor John D. Weeks
Department of Chemistry and Biochemistry
Institute for Physical Science and Technology

Local Molecular Field (LMF) theory is a framework for modeling the long range forces of a statistical system using a mimic system with a modified Hamiltonian that includes a self consistent molecular potential. This theory was formulated in the equilibrium context, being an extension of the Weeks Chandler Andersen (WCA) theory to inhomogeneous systems. This thesis extends the framework further into the nonequilibrium regime. It is first shown that the equilibrium derivation can be generalized readily by using a nonequilibrium ensemble average and its relevant equations of motion. Specifically, the equations of interest are fluid dynamics equations which can be generated as moments of the BBGKY hierarchy. Although this approach works well, for the application to simulations it is desirable to approximate the LMF potential dynamically during a single simulation, instead of a nonequilibrium ensemble. This goal was pursued with a variety of techniques, the most promising of which is a nonequilibrium force balance approach to dynamically approximate the relevant ensemble averages. This method views a quantity

such as the particle density as a field, and uses the statistical equations of motion to propagate the field, with the forces in the equations computed from simulation. These results should help LMF theory become more useful in practice, in addition to furthering the theoretical understanding of near equilibrium molecular fluids.

LOCAL MOLECULAR FIELD THEORY
FOR NON-EQUILIBRIUM SYSTEMS

by

Edward B. Baker III

Dissertation submitted to the Faculty of the Graduate School of the
University of Maryland, College Park in partial fulfillment
of the requirements for the degree of
Doctor of Philosophy
2019

Advisory Committee:

Professor John Weeks, Chair/Advisor

Professor Christopher Jarzynski

Professor Jeffery Klauda

Professor Pratyush Tiwary

Professor Silvina Matysiak, Dean's Representative

© Copyright by
Edward B. Baker III
2019

Acknowledgements

I want to begin by thanking my advisor, Professor John Weeks, for his guidance and support. He has a deep intuition for the behavior of statistical systems, and has the ability to get to the heart of a physical problem through a process of seeing the physics behind the mathematics. His approach has helped me try to see the forest through the trees of technical detail in a theory.

I would also like to thank Professors Chris Jarzynski, Pratyush Tiwary, Jefferey Klauda and Silvina Matysiak for serving on my committee. I very much appreciate their effort and time. I owe a special debt of gratitude to Professors Michael Coplan, Chris Jarzynski, Pratyush Tiwary and J. Robert Dorfman. Michael and Chris were very supportive during a difficult time in my graduate studies, and Chris has been an inspiring influence for my research. Pratyush Tiwary and J. Robert Dorfman have both been helpful in furthering my research and suggesting new avenues I could pursue to make my results more relevant and interesting.

I would also like to thank the current and past members of the Weeks group. In particular, Rick Remsing and Jocelyn Rodgers have suggested many interesting avenues to pursue, in addition to helping with the nuts and bolts of the projects contained in this thesis. I also enjoyed working with Ang Gao, who has a different approach to LMF theory that has led to deeper understanding of the theory, and shows great promise for applications.

Finally, I would like to thank my friends and family for their support during my nonlinear journey through graduate studies. I want to thank my mom, whose

constant support has been a guiding influence in my life. I want to thank my wife Melissa Wilf for her support, my best friend Vlad Tenev, my sister Alexis Baker and dad Edward Baker Jr., and my daughter Amalie Wilf Baker. I'd also like to thank former student Mick Warehime, and Eleonora Mavroeidi for helping me through the earlier parts of the program.

Table of Contents

Acknowledgements	ii
Table of Contents	iv
List of Figures	vi
List of Abbreviations	vii
1 Introduction	1
2 Background	8
2.1 Review of LMF and WCA Theory	9
2.2 LMF theory for electrostatics	16
2.3 BBGKY and YBG hierarchies	20
2.4 Fluid dynamics equations	24
3 Ensemble Averaged LMF Theory	28
3.1 Introduction	28
3.2 The non-equilibrium formalism	30
3.3 Implementation with slab geometry	38
3.4 Time dependent potentials	43
3.4.1 Nonequilibrium Relaxation to Changes in Electric Fields . . .	43
3.4.2 Sinusoidal field	45
3.5 Conclusions and Outlook	47
4 Non-equilibrium densities from force balance equations for single particle and constrained molecular systems	49
4.1 Introduction	49
4.2 Review of force sampling method	50
4.3 Generalization to non-equilibrium systems	52
4.4 Force sampling for constrained systems	54
4.5 Non-equilibrium constrained systems	61
5 Stochastic sampling for nonequilibrium LMF theory	68
5.1 Introduction	68
5.2 Stochastic local molecular field theory	69
5.3 Dielectric response	76

5.4	Slab geometry	82
5.5	Conclusion	85
6	Approximate thermofield dynamics of interacting fermions	86
6.1	Introduction	86
6.2	Thermal coherent states	89
6.3	Interacting dynamics	94
6.4	Optimized basis set	98
6.5	Thermal coherent state evolution	102
6.6	Simplified basis	106
6.7	Approximate dynamics	109
6.8	Homogeneous electron gas	112
6.9	Conclusion	114
A	Detailed simulation methods	115
B	Alternative approaches to non-equilibrium LMF theory	116
B.1	Introduction	116
B.2	Non equilibrium LMF with Hamiltonian LMF dynamics	117
B.3	Generalized linear response approach to non-equilibrium LMF theory	126
C	Thermofield dynamics background and calculations	132
C.1	Canonical transformations	132
C.2	Incremental optimization	133
C.3	Relations between unitary transformations	134
	Bibliography	138

List of Figures

2.1	Illustration of the concepts underlying WCA theory	10
2.2	Illustration of the concepts underlying LMF theory	12
3.1	Ensemble averaging for LMF theory	32
3.2	Slab geometry with hydrophobic walls	40
3.3	Slab geometry under external field	42
3.4	Abrupt change to electric field in slab geometry	43
3.5	Sinusoidal field in slab geometry	46
4.1	Density averaging versus force sampling for LJ fluid	52
4.2	Force sampling for constrained system	55
4.3	Force sampling for flexible water model	56
4.4	Force sampling for SPC/E water in the slab geometry	58
4.5	Force sampling for LJ nm potential	60
5.1	Summary of SLMF method	71
5.2	One dimensional system illustration	74
5.3	Autocorrelation functions for linear response analysis	77
5.4	Autocorrelation functions analyzing parameters of SLMF theory	80
5.5	SLMF results for slab geometry simulation	82
5.6	SLMF for sinusoidally oscillating field	83

List of Abbreviations

BBGKY	Bogoliubov–Born–Green–Kirkwood–Yvon
GT	Gaussian-truncated
LAMMPS	Large-scale Atomic/Molecular Massively Parallel Simulator
LMF	Local Molecular Field Theory
LJ	Lennard-Jones
MD	Molecular Dynamics
NVT	Canonical; constant number of particles, volume and temperature
PPPM	Particle-particle-particle mesh Ewald
SC	Strong coupling
SLMF	Stochastic LMF
SOR	Successive over-relaxation
SPC/E	Extended simple point charge
VDW	van der Waals
WCA	Weeks-Chandler-Andersen
YBG	Yvon-Born-Green

Chapter 1: Introduction

Molecular dynamics simulations are an essential part of modern statistical mechanics research, providing the ability to computationally probe important physical systems, in addition to investigating toy models to further improve and test theoretical techniques. In order to successfully use these simulations, it is important to develop theoretical tools to fully understand computational results, leading the way for new understanding of the underlying systems of study. One challenging aspect of molecular dynamics simulations has been modeling the long range components of the forces involved, particularly for the Coulomb force, which is slowly decaying. This problem is challenging both computationally and theoretically [1, 2, 3]. From the standpoint of computation, Ewald summation and its variants have become standard methods to compute these long range forces. The more efficient algorithms that have been developed rely on Fourier transformations of the long range potential, and therefore can be computationally expensive, and do not scale well with larger simulation boxes [4, 5, 6]. From a theoretical point of view, larger wavelength components can show a more coarse grained picture of what is happening in a simulation, and therefore a more advanced understanding of these components can lead to greater insight into the underlying physics of the simulation [7, 8]. Also, finite

size effects can lead to artifacts in the resulting dynamics [9]. For these reasons and more, it is interesting to investigate the long range interactions in a simulation.

Local Molecular Field (LMF) theory is a framework that has been developed to formalize this separation of the complicated, microscopic degrees of freedom in a simulation from the slowly varying, long range components [10, 11, 12, 13]. To deal with the long range part, LMF theory uses a rigorous statistical mechanics approach to the problem, and therefore yields an abstracted level of description that avoids some of the complications inherent in all atom simulations. Furthermore, in some cases LMF theory can provide computational savings in these simulations, by avoiding the use of Ewald summations and related algorithms, which can be bottlenecks in simulation. This could allow for pushing the boundaries of the time scales and length scales that simulations are able to probe.

Many of the results that have been found for LMF theory were derived in the equilibrium context. A classic example is that of a solute fixed at the origin in the presence of a molecular solvent, such as water. In this example, one introduces an LMF mimic system with a renormalized LMF potential. The mimic system has truncated short pair interactions, and the renormalized potential is chosen to reproduce the molecular structure of the full system by incorporating the average long range components of the forces in a self consistent fashion. In this example, the renormalized potential must be constant in time, and therefore this theory is fundamentally formulated in the context of equilibrium statistical mechanics. The theory has been shown to work extremely well in this context, and many other interesting systems have been studied in the context of LMF theory.

Despite the successes of this theory, there are many systems for which one might be interested in questions regarding dynamics. Furthermore, even in equilibrium systems, if there is a large bio-molecular solute that is not fixed, then the LMF potential would have to be computed self consistently for each configuration of the solute. This is computationally difficult, and also does not seem to be the best approach for dealing with this situation. Furthermore, for applications of the theory, it would be optimal to have techniques that could approximate the LMF potential dynamically as a simulation progress, so that people could use this as a “black box” algorithm. It is the goal of this thesis to investigate the extension of the formalism of LMF theory to non-equilibrium systems, and to develop some possible paths toward the dynamic approximation of the LMF potential in a black box algorithm.

It turns out that the extension of the underlying formalism of LMF theory to non-equilibrium contexts can be carried out effectively using a similar argument as in the original derivation. In order to achieve this, it is necessary to use the more general equations of non-equilibrium statistical mechanics, to change the interpretation of the ensembles under consideration, and to adjust the arguments underpinning the proof. This can be carried out relatively quickly, and works very well, just like in the equilibrium context. A more difficult goal is to obtain an effective method of dynamically approximating the LMF potential for a single simulation as it progresses, which would arguably be the best way to implement LMF theory in practice. In the pursuit of this goal, a number of different techniques have been attempted, with varying levels of success.

In attempting to approximate the LMF potential dynamically, one of the most difficult issues one faces is to generate an adequate statistical sampling of the particle densities, while simultaneously updating the potential quickly enough to reflect the current state of the system. The general approach taken in this thesis is to achieve these dynamical updates through evolution equations of the LMF potential, so that each timestep only changes the potential slightly. This allows the potential to reach self-consistency dynamically, as opposed to the iterative procedures [13] and linear response methods [14] that have been used previously. Intuitively, one can understand this as being a very large number of very small iterations, and so the two approaches are related. This approach can lead to more stable relaxation of the potential, and therefore is arguably superior to the iterative procedures used before.

There are some drawbacks to this approach to the problem, however. With any of these methods, there is an inherent time scale of averaging that must appear in the evolution equations, in one form or another. This means that the method must be used for systems where the time scales under study are much longer than the effective time scales of averaging, and therefore can not be used as a generic approximation for all systems. This also leads generally to a lag in the dynamics of the mimic system relative to the full system, which is on the order of the time scale of averaging. As this time scale gets shorter, the approximation of the LMF potential generally degrades due to poor statistics.

Furthermore, it would be desirable for the evolution equation of the LMF potential to be obtained from some physically motivated approximation, because

this would reflect the underlying physics and ideally lead to more accuracy. A few different approaches were taken along these lines, with varying degrees of success. In some cases, it is also useful to include ad hoc terms in the equations, to help with convergence. The ad hoc terms can also be physically motivated, such as the viscous term in the Navier Stokes equation, to be discussed in [chapter 4](#). In this way, many variants of non-equilibrium LMF theory can arise, and lead to different results and conclusions.

We begin in [chapter 2](#) with a review of equilibrium LMF theory, and its motivation coming from the force cancellation arguments of Widom and the theory of Weeks Chandler and Andersen. We then review further background material, including a detailed derivation of the YBG and BBGKY hierarchies, and their use in the derivation of fluid dynamics equations, to be developed more in [chapter 3](#). We then review some formalism used to describe constrained systems, which is relevant for the material in [chapter 4](#).

In [chapter 3](#), we introduce the ensemble averaged approach to non-equilibrium LMF theory. In this approach, one defines a non-equilibrium ensemble as a phase space distribution function which evolves according to the Liouville equation. We then use these equations to arrive at the Cauchy momentum equation, and make a near equilibrium approximation to bring this to a form that is similar to the YBG hierarchy. It is then possible to use the techniques from equilibrium LMF theory to derive a non-equilibrium LMF equation, and show that the resulting mimic system will evolve similarly to the full system, even though the arguments are not exactly the same as in equilibrium. We then show that this theory works well for a collection

of non-trivial toy models.

In [chapter 4](#) we present the most promising practical implementation of non-equilibrium LMF theory. This method is inspired by a series of papers written on an alternate method of approximating observables in simulation, such as the single particle density, which will be called the force balance approach. This approach uses the YBG hierarchy equation to probe the density of the system indirectly, by instead sampling the force density. This leads naturally to a way of approximating the LMF potential using the force balance method. The theory behind this approach is developed out of equilibrium and for constrained systems, and then some preliminary simulations are presented.

In [chapter 5](#) yet another approach to non-equilibrium LMF theory is introduced, this time more computationally inspired. This approach could be used by itself, or in conjunction with the methods of [chapter 4](#), because it deals with a separate set of difficulties. The main idea is to sample the smooth charge density stochastically, and then use this stochastic sampling to source an iterative Poisson solver. Because sampling the charge density and interpolating to a grid is one of the more computationally expensive steps in the Ewald algorithm, this alternative could provide significant computational savings in cases where a separation of time scales allows for statistically meaningful averaging of the field. This idea of separation of time scales is investigated using the theory of dielectric response, and some preliminary results are presented.

In [chapter 6](#), a line of research not directly related to LMF theory is presented, but having to do with molecular simulations. Here an alternative approach to finite

temperature quantum simulations is presented, which is called approximate thermofield dynamics. With the simplest approximation of a thermal coherent state, this method reduces to the Hartree-Fock-Bogoliubov method for temperature dependent evolution of a system. As an example this method is applied to the homogeneous electron gas.

In the appendices, some alternate approaches to non-equilibrium LMF theory are also presented, which did not yield interesting enough results to be pursued seriously by the author.

Chapter 2: Background

In this chapter we provide a review of topics that are relevant for the research contained in this thesis. We begin with a review of the theory of Weeks Chandler and Andersen (WCA) and the force cancellation argument which underlies the development of LMF theory. We will then proceed to the formalism of LMF theory, deriving the LMF equation and arguing that the mimic system introduced will approximate the full system very well for a general class of systems. We will then proceed to review the derivation of the BBGKY hierarchy, and the YBG hierarchy, on which LMF theory depends. These hierarchies play an important role in the developments of this thesis, and therefore we will present a pedagogical derivation.

After this introductory material, the focus will be on techniques that are useful for the development of non-equilibrium LMF theory and related applications. First we will show how the moments of the BBGKY hierarchy equations lead directly to the Navier-Stokes and energy conservation equations in a liquid. This formalism is important for the ensemble averaged approach to non-equilibrium LMF theory.

2.1 Review of LMF and WCA Theory

Local Molecular Field theory is a framework for understanding the long range interactions in a statistical system, while abstracting out the complicated short range dynamics of the interacting particles. The key insight underlying the development of LMF theory was originally made by Widom [15], and regards the concept of force cancellation for a bulk fluid. This idea was further developed by Weeks, Chandler and Andersen to create the WCA theory for Lennard-Jones fluids [16, 17].

Force cancellation is a property satisfied for many uniform, dense fluids. The first and most well known example is that of a uniform fluid of particles interacting under the Lennard-Jones pair potential

$$u_{LJ}(r) = 4\varepsilon_{LJ} \left[\left(\frac{\sigma_{LJ}}{r} \right)^{12} - \left(\frac{\sigma_{LJ}}{r} \right)^6 \right]. \quad (2.1)$$

In this example, the force is strongly repulsive at short range, but is weakly attractive as the distance increases. For the weak attractive forces, the force cancellation argument states that although these forces are not negligible for any individual interaction, the vector sum of the forces from all of the different particles vanishes on average, and also makes only a small contribution to the structural properties of the fluid. In particular, if one considers the radial distribution function $g(r)$ for this fluid, the structure should be almost identical if one ignores the long range attractions.

This intuition was formalized in WCA theory, where the Lennard-Jones po-

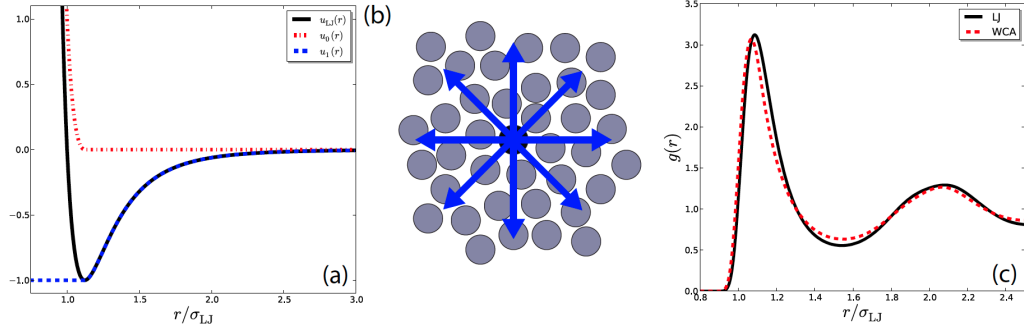


Figure 2.1: (a) The WCA potential defined by equation (2.2), showing the natural splitting between the short range and long range parts. (b) Illustration of the concept of force cancellation, coming from overall cancellation in the vector sum of forces involved. (c) $g(r)$ for a Lennard-Jones fluid and its short range reference system for $T^* = .65$ and $\rho^* = .85$. (figure credit to Richard Remsing in his thesis [18])

tential is split into two distinct parts

$$u_0(r) = \begin{cases} u_{LJ}(R) + \varepsilon_{LJ} & r < r_0 \\ 0 & r > r_0 \end{cases} \quad (2.2)$$

$$u_1(r) = \begin{cases} -\varepsilon_{LJ} & r < r_0 \\ u_{LJ}(r) & r > r_0, \end{cases} \quad (2.3)$$

where r_0 is the position of the minimum of the LJ potential, and $u_0(r)$ is known as the WCA potential. This splitting is illustrated in figure 2.1a. The force cancellation argument suggests that the long range forces from the u_1 potential will cancel on average, and therefore will not contribute significantly to the pair correlation function $g(r)$. This is rigorously true on average for a uniform fluid, but it turns out to be a very good approximation for individual equilibrated configurations, and therefore the structure of the fluid does remain almost the same if one completely

neglects the long range component. The dominant contribution from these long range forces is a uniform background energy, which can be approximated with a mean field theory. This approximation led to a number of developments, including the use of a perturbation theory for uniform fluids, in addition to the ability to use the truncated reference system to infer thermodynamic properties of the full system. These developments are collectively known as WCA theory.

Local Molecular Field theory is a formalism for extending the intuition of the force cancellation arguments of WCA theory to inhomogeneous systems, where the force cancellation argument generally fails. To see why the argument fails, consider introducing a large spherical solute into a Lennard-Jones fluid, as depicted in figure 2.2a. The force cancellation argument relied on the uniformity of the fluid to argue that the vector sum of the long range forces on a fixed particle must vanish. However, due to the solute, there is an excluded volume in the system, and therefore the contribution from that region will create unbalanced forces. For this reason, in an inhomogeneous system, it is necessary to include corrections to the WCA approximation. LMF theory is the best way to include such corrections.

The idea behind LMF theory is to introduce a *mimic system*, in which the pair interactions are truncated, but a complementary field is introduced to approximately account for the neglected long range interactions. This is schematically illustrated

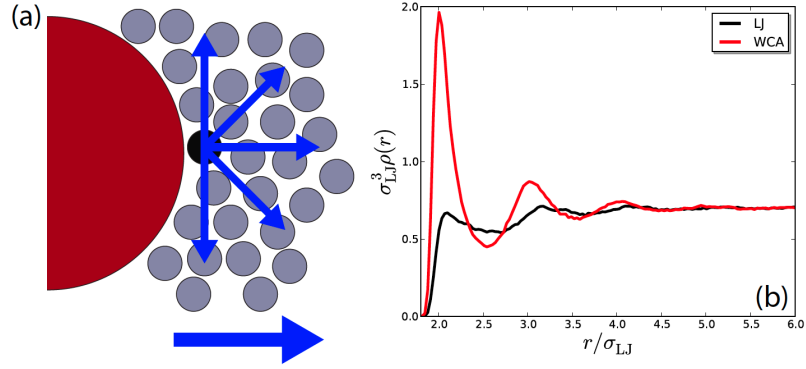


Figure 2.2: (a) Illustration of the failure of the force cancellation argument for an inhomogeneous Lennard-Jones liquid. (b) Particle density for the fluid and its reference system at $T^* = .85$ and $\rho^* = .70$. (figure credit to Richard Remsing in his thesis [18])

as follows

$$\begin{array}{ccc}
 \text{Full} & & \text{Mimic} \\
 \left\{ \begin{array}{c} w(r) \\ \phi(\mathbf{r}) \end{array} \right\} & \rightarrow & \left\{ \begin{array}{c} u_0(r) \\ \phi_R(\mathbf{r}) \end{array} \right\}.
 \end{array} \tag{2.4}$$

Here $w(r)$ is the pair potential in the full system, and $u_0(r)$ is the truncated pair potential. To account for the unbalanced forces that are neglected in the mimic system, the renormalized potential $\phi_R(\mathbf{r})$ is chosen to reproduce the structural properties of the full system. This idea will be developed more rigorously, leading to the LMF equation for the renormalized potential.

The derivation of LMF theory begins with the assumption that there exists a renormalized potential $\phi_R(\mathbf{r})$ that will reproduce the structure of the full system, so

that the single particle distribution function is the same for both systems, or

$$\rho^{(1)}(\mathbf{r}; [\phi]) = \rho_R^{(1)}(\mathbf{r}; [\phi_R]). \quad (2.5)$$

This is a very reasonable assumption, because the potential $\phi_R(\mathbf{r})$ is arbitrary, and is chosen precisely to make this condition true. This is particularly true given that the short range interactions play such a dominant role in the system, and therefore the renormalized potential should only add a slowly varying component to the interaction. For a more rigorous derivation showing that this hypothesis is indeed accurate, one could consider a density functional theory approach, where it can be shown that any single particle density can be reproduced by a given external field [19].

Given the previous assumption, it is now the goal of LMF theory to obtain an equation for the renormalized field $\phi_R(\mathbf{r})$. In order to do this, one introduces the YBG hierarchy equation

$$\beta^{-1} \nabla \ln \rho(\mathbf{r}; t) = -\nabla \phi(\mathbf{r}; t) - \int d\mathbf{r}' \rho(\mathbf{r}'|\mathbf{r}) \nabla w(|\mathbf{r} - \mathbf{r}'|). \quad (2.6)$$

Here $\rho(\mathbf{r}'|\mathbf{r})$ is the conditional singlet density, or the probability to find a particle at \mathbf{r}' given that there is a particle located at \mathbf{r} . Two different derivations of the YBG hierarchy will be given in the next section, and the equation is valid for any Hamiltonian system at equilibrium. In particular, the equation is valid for both the full and mimic systems, and therefore one can subtract this equation for the two

systems to find a formally exact relation between $\phi_R(\mathbf{r})$ and $\phi(\mathbf{r})$:

$$-\nabla\phi_R(\mathbf{r}) = -\nabla\phi(\mathbf{r}) - \int d\mathbf{r}' \rho_R(\mathbf{r}'; [\phi_R]) \nabla u_1(|\mathbf{r} - \mathbf{r}'|) \quad (2.7a)$$

$$- \int d\mathbf{r}' \left(\rho(\mathbf{r}'|\mathbf{r}; [\phi]) - \rho_R(\mathbf{r}'|\mathbf{r}; [\phi_R]) \right) \nabla u_0(|\mathbf{r} - \mathbf{r}'|) \quad (2.7b)$$

$$- \int d\mathbf{r}' \left(\rho(\mathbf{r}'|\mathbf{r}'; [\phi]) - \rho(\mathbf{r}'; [\phi_R]) \right) \nabla u_1(|\mathbf{r} - \mathbf{r}'|), \quad (2.7c)$$

where we have also used equation (2.5).

We will argue that the terms (2.7b) and (2.7c) will be small, and therefore can be safely neglected. The error term (2.7b) probes the difference in the full and mimic systems of the conditional singlet density. In general, we do not necessarily expect that these quantities are the same, due to the long range interactions neglected in the mimic system. However, the force from the short range force $F_0(\mathbf{r}) = -\nabla u_0(r)$ vanishes for large r by assumption, and therefore this term only probes the short range difference of the conditional singlet densities for the two systems. Because the short range interactions are the same for these two systems, we do expect the conditional singlet densities to be close at short distances, and therefore we expect the relevant convolution to be small. The term (2.7c) probes the difference between the conditional singlet density in the full system, and the singlet density in the mimic system. This is convolved with the force from the long range part of the potential, $F_1(\mathbf{r}) = -\nabla u_1(r)$, and this force vanishes at short distances, again by assumption. We do expect that at large distances the conditional singlet density is approximately equal to the single particle density, because the correlations should

be short ranged for systems that are not near a critical point. Therefore, we also expect this term to be small.

After neglecting the terms above which involve higher order correlation functions, we have effectively truncated the hierarchy and are left with the equilibrium LMF equation

$$\nabla\phi_R(\mathbf{r}) = \nabla\phi(\mathbf{r}) + \int d\mathbf{r}' \rho_R(\mathbf{r}'; [\phi_R]) \nabla u_1(|\mathbf{r} - \mathbf{r}'|). \quad (2.8)$$

This relates the renormalized potential $\phi_R(\mathbf{r})$ to the potential of the full system and the singlet density in the mimic system. Although this equation takes the form of a mean field type equation, it is important to understand the difference between this and a mean field approach. This is a self consistent equation, which must be iteratively solved in order to obtain a converged solution which satisfies the equation. Furthermore, this equation came directly from a series of controlled approximations to the exact YBG hierarchy, as opposed to the usual mean field approach.

In order to fully understand the difference in these two approaches, it is interesting to consider in what cases these approximations could fail, and why. One way in which this approach could fail is if the separation between the short range and long range forces was too short. In other words, if the short range forces did not adequately account for the forces at distances for which correlations still exist in the liquid, then one would expect the approximation to break down. This becomes particularly apparent in the context of electrostatics, where the splitting has an explicit length scale of smoothing σ , to be discussed. Therefore, this derivation not

only proves that the approximations are reasonable, but also give immediate insight into when they might fail. This will lead to an appropriate choice of the parameter σ .

Another interesting question is whether LMF theory is a good approximation for the dynamics of the theory. Velocity autocorrelation functions were studied for an LJ fluid by Rick Remsing in his thesis [18], where he showed that LMF theory reproduces the autocorrelation function accurately at short and intermediate timescales, with small deviations for the longer timescales. In his thesis, Ang Gao considered the velocity autocorrelation function and diffusion coefficient for fullerene solutes in water [20], which also showed slight discrepancies, but overall good agreement. This is an area that could be investigated more thoroughly in future work.

2.2 LMF theory for electrostatics

The previous derivation was valid for a system with only a single particle species, and therefore is not as general as it could be. In particular, for a system involving electrostatic interactions, one may be interested in site-site molecular models, for which different particle species have different charges. LMF theory can be extended to these situations, and have been studied extensively for single species molecular models. In order to accomplish this, a site site YBG hierarchy equation was derived, which encompasses effects from both intra-particle and inter-particle interactions [21, 22]. Although the full derivation is not contained here, the discussion regarding constrained systems in [chapter 4](#) will contain equations that are

valid in this broader context. For the present discussion, we will derive the LMF equation for electrostatics, and discuss the splitting of the Coulomb potential used in this context.

To obtain the LMF equation for mixtures, one introduces the relevant LMF equation for a species α in a mixture of species indexed by γ and including α

$$\phi_{R,\alpha}(\mathbf{r}) = \phi_\alpha(\mathbf{r}) + \sum_\gamma \int d\mathbf{r}' \rho_{R,\gamma}(\mathbf{r}') u_{1,\alpha\gamma}(|\mathbf{r} - \mathbf{r}'|). \quad (2.9)$$

For a general set of interactions, this would be the furthest simplification possible. However, due to the universal character of the electrostatic interaction, one can further simplify the equation. To do so, we consider the following splitting of the Coulomb potential

$$\frac{1}{r} = v_0(r) + v_1(r) \quad (2.10)$$

where

$$v_0(r) = \frac{\text{erfc}(r/\sigma)}{r}, \quad v_1(r) = \frac{\text{erf}(r/\sigma)}{r}. \quad (2.11)$$

In addition to LMF theory, this splitting is also used in standard Ewald summation techniques. The long range potential $v_1(r)$ here is that due to a Gaussian smoothed charge density of unit charge

$$\rho_G(r) = \frac{1}{\pi^{3/2}\sigma^3} \exp\left(-\frac{r^2}{\sigma^2}\right). \quad (2.12)$$

Because this potential arises from Gaussian smoothing, the Fourier transform of the

resulting potential is also well behaved, which is one of the reasons this splitting is chosen.

If one chooses the same smoothing length σ for all electrostatic interactions in a system, then the LMF equations written previously take the universal form

$$\phi_{R,\alpha}(\mathbf{r}) = \phi_\alpha(\mathbf{r}) + \frac{q_\alpha}{\epsilon} \int d\mathbf{r}' \rho_R^q(\mathbf{r}') v_1(|\mathbf{r} - \mathbf{r}'|), \quad (2.13)$$

where we have defined the charge density

$$\rho^q(\mathbf{r}) = \sum_\gamma q_\gamma \rho_\gamma(\mathbf{r}). \quad (2.14)$$

One can further define the renormalized potential $\phi_{R,\alpha}(\mathbf{r})$ in terms of a renormalized electrostatic potential $\mathcal{V}_R(\mathbf{r})$ through the equation

$$\phi_{R,\alpha}(\mathbf{r}) = \phi_{ne,\alpha}(\mathbf{r}) + q_\alpha \mathcal{V}_R(\mathbf{r}), \quad (2.15)$$

where $\phi_{ne,\alpha}(\mathbf{r})$ encompasses the potential due to interactions that are not electrostatic, and therefore are not relevant to the current discussion. With this definition, the LMF equation further simplifies to

$$\mathcal{V}_R(\mathbf{r}) = \mathcal{V}(\mathbf{r}) + \frac{1}{\epsilon} \int d\mathbf{r}' \rho_R^q(\mathbf{r}') v_1(|\mathbf{r} - \mathbf{r}'|), \quad (2.16)$$

which is the LMF equation for electrostatics.

It is now clear how the length scale σ appears naturally in the LMF equation

for electrostatics. As discussed previously, the choice of σ is important for the LMF approximation to be accurate, and the derivation illustrates in what way this is the case. In particular, we want the short range part of the interaction to be enough to properly account for the short range structure of the fluid, and long range enough that the interparticle correlations become small at the relevant length scale. For fluids near the triple point, this requirement implies that the smoothing length should be long enough to encompass at least a few molecular shells. If the value of σ is greater than this minimal distance, denoted σ_{min} , then the LMF approximation should be valid. For example, in water at room temperature, it has been found empirically that a choice of $\sigma_{min} = 4.5\text{\AA}$ is sufficient for LMF theory to be valid.

For most cases of interest, there are two relevant parts of an electrostatic potential. One is due to the fixed external charges, and the other is due to the induced structure in the liquid. If one applies the same smoothing to the fixed external charges, then it is useful to define the total restructured LMF correction

$$\mathcal{V}_{R1}(\mathbf{r}) = \frac{1}{\epsilon} \int d\mathbf{r}' \rho_{R,tot}^q(\mathbf{r}') v_1(|\mathbf{r} - \mathbf{r}'|), \quad (2.17)$$

where $\rho_{R,tot}^q$ includes all charges in the system, including fixed charges. This equation can also be written schematically as $\mathcal{V}_{R1} = \rho_{R,tot}^q \star v_1 = \rho_{R,tot}^q \star \rho_G \star \frac{1}{r}$. Using the associativity of convolution, this is also equal to $\mathcal{V}_{R1} = \rho_{R,tot}^{q\sigma} \star \frac{1}{r}$, where the smooth charge density is defined by $\rho_{R,tot}^{q\sigma} = \rho_{R,tot}^q \star \rho_G$. More explicitly, we have

$$\mathcal{V}_{R1}(\mathbf{r}) = \frac{1}{\epsilon} \int d\mathbf{r}' \rho_{R,tot}^{q\sigma}(\mathbf{r}') \frac{1}{|\mathbf{r} - \mathbf{r}'|}, \quad (2.18)$$

where the smooth charge density is defined by

$$\rho_R^{q\sigma}(\mathbf{r}') = \int d\mathbf{r}' \rho_{R,tot}^q(\mathbf{r}') \rho_G(|\mathbf{r} - \mathbf{r}'|). \quad (2.19)$$

From these equations, we see that the potential $\mathcal{V}_{R1}(\mathbf{r})$ is the electrostatic potential given by the smoothed charge density $\rho_{R,tot}^{q\sigma}(\mathbf{r})$. In particular, this potential satisfies the Laplace equation

$$\nabla^2 \mathcal{V}_{R1}(\mathbf{r}') = -\frac{4\pi}{\epsilon} \rho_{R,tot}^{q\sigma}(\mathbf{r}). \quad (2.20)$$

This equation will be useful for motivating some of the approximations that will be introduced in non-equilibrium LMF theory.

2.3 BBGKY and YBG hierarchies

In this section, we will derive the BBGKY and first of the YBG hierarchy equations, which are of central importance to LMF theory and this thesis. We will derive the first equation of the YBG hierarchy in two different ways, both of which are useful and relevant to the later discussion. Part of the presentation here follows Hansen and McDonald [23].

The first method to derive the first of the YBG hierarchy equations is the most straightforward, and can be generalized most easily for more complicated situations. To begin, we define the reduced particle density $\rho^{(1)}(\mathbf{r})$ for a single particle species

in an equilibrium canonical ensemble by

$$\rho^{(1)}(\mathbf{r}) = \mathcal{Z}^{-1} N \int e^{-\beta \mathcal{H}} d^{N-1} \mathbf{r}. \quad (2.21)$$

Here \mathcal{Z} is the partition function, N is the total number of particles, $\beta = (kT)^{-1}$ and \mathcal{H} is the Hamiltonian. Here the integral is over all but one particle, which is held fixed, and the particles are assumed to be identical. Taking a gradient of this equation, we find

$$\nabla \rho^{(1)}(\mathbf{r}) = -\beta \mathcal{Z}^{-1} N \int \nabla \mathcal{H} e^{-\beta \mathcal{H}} d^{N-1} \mathbf{r} d^N \mathbf{p}. \quad (2.22)$$

We will take the Hamiltonian to have the form of a kinetic term added to an external potential and a pair interaction

$$\mathcal{H} = \sum_i \frac{\mathbf{p}_i^2}{2m} + \sum_i \phi(\mathbf{r}_i) + \sum_{i \neq j} w(\mathbf{r}_i, \mathbf{r}_j), \quad (2.23)$$

which yields the equation

$$\nabla \rho^{(1)}(\mathbf{r}) = -\beta \rho(\mathbf{r}) \nabla \phi(\mathbf{r}) - \beta \int d\mathbf{r}' \rho^{(2)}(\mathbf{r}', \mathbf{r}) \nabla w(\mathbf{r}, \mathbf{r}'). \quad (2.24)$$

where $\rho^{(2)}(\mathbf{r}, \mathbf{r}') = \mathcal{Z}^{-1} N(N-1) \int e^{-\beta \mathcal{H}} d^{N-2} \mathbf{r} d^N \mathbf{p}$ is the two particle density. Dividing this equation by $\rho^{(1)}(\mathbf{r})$ we find the first of the YBG hierarchy equations

$$\nabla \ln \rho^{(1)}(\mathbf{r}) = -\beta \nabla \phi(\mathbf{r}) - \beta \int d\mathbf{r}' \rho(\mathbf{r}'; \mathbf{r}) \nabla w(\mathbf{r}, \mathbf{r}'), \quad (2.25)$$

where we have defined the conditional singlet density

$$\rho(\mathbf{r}'; \mathbf{r}) = \frac{\rho^{(2)}(\mathbf{r}', \mathbf{r})}{\rho^{(1)}(\mathbf{r})}. \quad (2.26)$$

The second derivation of the YBG hierarchy equations will be as the equilibrium limit of the BBGKY hierarchy equations, which are the non-equilibrium generalization of the hierarchy. The derivation of the BBGKY hierarchy starts with the Liouville equation, which follows from the continuity equation in phase space

$$\frac{\partial f^{(N)}}{\partial t} + \sum_{i=1}^N \left(\frac{\partial f^{(N)}}{\partial \mathbf{r}_i} \cdot \dot{\mathbf{r}}_i + \frac{\partial f^{(N)}}{\partial \mathbf{p}_i} \cdot \dot{\mathbf{p}}_i \right) = 0. \quad (2.27)$$

Using Hamilton's equations for the Hamiltonian (2.23), this can be written

$$\left(\frac{\partial}{\partial t} + \sum_{i=1}^N \frac{\mathbf{p}_i}{m} \cdot \frac{\partial}{\partial \mathbf{r}_i} - \sum_{i=1}^N \frac{\partial \phi}{\partial \mathbf{r}_i} \cdot \frac{\partial}{\partial \mathbf{p}_i} \right) f^{(N)} = \sum_{i,j=1}^N \frac{\partial w(\mathbf{r}_i, \mathbf{r}_j)}{\partial \mathbf{r}_i} \cdot \frac{\partial f^{(N)}}{\partial \mathbf{p}_i}. \quad (2.28)$$

To derive the BBGKY hierarchy, we first define the reduced phase space distribution functions

$$f^{(n)}(\mathbf{r}^n, \mathbf{p}^n; t) = \frac{N!}{(N-n)!} \int \int f^{(N)}(\mathbf{r}^N, \mathbf{p}^N; t) d\mathbf{r}^{N-n} d\mathbf{p}^{N-n}. \quad (2.29)$$

With this definition, we integrate the Liouville equation over $(N-n)$ coordinates

to find

$$\left(\frac{\partial}{\partial t} + \sum_{i=1}^n \frac{\mathbf{p}_i}{m} \cdot \frac{\partial}{\partial \mathbf{r}_i} - \sum_{i=1}^n \frac{\partial \phi}{\partial \mathbf{r}_i} \cdot \frac{\partial}{\partial \mathbf{p}_i} \right) f^{(n)} = \sum_{i,j=1}^n \frac{\partial w(\mathbf{r}_i, \mathbf{r}_j)}{\partial \mathbf{r}_i} \cdot \frac{\partial f^{(n)}}{\partial \mathbf{p}_i} + \sum_{i=1}^n \int \int \frac{\partial w(\mathbf{r}_i, \mathbf{r}_{n+1})}{\partial \mathbf{r}_i} \cdot \frac{\partial f^{(n+1)}}{\partial \mathbf{p}_i} d\mathbf{r}_{n+1} d\mathbf{p}_{n+1}, \quad (2.30)$$

which is the BBGKY hierarchy. The first equation of the hierarchy is

$$\left(\frac{\partial}{\partial t} + \frac{\mathbf{p}_1}{m} \cdot \frac{\partial}{\partial \mathbf{r}_1} - \frac{\partial \phi}{\partial \mathbf{r}_1} \cdot \frac{\partial}{\partial \mathbf{p}_1} \right) f^{(1)} = \int \int \frac{\partial w(\mathbf{r}_1, \mathbf{r}_2)}{\partial \mathbf{r}_1} \cdot \frac{\partial f^{(2)}}{\partial \mathbf{p}_1} d\mathbf{r}_2 d\mathbf{p}_2. \quad (2.31)$$

To find the equilibrium limit of equation (2.31), we first neglect the time derivative, as the equilibrium phase space distribution is independent of time. Also, at equilibrium the momentum dependence of the distribution functions takes the form of a Maxwell distribution

$$f_M(\mathbf{p}) = \frac{\exp(-\beta|\mathbf{p}|^2/2m)}{(2\pi m k_B T)^{3/2}}, \quad (2.32)$$

so that $f^{(1)}(\mathbf{r}_1, \mathbf{p}_1) = \rho^{(1)}(\mathbf{r}_1) f_M(\mathbf{p}_1)$, and similarly for $f^{(2)}$. Upon substituting the Maxwell distribution into equation (2.31) and simplifying, we find

$$\mathbf{p}_1 \cdot (\beta^{-1} \nabla_1 - \nabla_1 \phi) \rho^{(1)}(\mathbf{r}_1) = \mathbf{p}_1 \cdot \int \nabla w(\mathbf{r}_1, \mathbf{r}_2) \rho^{(2)}(\mathbf{r}_1, \mathbf{r}_2) d\mathbf{r}_2. \quad (2.33)$$

Noting that this equation is true for all \mathbf{p}_1 , one can neglect the dot product with

\mathbf{p}_1 . Then, dividing through by $\rho^{(1)}$ and simplifying yields equation (2.25).

2.4 Fluid dynamics equations

In this section we will show how the moments of the BBGKY hierarchy lead to microscopic versions of fluid dynamics equations, including the Navier-Stokes equation and the equation for conservation of energy. The presentation here will follow that of Harris [24], with some modifications to agree with our conventions. Many of these ideas are also expounded in more detail in Landau and Lifshitz [25][26]. This procedure forms the basis of the formalism necessary to extend LMF theory to the non-equilibrium situation in the ensemble averaged approach, to be discussed in chapter 3.

To begin, we define the moments of the reduced phase space density $f^{(1)}(\mathbf{r}, \mathbf{p}; t)$ with respect to momentum by

$$M_{\alpha\beta\dots} = \int d\mathbf{p} \mathbf{p}_\alpha \mathbf{p}_\beta \dots f(\mathbf{r}, \mathbf{p}; t), \quad (2.34)$$

where the indices α, β, \dots are spatial indices. The first few moments have direct physical significance in the context of fluid dynamics. The zeroth moment is the particle density

$$\rho(\mathbf{r}; t) = \int d\mathbf{p} f(\mathbf{r}, \mathbf{p}; t), \quad (2.35)$$

and the first moment is related to the fluid flow velocity $\mathbf{u}(\mathbf{r}; t)$ by

$$\rho(\mathbf{r}; t)\mathbf{u}(\mathbf{r}; t) = \int d\mathbf{p} \frac{\mathbf{p}}{m} f(\mathbf{r}, \mathbf{p}; t). \quad (2.36)$$

In order to study higher moments, it is useful to introduce the relative flow velocity

$$\mathbf{v}_0 = \frac{\mathbf{p}}{m} - \mathbf{u}, \quad (2.37)$$

which measures the speed of a particle in the reference frame of the fluid with average velocity \mathbf{u} . Using this quantity, the energy density $E = \int d\mathbf{p} p^2/2m f$ of the system can be written as a sum of a local internal energy $\xi = \int d\mathbf{p} m v_0^2/2 f$ and the kinetic energy of the bulk fluid, or

$$E = \xi + \frac{1}{2}\rho m u^2. \quad (2.38)$$

For a system of structureless particles, the equipartition theorem states that the internal energy is given by

$$\xi = \frac{3}{2}kT. \quad (2.39)$$

By considering an infinitesimal volume element around a point \mathbf{r} , one can show that the pressure tensor is related to the relative flow velocity through the equation

$$\mathbf{P} = \int d\mathbf{p} \mathbf{v}_0^T \mathbf{v}_0 f(\mathbf{r}, \mathbf{p}; t). \quad (2.40)$$

Furthermore, defining the heat and energy flux densities as

$$\mathbf{E} = \int d\mathbf{p} \frac{p^2}{2m^2} \mathbf{p} f(\mathbf{r}, \mathbf{p}; t), \quad \mathbf{Q} = \int d\mathbf{p} \frac{mv_0^2}{2} \mathbf{v}_0 f(\mathbf{r}, \mathbf{p}; t), \quad (2.41)$$

we have the relation

$$\mathbf{E} = \mathbf{Q} + \mathbf{u} \cdot \mathbf{P} + \mathbf{u} \rho E, \quad (2.42)$$

which is a local thermodynamic decomposition for fluids.

With these definitions, one sees how the local microscopic definitions of statistical mechanics translate to macroscopic variables used in the study of fluid dynamics. Furthermore, by taking moments of the BBGKY hierarchy equation (2.31), one obtains the equations of fluid dynamics. The zeroth moment yields the continuity equation

$$\frac{\partial \rho}{\partial t} + \nabla \cdot (\rho \mathbf{u}) = 0. \quad (2.43)$$

The first moment yields an equation for the fluid velocity

$$\frac{\partial}{\partial t} (\rho \mathbf{u}) + \nabla \cdot (\rho \mathbf{u}^T \mathbf{u} + \mathbf{P}) = \langle \mathbf{F} \rangle, \quad (2.44)$$

where we have defined the force density

$$\langle \mathbf{F}(\mathbf{r}) \rangle = -\rho(\mathbf{r}) \nabla \phi(\mathbf{r}) - \int \int \int \nabla w(\mathbf{r}, \mathbf{r}') f^{(2)}(\mathbf{r}, \mathbf{p}, \mathbf{r}', \mathbf{p}'; t) d\mathbf{r}' d\mathbf{p}' d\mathbf{p}. \quad (2.45)$$

Equation (2.44) is the microscopic version of the Cauchy momentum equation written in conservation form, which gives rise to the Navier-Stokes equation after further

simplification. We have therefore derived macroscopic fluid dynamics equation directly from the microscopic equations of motion.

Finally, multiplying equation (2.31) by $p^2/2m$ and integrating yields an energy conservation equation

$$\frac{\partial}{\partial t} E + \nabla \cdot \mathbf{E} = \langle \mathbf{p} \cdot \mathbf{F} \rangle. \quad (2.46)$$

Together, these constitute the fundamental equations of macroscopic fluid dynamics. However, because of the ensemble averages in these equations, they do not constitute a closed system of equations, and cannot be solved explicitly. These equations are useful theoretically, and can be used in molecular dynamics simulations.

Chapter 3: Ensemble Averaged LMF Theory

3.1 Introduction

In this chapter we will take our first step towards generalizing LMF theory to non-equilibrium systems. This approach relies on the use of non-equilibrium ensemble averages, which correspond to averages over a number of realizations of the same system subjected to the same external force, starting from equilibrium. This idea is a powerful tool in non-equilibrium statistical mechanics [27], being the natural generalization of the ensemble average in equilibrium. Understanding LMF theory within this general formalism is an important first step in the development of non-equilibrium LMF theory, serving as an important theoretical basis for the investigation of further approximation methods.

Another difference between the equilibrium and non-equilibrium formalism are the underlying equations that are used, and the character of these equations. The equilibrium derivation of the LMF equation relied on the use of the first of the equilibrium Yvon-Born-Green (YBG) hierarchy equations, which provides a self-consistent LMF potential that can be found iteratively in simulation [28], or through the use of linear response methods [14]. In this case we will use the time dependent Bogoliubov-Born-Green-Kirkwood-Yvon (BBGKY) hierarchy, adapting

a similar derivation in this more general framework. We begin by deriving a form of the BBGKY equation which makes manifest the reduction to equilibrium, using this equation as a key tool in the derivation of the non-equilibrium LMF equation. With this form of the equation, it will become clear that the original self consistency condition of equilibrium becomes a dynamic relaxation condition, and LMF theory will imply that the full and mimic systems will satisfy the same differential equation. The solution to this differential equation is unique, and therefore we expect the two systems to evolve in the same way. Through this mechanism, the original self-consistency condition for the LMF equation becomes a dynamic relaxation property of a non-equilibrium ensemble. This is a phenomenon that underscores the fundamental difference between the equilibrium and non-equilibrium approach to LMF theory.

After developing the non-equilibrium formalism, we apply the result to a model system consisting of water molecules confined between two hydrophobic walls in the presence of an external electric field. For a time independent external field, this system has been an important test case for the development of LMF theory [28][29][30], and therefore provides a useful model system with which to test this methodology. We first demonstrate how a system far from equilibrium dynamically relaxes to the correct equilibrium configuration in the presence of a time-independent field, and then show that the resulting configuration agrees with previous published data on equilibrium LMF theory. In this case neglecting the long range forces entirely fails dramatically, and so this serves as a good test model for the theory. We then consider the effect of an oscillating electric field and instantaneous perturbing electric

field, illustrating the efficacy of the non-equilibrium approach for investigating the dynamics of a dielectric medium.

3.2 The non-equilibrium formalism

LMF theory starts with a splitting of the Coulomb potential into a short and long range component

$$\frac{1}{r} = v_0(r) + v_1(r), \quad (3.1)$$

where the long range component is the potential generated by a unit Gaussian charge density of width σ , which is a smoothing length chosen appropriately for the system under consideration. Here σ will be chosen to be 4.5 Å, which should be adequate for SPC/E water[30]. If one neglects the long range forces completely for all charges in the system, the answer can be correct in certain cases, specifically for bulk solvent. This approximation is denoted *strong coupling*.

In LMF theory, the long range force is taken into account through a self consistent potential satisfying the equilibrium LMF equation

$$V_{R1}(\mathbf{r}) = \frac{1}{\epsilon} \int d\mathbf{r}' \rho_{R,tot}^{q\sigma}(\mathbf{r}') \cdot \frac{1}{|\mathbf{r} - \mathbf{r}'|}, \quad (3.2)$$

where $V_{R1}(\mathbf{r})$ is the LMF potential excluding the external field, and $\rho_{R,tot}^{q\sigma}(\mathbf{r}')$ is the average smooth charge density of the strong coupling system in the presence of the LMF potential. This auxiliary system, which approximately takes account of the long range forces, is known as the *mimic system*, which is indicated by the subscript

R. The fundamental argument of LMF theory proves that the equilibrium single particle density of the mimic system is very close to that of the full system, under a set of mild physically motivated approximations. Equation (3.2) is a solution to Poisson's equation sourced by the smooth charge density

$$\nabla^2 V_{R_1}(\mathbf{r}) = -\frac{4\pi}{\epsilon_0} \rho_{R,tot}^{q\sigma}(\mathbf{r}). \quad (3.3)$$

The assumptions and validity of LMF theory is discussed in detail in previous publications, in addition to a detailed derivation using the first of the YBG hierarchy [28][29][30].

In the non-equilibrium context, the most natural way to obtain a mean field for the long range forces is to consider an ensemble of systems characterized by a non-equilibrium phase-space density $f^{(N)}(\mathbf{r}^{(N)}, \mathbf{p}^{(N)}; t, \phi(t))$, and the corresponding reduced phase space densities, defined by integrating out all but a subset of the identical particles considered. For an ensemble close to equilibrium, the long ranged forces from the reduced densities tend to smooth out statistical fluctuations occurring for an individual realization, resulting in a mean field that accounts for the average long range force of the ensemble. This averaging is illustrated in figure 3.1.

We will be most interested in the single particle reduced phase space density,

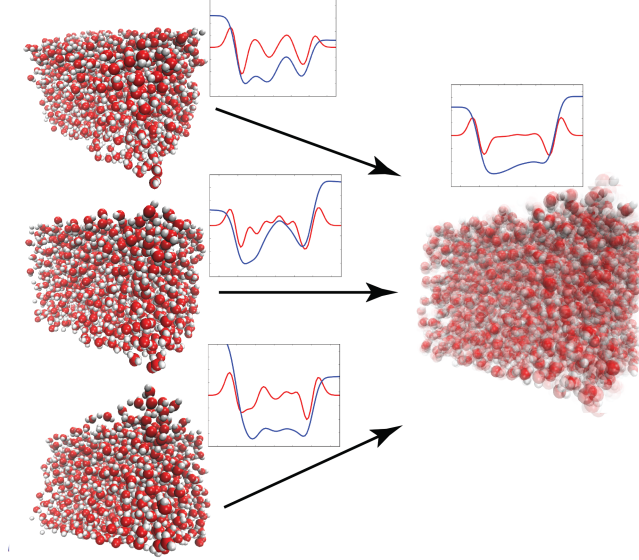


Figure 3.1: Illustration of the statistical smoothing that occurs when considering an ensemble of systems as opposed to a single realization, with the smooth charge density (red) and LMF potential (blue) plotted next to each system. We show in this paper that a system close to equilibrium evolving under this mean field will have the same non-equilibrium single particle density as one that evolves under the full dynamics.

which evolves according to the first of the BBGKY hierarchy equations [31]

$$\left(\frac{\partial}{\partial t} - \nabla\phi(\mathbf{r}; t) \cdot \frac{\partial}{\partial \mathbf{p}} + \frac{\mathbf{p}}{m} \cdot \nabla\right) f^{(1)}(\mathbf{r}, \mathbf{p}; t) = \int \int \nabla w(|\mathbf{r} - \mathbf{r}'|) \cdot \frac{\partial}{\partial \mathbf{p}} f^{(2)}(\mathbf{r}, \mathbf{p}, \mathbf{r}', \mathbf{p}'; t) d\mathbf{r}' d\mathbf{p}', \quad (3.4)$$

where $f^{(n)}(\mathbf{r}^{(n)}, \mathbf{p}^{(n)}; t)$ are time dependent reduced phase space distributions, $\phi(\mathbf{r}; t)$ is a time dependent external potential, and $w(r)$ is the interparticle potential. At equilibrium, the phase space distribution functions have simple momentum dependence which leads to the YBG hierarchy, used in the derivation of LMF theory [10]. To make use of the approximations in the original derivation, we will first derive a form of this equation that manifests the reduction to equilibrium. This is related

to the derivation of hydrodynamical equations from statistical mechanical origins, which are explained in more detail by Harris [24] and Landau [25][26].

To begin, integrate equation (3.4) with respect to \mathbf{p} to get the continuity equation

$$\frac{\partial}{\partial t}\rho + \nabla \cdot (\rho\mathbf{u}) = 0,$$

where we have defined the non-equilibrium singlet density and velocity field

$$\rho(\mathbf{r}; t) = \int f^{(1)}(\mathbf{r}, \mathbf{p}; t)d\mathbf{p}, \quad \mathbf{u}(\mathbf{r}; t) = \rho^{-1} \int \frac{\mathbf{p}}{m} f^{(1)}(\mathbf{r}, \mathbf{p}; t)d\mathbf{p}.$$

In order to study higher moments, it is useful to introduce the relative flow velocity

$$\mathbf{v}_0 = \frac{\mathbf{p}}{m} - \mathbf{u}, \tag{3.5}$$

which measures the speed of a particle in the reference frame of the fluid. The pressure tensor is related to the relative flow velocity through the equation

$$\mathbf{P} = \int d\mathbf{p} \mathbf{v}_0^T \mathbf{v}_0 f(\mathbf{r}, \mathbf{p}; t). \tag{3.6}$$

As discussed in section 2.4, taking the first moment with respect to momentum of equation (3.4) yields the Cauchy momentum equation written in conservation form

$$\frac{\partial}{\partial t}(\rho\mathbf{u}) + \nabla \cdot (\rho\mathbf{u}^T \mathbf{u} + \mathbf{P}) = \mathbf{F}, \tag{3.7}$$

where we have defined the average force density

$$\mathbf{F}(\mathbf{r}; t) = -\rho(\mathbf{r}; t)\nabla\phi(\mathbf{r}; t) - \int \int \int \nabla w(\mathbf{r}, \mathbf{r}') f^{(2)}(\mathbf{r}, \mathbf{p}, \mathbf{r}', \mathbf{p}'; t) d\mathbf{r}' d\mathbf{p}' d\mathbf{p}. \quad (3.8)$$

For systems that are in equilibrium, the momentum dependence of $f^{(1)}(\mathbf{r}, \mathbf{p}; t)$ takes the form of a Maxwell distribution. For systems that are locally equilibrated around the flow velocity \mathbf{u} , the momentum distribution should be well approximated by a Maxwell distribution centered at \mathbf{u} . We are therefore motivated to define the modified phase space density

$$\tilde{f}^{(1)}(\mathbf{r}, \mathbf{p}; t) = \frac{f^{(1)}(\mathbf{r}, \mathbf{p}; t)}{f_M(\mathbf{v}_0)},$$

where $f_M(\mathbf{v})$ denotes the Maxwell distribution

$$f_M(\mathbf{v}) = \frac{\exp(-\beta m |\mathbf{v}|^2 / 2)}{(2\pi m k_B T)^{3/2}}.$$

In terms of this function, the pressure tensor $\mathbf{P}(\mathbf{r}; t)$ can be written

$$\mathbf{P}(\mathbf{r}; t) = \frac{\rho(\mathbf{r}; t)}{\beta m} \mathbf{I} + \tilde{\mathbf{P}}(\mathbf{r}; t),$$

where \mathbf{I} is the identity matrix, and we have defined

$$\tilde{\mathbf{P}}(\mathbf{r}; t) = \int \frac{f_M(\mathbf{v}_0)}{m^2 \beta^2} \frac{\partial}{\partial \mathbf{v}_0} \frac{\partial}{\partial \mathbf{v}_0^T} \tilde{f}^{(1)}(\mathbf{r}, \mathbf{p}; t) d\mathbf{p}.$$

We expect the modified density $\tilde{f}(\mathbf{r}, \mathbf{p}; t)$ to have weak momentum dependence for systems that are close to equilibrium. For this reason we expect $\tilde{P}(\mathbf{r}; t)$ to be suppressed in magnitude by the two derivatives with respect to \mathbf{v}_0 .

With these definitions, equation (3.7) becomes

$$m\rho^{-1}\left(\frac{\partial}{\partial t}(\rho\mathbf{u}) + \nabla \cdot (\rho\mathbf{u}^T\mathbf{u} + \tilde{\mathbf{P}})\right) = -\beta^{-1}\nabla \ln \rho + \rho^{-1}\mathbf{F}, \quad (3.9)$$

The right hand side of this equation is the first of the YBG hierarchy. Naturally, at equilibrium the terms on the left hand side vanish, which manifests how this equation reduces to the equilibrium situation, even though it is exact for the non-equilibrium case as well.

The derivation leading to the non-equilibrium LMF equation now proceeds just as in the equilibrium case. First we introduce the LMF mimic system, which evolves under a truncated potential $u_0(r)$ and a renormalized field $\phi_R(\mathbf{r}; t)$ chosen to reproduce the exact non-equilibrium phase space density, or

$$\rho(\mathbf{r}; t, [\phi]) = \rho_R(\mathbf{r}; t, [\phi_R]).$$

The existence of such a potential is not a strong assumption, especially when the potential $u_0(\mathbf{r})$ is chosen to reproduce the short ranged intermolecular forces. We

then subtract equation (3.9) for the full and mimic systems, which gives

$$\frac{m}{\rho(\mathbf{r}; t)} \left(\frac{\partial}{\partial t} \delta(\rho \mathbf{u}) + \nabla \cdot \delta(\rho \mathbf{u}^T \mathbf{u} + \tilde{\mathbf{P}}) \right) = \quad (3.10a)$$

$$\nabla \left(\phi_R(\mathbf{r}; t) - \phi(\mathbf{r}; t) - \int \rho_R(\mathbf{r}'; t, [\phi_R]) u_1(|\mathbf{r} - \mathbf{r}'|) d\mathbf{r}' \right) \quad (3.10b)$$

$$- \int \left(\rho(\mathbf{r}'|\mathbf{r}; t, [\phi]) - \rho_R(\mathbf{r}'|\mathbf{r}; t, [\phi_R]) \right) \nabla u_0(|\mathbf{r} - \mathbf{r}'|) d\mathbf{r}' \quad (3.10c)$$

$$- \int \left(\rho(\mathbf{r}'|\mathbf{r}'; t, [\phi]) - \rho(\mathbf{r}'; t, [\phi_R]) \right) \nabla u_1(|\mathbf{r} - \mathbf{r}'|) d\mathbf{r}', \quad (3.10d)$$

where δ denotes the difference between the full and mimic system. For example, we define $\delta(\rho \mathbf{u}) = \rho_R \mathbf{u}_R - \rho \mathbf{u}$.

The expressions on the right hand side of this equation are familiar from the original derivation of LMF theory [28], where the terms (3.10c) and (3.10d) are the two error terms neglected in that derivation. For a large class of systems we expect that these two terms will be close to zero for the same reasons as originally. In particular, term (3.10c) is a convolution of the gradient of the short range force with the difference in the conditional singlet densities. Because the mimic system has the same short range interactions as the full system, we expect that the conditional singlet densities for the two systems should be close together at short distances. At farther distances, where this may not be the case, the integral is suppressed by convolution with $\nabla u_0(r)$, which quickly approaches zero at large r . For term (3.10d), the integral contains the difference between the conditional singlet density and singlet density for the full system. In general, these densities are substantially different at short distances, but should become approximately equal at larger dis-

tances [32]. Conversely, the gradient of the long range force is chosen to be small at short distances, and large only at length scales larger than σ .

We will also neglect the term $\delta\tilde{P}_{ij}(\mathbf{r}; t)$ for two reasons. First, as noted previously, this term is already suppressed by two derivatives of $\tilde{f}(\mathbf{r}, \mathbf{p}; t)$, which we expect to suppress this term for systems that are moderately close to equilibrium. Secondly, this term is the difference between $\tilde{P}(\mathbf{r}; t)$ for the full and mimic system. The term is local in space, so the two systems should have the same characteristics at that length scale because the short range interactions are the same for the two systems. For this reason, we expect that this difference will also be suppressed further.

Term (3.10b) is the non-equilibrium LMF equation

$$\phi_R(\mathbf{r}; t) = \phi(\mathbf{r}; t) + \int \rho_R(\mathbf{r}'; t, [\phi_R]) u_1(|\mathbf{r} - \mathbf{r}'|) d\mathbf{r}' + C, \quad (3.11)$$

which defines the renormalized potential in the mimic system. After neglecting the terms discussed above, demanding that the LMF equation holds, and then using the continuity equation, we find

$$\delta \frac{D}{Dt} \mathbf{u}(\mathbf{r}; t) = 0. \quad (3.12)$$

Here we have defined the material derivative

$$\frac{D}{Dt} = \frac{\partial}{\partial t} + \mathbf{u} \cdot \nabla \quad (3.13)$$

familiar from hydrodynamics. Clearly, a particular solution of this equation is given

by $\mathbf{u} = \mathbf{u}_R$. As these equations are slowly varying due to the Gaussian smoothing, we do not expect any pathological behavior in the differential equations, and therefore this particular solution should be unique for systems with the same initial conditions. For this reason we expect the two systems to evolve similarly. Additionally, even if the systems start to diverge slightly, they are both driven towards the equilibrium solution, which is a fixed point of equation (3.9). The equilibrium derivation of the LMF equation is true regardless of the dynamics of the system, so we always expect the two systems to stay close together.

We therefore find that the LMF mimic system will yield an accurate approximation to the dynamics of the full system for a large class of models, assuming that they are moderately close to equilibrium, in the sense that the momentum dependence is close to Maxwellian. In the following we will apply this approximation to a variety of cases, which are even farther from equilibrium than one might expect, showing that the approximation is indeed valid in many interesting situations.

3.3 Implementation with slab geometry

We illustrate these modified LMF dynamics with an important model system - water confined between hydrophobic walls in the slab geometry. This geometry is one of the simplest non-trivial examples of a non-uniform system, illustrates subtleties in methods for handling electrostatics, and shows non-trivial equilibrium and dynamic properties. Water confined between hydrophobic walls in the slab geometry has been well studied in the context of LMF theory[14][30]. In this case, the strong

coupling approximation fails in a number of ways [33], and is corrected by the long range LMF field. The LMF potential applies a torque near the walls, and goes to zero in the center of the slab, where bulk water properties are recovered.

Computationally, the ensemble of realizations used in the derivation above is obtained by simulating a number of independent copies of the system evolving under the mean long range force averaged over the entire ensemble. As opposed to the usual self-consistent method of solving the LMF equation, this ensemble dynamically relaxes to the correct solution under the non-equilibrium LMF prescription. From the self-consistent field point of view, we can understand this as the LMF field correcting itself slightly at each time step, instead of a large correction being applied at the end of each simulation. Both methods rely on updates to the field based on new statistical data, but it is clear that if these corrections are small and made frequently, then the convergence of these methods should be smoother, assuming that the underlying equations are well behaved. This is a significant departure from previous methods, and offers some advantages in terms of convergence for arbitrary initial choices of field.

The approach to equilibrium under this formalism is illustrated in figure 3.2. We note that in this figure the initial potential drop is very large, because the system started in a very unphysical (ice-like) structure. The time scale of the equilibration is rather impressive given the long time scales necessary for LMF equilibration with previous methods. This is a first illustration of why dynamic relaxation is a promising approach to LMF theory.

According to equation (3.11), the mimic system evolves under the instant-

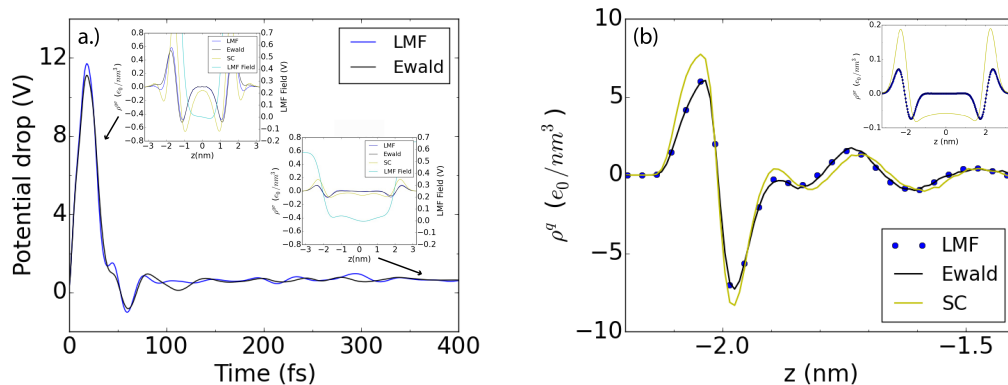


Figure 3.2: Simulations were performed for the slab geometry with hydrophobic walls, with the dynamic approach to equilibrium illustrated in (a). The blue line corresponds to the potential drop over the wall, with the corresponding LMF field and smooth charge density shown for selected times. In (b) the charge density is shown averaged over time, with the inset again showing the average field and smooth charge density.

neous average long range force of the entire ensemble, which in the slab geometry also includes averaging over the x and y directions. For the spatial averaging, we are taking advantage of the translational symmetry in two of the dimensions to further improve the statistics necessary to create a reasonable ensemble. In this sense we are viewing the translational symmetry similarly to an independent realization of the dynamics, which was a simplification also used in the equilibrium context [30]. In practice, we also set the x and y components of the force to zero because of the symmetry, and use the averaging to compute the z-component of the force, which is the only non-zero component in the limit where the number of realizations goes to infinity.

We performed simulations using the LAMMPS molecular modeling software. SPC/E water was confined between two hydrophobic smoothed LJ walls, modeling paraffin [34]. The box used varied in size (see appendix A), and for npt simula-

tions the x and y directions were allowed to change size. For most simulations, 12 realizations of the system were modeled simultaneously, with averaging over the realizations and the x and y directions to obtain the average LMF field in the z direction, assumed to be constant in the other directions. Each realization was equilibrated for 200 ps at 298 C under a Nose-Hoover type thermostat, and a barostat of one atm for constant pressure simulations. In studying this system for a time independent potential, we show that the dynamic LMF equation derived above asymptotically reproduces the equilibrium LMF dynamics, and in fact approaches the correct solution rather quickly. We also demonstrate the effect of an electric field on the structure of the water, using these dynamics as a sensitive test of properties such as the field dependent dielectric constant.

In figure 3.2, we show the smoothed charge density and LMF field obtained in the absence of an electric field. The agreement between this result and previously published data [30] verifies that this dynamic method agrees with the self-consistent equilibrium way of solving the LMF equation, which is non-trivial given the dramatically different simulation techniques. In this case, the field dynamically relaxes to the equilibrium configuration, as opposed to the sequential equilibrium simulations followed by a linear response correction employed previously [14]. We therefore have a new interpretation of the equilibrium LMF equation as the asymptotic solution of the non-equilibrium solution for a time-independent external field.

In the presence of an electric field, the failure of the strong coupling approximation is even more dramatic, and can be clearly seen in the density profiles of the system. In this context, we applied the strong coupling approximation to the

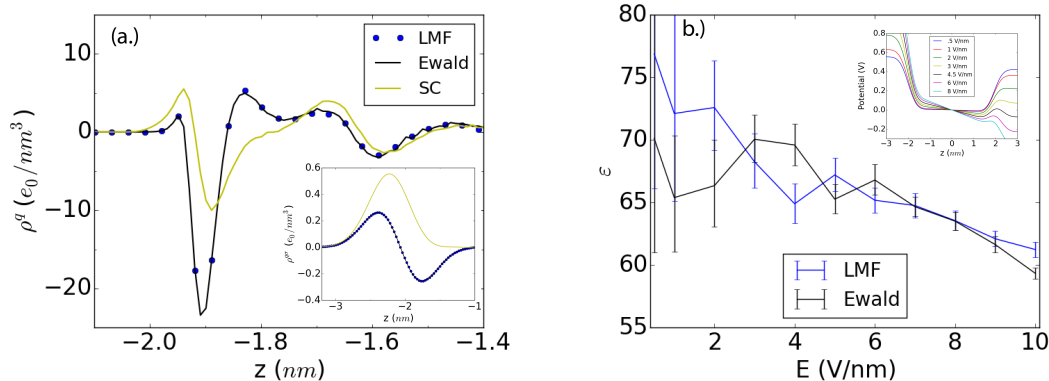


Figure 3.3: Simulations were performed for the slab geometry with an electric field of 10 V/nm , and the charge density is shown in (a), with the smooth charge density in the inset. The approximate dielectric constant is plotted as a function of external applied field in (b), with the corresponding LMF potentials in the inset.

charges of the water, and the charge on the wall responsible for the applied field, which is most natural because of the universality of the Coulomb force. Figure 3.3 shows the charge density for an applied field of 10 V/nm . In this case, the long range forces of the full model diminish the total electric field by a factor of ϵ^{-1} , as predicted by elementary electrostatics.

Using LMF theory, it is possible to probe the dielectric behavior of the water more carefully, and to test the validity of the theory. The dielectric properties of water confined in a slab has been studied for large fields, and is known to be reduced at very large fields due to saturation of the alignment of the water molecules [35]. Figure 3.3 illustrates this dielectric constant for smaller fields than usually studied, also showing the agreement between the LMF and Ewald results for this calculation, up to statistical fluctuations.

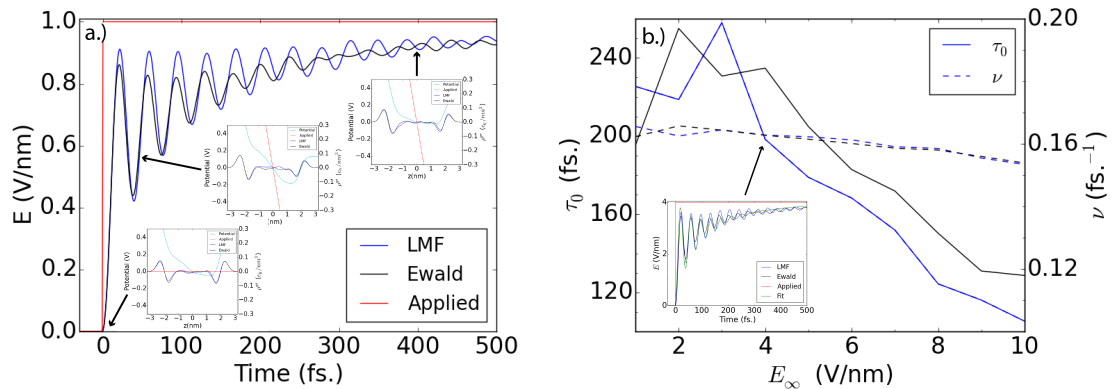


Figure 3.4: An abrupt change in electric field was simulated after equilibration at zero field. The approach to equilibrium is illustrated in (a), where the insets show the instantaneous smooth charge density and potential of the different systems. In (b.) the timescale of relaxation and frequency of oscillations as a function of electric field are plotted.

3.4 Time dependent potentials

We will now consider the effect of a time varying external field on the charge density of water evolving under the non-equilibrium LMF equation. To this end, we have considered the slab geometry subject to both an abrupt change in the applied electric field, and an electric field oscillating sinusoidally in time. All of these simulations were performed with a Nosé-Hoover thermostat cooling the system while the changing field increased the temperature, leading to a temperature slightly above room temperature.

3.4.1 Nonequilibrium Relaxation to Changes in Electric Fields

We first considered the response of a system to a rapid change in the electric field, by equilibrating the system at zero field, and then abruptly turning on a finite field to visualize the dielectric relaxation of the medium. The response of

a dielectric medium to an abrupt change in field is both conceptually simple and physically interesting, because of its relation to the charge transfer problem and ionic solvation [36][37]. Although an instantaneous change in the charge density of the slab geometry is somewhat artificial, it does capture the essential physics of the charge transfer problem for large solutes. Additionally, this problem represents a simple and direct test of the non-equilibrium formalism developed previously.

Figure 3.4 illustrates the approach to equilibrium with the average bulk polarization field versus time, with some snapshots shown additionally. We used a non-linear least squares fit to approximate this approach to equilibrium by a function of the form

$$E \approx E_\infty - A_0 e^{-t/\tau_0} - A_1 e^{-t/\tau_1} \cos(\nu t), \quad (3.14)$$

and the corresponding value for τ_0 and ω are plotted. This functional form contains an average decay superposed onto a decaying oscillatory function, which are physically interpreted as the relaxation of the mean bulk electric field to its equilibrium value superposed onto the short range oscillatory fluctuations from the dielectric response of the medium. The parameter τ_0 is a timescale of this slow relaxation of the system, while the frequency ν is a measure of the frequency of the damped oscillations.

It is clear from this figure that dynamic LMF theory is again in very good agreement with the full system, although it is not perfect. This is to be expected, because when the field is changed the system is far from equilibrium, and therefore the approximations of LMF theory are not expected to hold perfectly. Also, we see

that the period of oscillation for the relaxation, ω , is approximately constant for both systems, although the full system has a slightly smaller amplitude of oscillation than the LMF dynamics. This can be understood in terms of the characteristic time scale of water fluctuations, related to the frequency dependent charge-charge autocorrelation function of water [38][39], which is investigated more in chapter 5.

3.4.2 Sinusoidal field

We also considered the response of the medium to a spatially constant electric field oscillating in time. This problem is natural to consider, being the paradigmatic example for the linear response formalism, and defining the complex dielectric constant [31][40]. Furthermore, this problem is directly related to the interaction of light with a dielectric medium, which are amenable to experimental investigation [41]. Because of the relation of this problem to the linear response of a dielectric medium, testing the behavior of the complex permittivity also probes the accuracy of the LMF approximation for systems evolving on the timescales of the order of the period, such as systems of biological interest.

We first considered a field with a period of 400 fs. and a maximum amplitude of 10 V/nm , which are very rapid and large fields relative to most systems of biological interest. We might expect that the approximations leading to equation (3.12) may be invalid in this case, as the system is not very close to equilibrium, but this is not the case. In figure 3.5, we have taken snapshots four times every period for a simulation of one nanosecond when the instantaneous applied field is zero. This

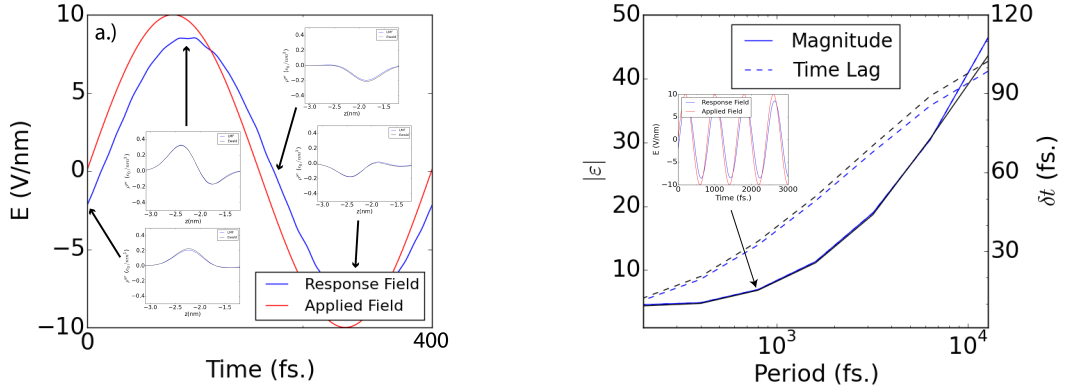


Figure 3.5: A simulation was performed with a spatially independent electric field with sinusoidal time variation. The bulk electric field as a function of time is plotted in (a), with snapshots of the smooth charge density for the LMF and Ewald systems shown at snapshots. The complex dielectric constant as a function of period is plotted in (b), with an inset showing the oscillating electric field that generates a data point.

allows us to get enough statistics for an instantaneous snapshot of a non-equilibrium system, due to the periodicity of the driving force. Due to the fast driving of the system, the instantaneous charge density is far from its equilibrium values. Here the LMF approximation is still very good, because the system is close enough to equilibrium to still satisfy the general arguments required for the validity of LMF theory.

For a sinusoidally varying field, the static dielectric response shows a time lag due to the finite time it takes for the dielectric medium to respond to the changing field. This can be expressed using a complex dielectric function, where the magnitude determines the ratio of the amplitudes of the displacement field and total electric field, and the phase determines the temporal offset of the two fields.

This function is defined by the equation

$$D_0 e^{i\omega(t-\delta t)} = |\varepsilon(\omega)| E_0 e^{i\omega t}, \quad (3.15)$$

where we have split the complex dielectric constant into a phase, given by the time offset, and a magnitude. These two quantities are plotted in figure 3.5, which also illustrates the applied field and polarization density for a few periods. To some degree, it is surprising how well the LMF and Ewald results agree for this broad range of periods, given how far from equilibrium these systems are.

3.5 Conclusions and Outlook

We have generalized the formalism of LMF theory to the non-equilibrium context, which required the use of the mean field of an ensemble of systems evolving under the same time-dependent external field. We showed that the same approximations that are required in equilibrium can be used in the non-equilibrium derivation, and that ensembles that are reasonably close to equilibrium still satisfy these approximations to a high degree of accuracy.

We first showed that the steady state configurations obtained for a time-independent external field agree with those obtained in equilibrium LMF theory, lending credence to the proposed formalism. We then showed that the dynamics of the full and LMF systems are very close for two systems reasonably far from equilibrium, at least relative to most biological simulations of interest, showing that the necessary approximations are even true out of equilibrium.

In practice, these methods could be used for a dynamical use of LMF theory used in molecular dynamics simulations. In general, it is not always practical to simulate multiple realizations of a system evolving according to LMF dynamics, however it may be possible to obtain approximate statistics for the mean LMF field by using the assumed ergodicity of a solvent interacting with particles that evolve on a slower dynamic time-scale. These issues will be investigated further in alternate versions on non-equilibrium LMF theory presented in the next few chapters.

Chapter 4: Non-equilibrium densities from force balance equations for single particle and constrained molecular systems

4.1 Introduction

Recently, a new method for sampling ensemble averages through force balance equations was investigated by Borgis et. al. [42] and Heras et. al. [43]. This could be a new type of enhanced sampling, and has parallels to the theory of adaptive biasing force [44]. This approach relies on the YBG hierarchy equation written as a force balance equation as shown below:

$$\mathbf{F}(\mathbf{r}) - \beta^{-1}\nabla\rho(\mathbf{r}) = 0. \quad (4.1)$$

The idea is to sample the force density instead of the smooth charge density, which leads to reduced statistical noise in the resulting distribution. Indeed, a reasonable approximation to $g(r)$ was obtained from a single equilibrated configuration of an LJ fluid in the case studied by Borgis et al., which is an impressive achievement for this methodology.

This could be a useful development in the context of LMF theory. Solving the LMF equation relies on accurate approximation of smoothed particle densities, so

the force sampling approach could provide a useful tool for approximating the LMF potential at a snapshot in time. This is particularly important for non-equilibrium systems, in which it is generally necessary to find a time dependent LMF potential that changes as the simulation progresses. The more accurate this approximation is, the more accurate the LMF procedure would be. Furthermore, it is desirable to generalize this procedure to molecular solvents such as water, because single particle systems such as Lennard-Jones fluids are usually not as interesting for applications.

In this chapter we will generalize the force balance approach to non-equilibrium systems, and to constrained molecular systems. We start by reviewing the force sampling approach, calling attention to some benefits and drawbacks of the method. We then consider the generalization to nonequilibrium problems, starting with the equations derived in the previous chapter. We then consider constrained systems, first deriving the constrained force balance equation in equilibrium, and then generalizing to non-equilibrium systems. We then test these results on a model system, and discuss how the procedure could be extended for use with LMF theory.

4.2 Review of force sampling method

The force sampling approach is a method for approximating particle densities in an equilibrium system using the force balance equation [23]

$$\mathbf{F}(\mathbf{r}) - \beta^{-1}\nabla\rho(\mathbf{r}) = 0, \quad (4.2)$$

This can be derived from the first of the YBG hierarchy equations

$$\beta^{-1}\nabla\ln\rho(\mathbf{r}) = -\nabla\phi(\mathbf{r}) - \int \nabla w(|\mathbf{r} - \mathbf{r}'|)\rho(\mathbf{r}|\mathbf{r}')d\mathbf{r}' \quad (4.3)$$

by defining the force density

$$\mathbf{F}(\mathbf{r}) = \left\langle \sum_i \mathbf{F}_i(\mathbf{r}^N)\delta(\mathbf{r} - \mathbf{r}_i) \right\rangle.$$

This is for a system evolving under the external field $\phi(\mathbf{r})$ and pair potential $w(\mathbf{r}-\mathbf{r}')$, this can be written

$$\mathbf{F}(\mathbf{r}) = -\rho(\mathbf{r}; t) \left(\nabla\phi(\mathbf{r}; t) + \int \nabla w(|\mathbf{r} - \mathbf{r}'|)\rho(\mathbf{r}|\mathbf{r}'; t)d\mathbf{r}' \right).$$

Inserting this equality into the YBG hierarchy equation yields the force balance equation (4.2).

The force sampling method is a way of calculating the density $\rho(\mathbf{r})$ in an indirect fashion, which has certain desirable convergence properties. The standard approach to finding the particle density is to make a direct histogram of this quantity for a given amount of sampling, and use the average value obtained as the density. The force sampling approach is to compute the force density in this way, and then to solve equation (4.2) to find the particle density. For Lennard-Jones systems, this leads to less statistical noise for small sample sizes, which is desirable in simulations where computational cost is a concern.

An example of this increased convergence is illustrated in figure 4.1. In this

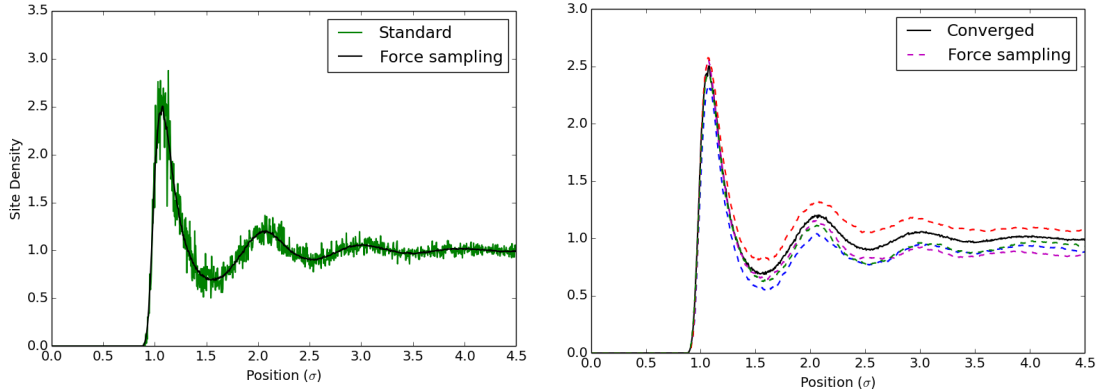


Figure 4.1: Density profile for an LJ fluid in the slab geometry as calculated with the density averaging and force sampling methods. The finite sample size curves are calculated by averaging over 3000 independent particles, then compared to the converged result. The grid spacing is chosen to be $\Delta r = .004\sigma$. For the force sampling method, multiple trials are shown to exhibit the scatter in the asymptotic density.

simulation, 1000 atoms were confined in a box with a reduced density $\rho^* = .8$ and a reduced temperature of $T^* = 1.35$, as considered by Borgis et. al. [42]. However, this figure also illustrates a generic issue with this method, which is systematic error that can be introduced. To understand this, note that the force balance equation relates the integral of the force to the density, and the integration smooths out the statistical noise, leading to the smoothness of the curves. However, the error in the forces leads to cumulative error in the average value of the density, whereas the usual method is scattered around the correct value. This issue was also considered by Heras et. al. [43], and will be investigated more closely in a different context.

4.3 Generalization to non-equilibrium systems

As of now, the force sampling method has been applied only to equilibrium systems. As is the case with LMF theory, there are potential advantages to general-

izing this method to non-equilibrium systems. This is for a similar reason, namely that the method yields a dynamically converging quantity that leverages both time and spatial averaging to reduce statistical noise. In fact, the two methods are complementary when viewed from this perspective.

In ensemble averaged LMF theory, the YBG hierarchy was generalized to equation (3.9), which can be rewritten

$$\mathbf{F} - \beta^{-1}\nabla\rho = m\left(\rho\frac{D\mathbf{u}}{Dt} + \nabla \cdot \tilde{\mathbf{P}}\right). \quad (4.4)$$

Here we have defined the material derivative $\frac{D}{Dt} = \frac{\partial}{\partial t} + \mathbf{u} \cdot \nabla$, and used the continuity equation. The left hand side of this equation is the force balance equation, and the right hand side is the non-equilibrium correction. This suggests a similar procedure as in equilibrium, using this equation to solve for ρ as a dynamically evolving field. However, this procedure is complicated by the introduction of new fields out of equilibrium, and it should be clarified exactly how this system should be solved for this method to work, which will be the topic of this section.

First, it is useful to recall that equation (4.4) is related to the Cauchy momentum equation, and therefore the Navier Stokes equation, where the pressure is chosen to reproduce the equilibrium YBG hierarchy equations. This motivates us to approximate the modified pressure tensor $\tilde{\mathbf{P}}$ with a dissipative term

$$\mathbf{F} - \beta^{-1}\nabla\rho = m\rho\frac{D\mathbf{u}}{Dt} - \mu\left(\nabla^2\mathbf{u} + \frac{1}{3}\nabla(\nabla \cdot \mathbf{u})\right), \quad (4.5)$$

where μ is the viscosity of the fluid. For our purposes, μ will be treated as a parameter that helps with the convergence of the approximation. However, the clear physical interpretation might be useful for applications, and the interpretation of results.

For the purposes of LMF theory, it is also important to solve for the smoothed density, or the smooth charge density in the case of electrostatics. For molecular fluids, this is complicated by the fact that these equations do not hold for constrained systems, and therefore will require more theoretical development, which will be pursued in the next subsection.

There is also difficulty with directly convolving equation (4.4) with a Gaussian to find an evolution equation for the Gaussian smoothed density. This will also lead to difficulty with finding the smooth charge density, but that also has other challenges due to the presence of constraints in molecular fluids. The difficulty with Gaussian smoothing arises because some of the terms are quadratic, and the convolution can only be absorbed into one term. For this reason, it is interesting to consider alternative algorithms for propagating the material derivative on a fixed grid. This will also be discussed in later sections.

4.4 Force sampling for constrained systems

As discussed previously, the force balance approach becomes more complicated in the case of molecular fluids. Molecular solvents are generally modeled as constrained systems, where the bond lengths are held fixed. However, the force

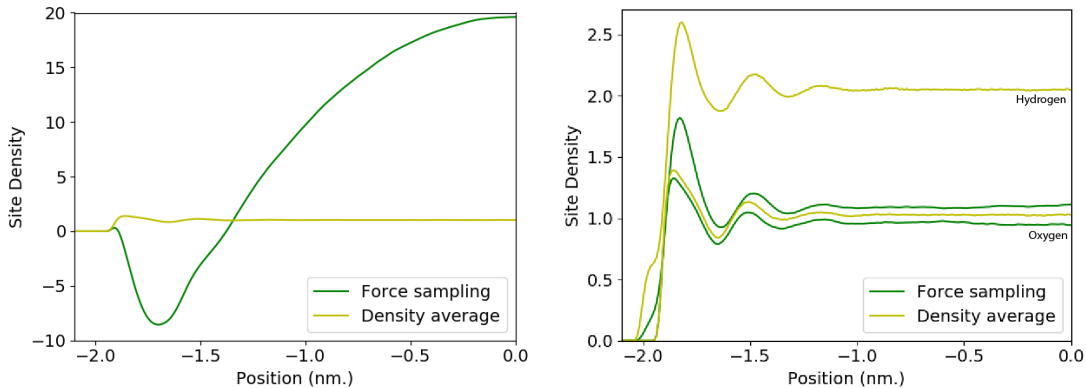


Figure 4.2: Density profiles calculated with the naïve force density approach for a system with constraints in the slab geometry. On the left is shown the oxygen density computed without including the additional constraint forces. On the right the result is shown for both the oxygen and hydrogen densities, including the SHAKE correction. Neither of these approaches gives the correct result.

sampling method no longer works in this case. This is particularly apparent in the slab geometry, the details of which are described in appendix A. The naïve approach to force sampling with constraints would be to try to use (4.2) without any modification. However, even with this approach one encounters a problem, because the forces generally include fictitious forces from the constraints, so there is a question of whether to include this contribution in the force density. The results of these two approaches is shown in the figure 4.2, both of which give incorrect results. It is also notable the difference in scale that arises from including the fictitious forces, which shows how large of a correction the constraints create.

To avoid issues with constraints, one can also consider a flexible model, which results in an unconstrained simulation. For this purpose, we considered the water model introduced by Voth et. al. [45]. In this case, the force sampling method converges extremely slowly, as illustrated in figure 4.3. This is because the harmonic potentials used to impose flexible constraints create very large forces in the simu-

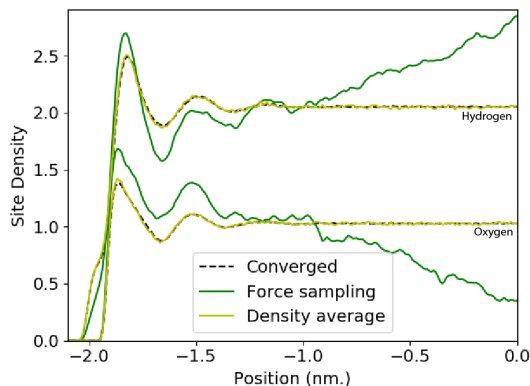


Figure 4.3: Density profile calculated using a flexible water model with 2000 independent samples, averaged over the periodic coordinates in the slab geometry. It is clear that the force sampling curves are very far from convergence, even though the usual method has already converged very well. This illustrates why using a flexible model is not a reasonable solution to the problem.

lation, so the force sampling method is inefficient due to the necessary statistical cancellation of these large forces. It does eventually converge, but the surprisingly slow convergence renders this method very undesirable for the computation of the particle densities. Flexible water models are more computationally intensive as well, so for this reason it is useful to derive a shake correction to the force sampling method. A similar correction was derived recently and independently by Coles et al. [46].

The study of non-Hamiltonian systems have been investigated by a number of researchers, including the original paper by Liouville [47]. More recently, these theories have been formulated in a coordinate invariant way using the theory of Lie groups [48][49][50]. The statistical mechanics of constrained systems, which can be applied to the study of algorithms such as SHAKE and RATTLE, has been investigated more recently [51][52]. Define the phase space of the system with a vector \mathbf{x} , which includes both the momenta \mathbf{p}_i and positions \mathbf{r}_i of the particles in

the system. Consider a system with K holonomic constraints

$$\sigma_\alpha(\mathbf{r}^N) = 0, \quad \alpha = 1, \dots, K. \quad (4.6)$$

For integration over phase space, we also impose the constraints $\dot{\sigma}_\alpha(\mathbf{r}^N, \mathbf{p}^N) = 0$.

For notational simplicity, define $\delta(\sigma) = \prod_\alpha \delta(\sigma_\alpha(\mathbf{r}^N))$, and similarly for $\delta(\dot{\sigma})$. Ciccotti et. al. [52] derived a constrained generalization of the equilibrium canonical ensemble .

$$\mathcal{P}(\mathbf{r}^N, \mathbf{p}^N) = \mathcal{Z}^{-1} N e^{-\beta \mathcal{H}(\mathbf{r}^N, \mathbf{p}^N)} |Z| \delta(\sigma) \delta(\dot{\sigma}), \quad (4.7)$$

where $\mathcal{Z} = \int d\mathbf{x} \mathcal{P}(\mathbf{x})$ is the partition function, and $|Z|$ is the determinant of the matrix

$$Z_{\alpha\beta} = \sum_{i=1}^N \frac{1}{m_i} \frac{\partial \sigma_\alpha}{\partial \mathbf{r}_i} \cdot \frac{\partial \sigma_\beta}{\partial \mathbf{r}_i}. \quad (4.8)$$

To generalize the YBG hierarchy, define the density of a given particle by integrating equation (4.7) over $(N - 1)$ particle positions and all momenta

$$\rho(\mathbf{r}) = \mathcal{Z}^{-1} N \int d^{N-1} \mathbf{r} d^N \mathbf{p} e^{-\beta \mathcal{H}} |Z| \delta(\sigma) \delta(\dot{\sigma}). \quad (4.9)$$

Denoting the fixed particle by the index $i = 1$, we take gradient of this expression to find

$$\nabla_1 \rho(\mathbf{r}_1) = \mathcal{Z}^{-1} N \int d^{N-1} \mathbf{r} d^N \mathbf{p} e^{-\beta \mathcal{H}} \left(-|Z| \delta(\sigma) \delta(\dot{\sigma}) \beta \nabla_1 \mathcal{H} + \nabla_1 (|Z| \delta(\sigma) \delta(\dot{\sigma})) \right). \quad (4.10)$$

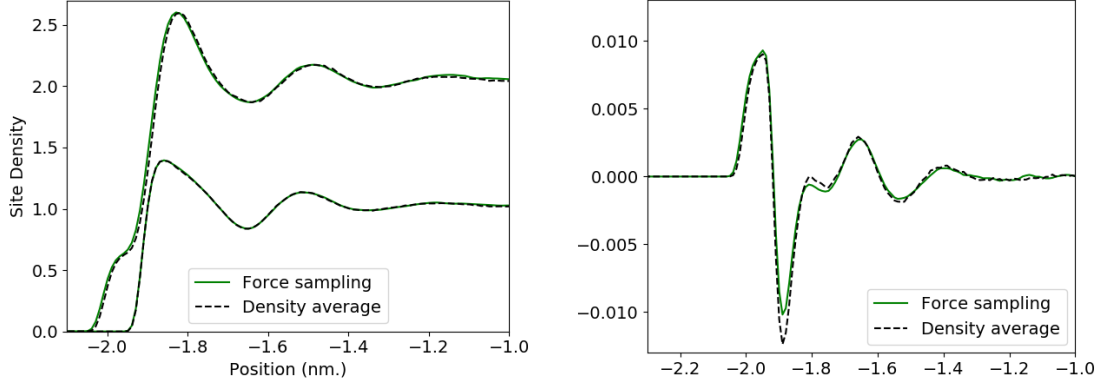


Figure 4.4: Density profile for SPC/E water in the slab geometry using the corrected force sampling method. The right figure shows the charge density.

The first term in this expression will yield terms that are familiar from the YBG hierarchy equation, but the second term is new, and yields a correction due to the constraints in the system.

To simplify equation (4.10) further, we first note that the derivatives of the delta functions are defined through integration by parts, and therefore we should search for a way to integrate those terms by parts. It turns out that this is very straightforward for constraints which are translationally invariant, which is a property that we will assume. This is a natural assumption, because most constraints we will consider depend on distances between particles instead of absolute positions, which are always translationally invariant. For a given particle, define the constrained cluster c_i as the set of particles that are connected to this atom by constraints. For a given constraint cluster c , any constraint σ_α will be invariant under translations of a shake cluster, which mathematically can be written $\sum_{i \in c} \nabla_i \sigma_\alpha = 0$, and readily implies

$$\sum_{i \in c}^N \nabla_i \left(|Z| \delta(\sigma) \delta(\dot{\sigma}) \right) = 0. \quad (4.11)$$

Using this relationship and integrating by parts for the second term in equation (4.10), we find

$$\nabla_1 \rho(\mathbf{r}_1) = -\mathcal{Z}^{-1} N \int d^{N-1} \mathbf{r} d^N \mathbf{p} |Z| \delta(\sigma) \delta(\dot{\sigma}) e^{-\beta \mathcal{H}} \sum_{i \in c} \beta \nabla_i \mathcal{H}, \quad (4.12)$$

where c contains the fixed particle located at \mathbf{r}_1 . We note that in the absence of constraints, all terms vanish besides that with $i = 1$, and so this equation reduces to the usual YBG hierarchy. If we define the cluster force as the total force on a cluster $\mathbf{F}_{c_i} = \sum_{i \in c_i} \mathbf{F}_i$, then equation (4.12) can be rewritten

$$\nabla \rho(\mathbf{r}) = \beta \left\langle \sum_i \mathbf{F}_{c_i} \delta(\mathbf{r} - \mathbf{r}_i) \right\rangle, \quad (4.13)$$

which generalizes the force balance equation (4.2). If one fixes a particle species, then one can restrict this sum to that particular species.

Equation (4.13) is a straightforward generalization of the force balance equation, and is the relevant equation to use when using this method with constrained systems. The results from this implementation are shown in figure 4.4, which show that this method does indeed give the correct results. The fluctuations from using this method, and for other LJ type simulations, will be studied further in the following sections.

In order to understand the convergence properties of the force sampling method we will consider the previous simulations in more depth, in addition to introducing a new set of model systems based on the (n,6) potentials considered by Clarke

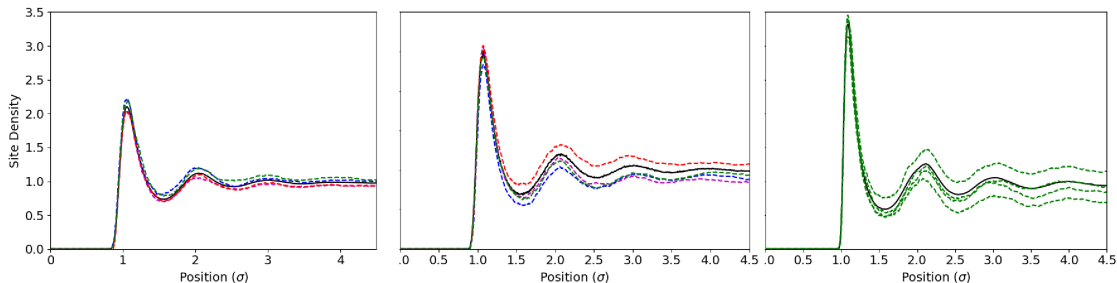


Figure 4.5: Density profiles for $(n,6)$ potentials for $n=8$, $n=12$, and $n=24$ from left to right.

et. al. [53], related to those studied by Stillinger et. al. [54]. To start, we first show the statistical fluctuations that occur in the simulation presented in figure 4.4. Based on this figure, it is clear that the issue of systematic error from the force sampling method is still a problem for molecular solvents, and is arguably worse in this context. Specifically, the charge density varies strongly for small sample sizes, and arguably shows more variation than the density averaging method, which seems to undermine the very reason for considering these methods.

To understand these fluctuations in more detail, and analyze their origins, we consider a series of (n,m) potentials of Lennard-Jones type, taking the form

$$E(r) = \frac{E_0}{n-m} \left[m \left(\frac{r_0}{r} \right)^n - n \left(\frac{r_0}{r} \right)^m \right]. \quad (4.14)$$

The purpose of introducing this potential is to investigate how the hardness of the particle core affects the convergence rate of the force sampling method, and for this reason we will fix $m = 6$ while varying n , keeping the well depth and location of the minimum fixed, which can be achieved by keeping E_0 and r_0 constant. We choose E_0 and r_0 to reproduce the LJ parameters of figure 4.1 for $n = 12$, in particular so

that $\rho^* = .8$ and $T^* = 1.35$.

The results from this analysis are shown in figure 4.5. It is clear from this figure that the softer potentials lead to less fluctuations in the asymptotic density, which is somewhat intuitive.

4.5 Non-equilibrium constrained systems

We will now discuss how to generalize the previous force balance approach to the non-equilibrium situation. We again define the phase space of the system by a set of vectors \mathbf{x}_i , which includes the momenta \mathbf{p}_i and positions \mathbf{r}_i of the particles in the system. The holonomic constraint equations are given by $\sigma_\alpha(\mathbf{r}^N) = 0$, and the particles satisfy a differential equation

$$\dot{\mathbf{x}}_i = \boldsymbol{\xi}_i, \tag{4.15}$$

where $\boldsymbol{\xi}_i(\mathbf{x})$ can be read off from the Hamiltonian equations of motion for a constrained system

$$\dot{\mathbf{r}}_i = \frac{\mathbf{p}_i}{m_i}, \tag{4.16}$$

$$\dot{\mathbf{p}}_i = -\frac{\partial\phi}{\partial\mathbf{r}_i} - \sum_\alpha \lambda_\alpha \frac{\partial\sigma_\alpha}{\partial\mathbf{r}_i}, \tag{4.17}$$

and λ_α are Lagrange multipliers for the Euler-Lagrange equations of type I. An ensemble undergoing these dynamics satisfies the generalized Liouville equation

$$\frac{\partial}{\partial t}(\gamma f) + \sum_i \frac{\partial}{\partial \mathbf{x}_i} \cdot (\boldsymbol{\xi}_i \gamma f) = 0, \quad (4.18)$$

where $f(\Gamma; t)$ is the phase space density, and $\gamma(\Gamma)$ is a metric factor that appears in the constrained dynamics, which is given by the determinant $|Z|$ of the matrix

$$Z_{\alpha\beta} = \sum_{i=1}^N \frac{1}{m_i} \frac{\partial \sigma_\alpha}{\partial \mathbf{r}_i} \cdot \frac{\partial \sigma_\beta}{\partial \mathbf{r}_i}. \quad (4.19)$$

as shown by Ciccotti et. al. [52]. In the case of Hamiltonian dynamics, the metric factor is constant and the divergence $\kappa = \sum_i \frac{\partial}{\partial \mathbf{x}_i} \cdot \boldsymbol{\xi}_i$ vanishes, so this equation reduces to the usual Liouville equation.

We will be interested in deriving a constrained generalization of equation (4.4), which will be useful for the application of non-equilibrium LMF theory to constrained systems, in addition to general theoretical interest. However, there are technical complications that arise due to the constraints, making the derivation more complicated, with less useful results. It turns out that the procedure simplifies if one considers the center of mass of a constrained cluster, which is a collection of particles that is not connected to any other particles through constraints. An important example of a constrained cluster will be a rigid water molecule.

Given the above consideration, we will begin by deriving a constrained generalization of the first of the BBGKY hierarchy equations for the center of mass of

a constrained cluster. Denote the constrained cluster by c , which is a collection of particle indices. The center of mass and momentum of this cluster are defined as usual,

$$\mathbf{r}_c = \frac{1}{M} \sum_{i \in c} m_i \mathbf{r}_i, \quad \mathbf{p}_c = \sum_{i \in c} \mathbf{p}_i, \quad (4.20)$$

where M is the mass of the cluster. These variables will collectively be denoted \mathbf{x}_c . To derive the BBGKY hierarchy equation, we integrate equation (4.18) over the hypersurface in phase space which satisfies the constraints, and with the constrained cluster fixed at coordinate $\mathbf{x}_c = \mathbf{x}$. To do this, define the singular measure

$$d\Gamma_c(\mathbf{x}) = \delta(\mathbf{x} - \mathbf{x}_c) \prod_{\alpha} \delta(\sigma_{\alpha}) \delta(\dot{\sigma}_{\alpha}) \prod_i d\mathbf{x}_i. \quad (4.21)$$

The first BBGKY equation can then be written

$$\int \left(\frac{\partial}{\partial t} (\gamma f) + \sum_i \frac{\partial}{\partial \mathbf{x}_i} \cdot (\boldsymbol{\xi}_i \gamma f) \right) d\Gamma_c(\mathbf{x}) = 0. \quad (4.22)$$

To simplify this equation further, we note that because the constraints are conserved by the dynamics, the delta functions preserving the constraints can be brought inside the derivatives. Furthermore, we can perform an orthogonal transformation on the coordinates so that the center of mass coordinates are phase space variables. With these simplifications, the equation becomes

$$\frac{\partial}{\partial t} f_c(\mathbf{x}; t) + \frac{\partial}{\partial \mathbf{x}} \cdot \int d\Gamma_c(\mathbf{x}) \boldsymbol{\xi}_c \gamma f(\mathbf{x}^N; t) = 0, \quad (4.23)$$

where we have defined $f_c(\mathbf{x}; t) = \int d\Gamma_c(\mathbf{x}) \gamma f(\mathbf{x}^N; t)$. To be more explicit, define the force density $\mathbf{F}_c(\mathbf{x}; t) = \int d\Gamma_c(\mathbf{x}) \dot{\mathbf{p}}_c \gamma f(\mathbf{x}^N; t)$, to find

$$\left(\frac{\partial}{\partial t} + \frac{\mathbf{p}}{M} \cdot \nabla \right) f_c(\mathbf{x}; t) + \frac{\partial}{\partial \mathbf{p}} \cdot \mathbf{F}_c(\mathbf{x}; t) = 0. \quad (4.24)$$

It is now clear how this reduces to the usual BBGKY hierarchy equation in the unconstrained case.

We can now derive the near equilibrium approximation by a similar procedure as before. First integrate equation (4.24) over \mathbf{p}_c to get the continuity equation

$$\frac{\partial}{\partial t} \rho_c(\mathbf{r}; t) = -\nabla \cdot \mathbf{j}_c(\mathbf{r}; t), \quad (4.25)$$

with the natural definitions of ρ_c and \mathbf{j}_c . Multiplying equation (4.24) by \mathbf{p}_c and integrating yields the natural generalization of equation (3.9)

$$\frac{\partial}{\partial t} \mathbf{j}_c + \nabla \cdot (\rho \mathbf{u}_c^T \mathbf{u}_c + \mathbf{P}_c) = \mathbf{F}_c, \quad (4.26)$$

where all the quantities are the natural center of mass generalizations. This is the point where considering the center of mass coordinates is most crucial. For constrained systems, the equilibrium momentum distribution is no longer a Maxwell distribution, but is instead given by the conditional probability density [52]

$$\mathcal{P}_C(\mathbf{p}^N | \mathbf{r}^N) = K e^{-\sum_i \frac{\beta}{2m_i} p_i^2} \prod_{\alpha} \delta(\sigma_{\alpha}), \quad (4.27)$$

where K is a normalization constant. In this expression, the delta functions make the momenta coupled, and therefore the usual Maxwell factor is quite complicated. However, the center of mass coordinates are necessarily unconstrained, because of the definition. Therefore, these variables do not suffer from the complications that arise for the individual coordinates of the particles in each cluster. In particular, the center of mass momentum will have a Maxwell distribution at equilibrium

$$f_M(\mathbf{p}_c) = \frac{\exp(-\beta p_c^2/2M)}{(2\pi M k_B T)^{3/2}}.$$

Given this simplification, we can proceed as before. Define a near equilibrium modified phase space density $\tilde{f}_c(\mathbf{x}; t)$ by the equation

$$f_c(\mathbf{x}; t) = \tilde{f}_c(\mathbf{x}; t) f_M(\mathbf{p}_c). \quad (4.28)$$

With this definition, we find

$$\mathbf{P}_c(\mathbf{r}; t) = \frac{\rho_c(\mathbf{r}; t)}{\beta M} \mathbf{I} + \tilde{\mathbf{P}}_c(\mathbf{r}; t).$$

Using this relationship, we get the natural generalization of equation (4.4)

$$\mathbf{F}_c - \beta^{-1} \nabla \rho_c = m \left(\rho_c \frac{D\mathbf{u}_c}{Dt} + \nabla \cdot \tilde{\mathbf{P}}_c \right). \quad (4.29)$$

A similar approximation will yield a generalization of the modified Navier-Stokes equation (4.5).

These generalizations are natural and convenient. However, one may not only be interested in the center of mass coordinates for constrained clusters. For example, in LMF theory for electrostatics one is generally interested in the expectation value of the smooth charge density, which depends on the precise locations of the charges within a constrained cluster, and not just the center of mass coordinates for that cluster. As stated previously, the relatively simple equations derived above become significantly more complicated for these coordinates, and indeed do not form a closed system of equations, giving them limited value.

An alternative approach is to take expectation values of quantities of interest given that a constrained cluster is fixed at position \mathbf{r} . For LMF theory, the primary example will be the polarization density of a charge neutral constrained cluster

$$\langle \boldsymbol{\mu}_c \rangle_{\mathbf{r}} = \int \boldsymbol{\mu}_c \gamma f d\Gamma_c(\mathbf{x}), \quad (4.30)$$

where we have defined the dipole moment $\boldsymbol{\mu}_c = \sum_{i \in c} q_i \mathbf{r}_i$. To obtain an equation of motion for this quantity, we multiply the Liouville equation (4.18) by $\boldsymbol{\mu}_c$ and integrate over the measure $d\Gamma_c$ to find

$$\int \boldsymbol{\mu}_c \left(\frac{\partial}{\partial t}(\gamma f) + \sum_i \frac{\partial}{\partial \mathbf{x}_i} \cdot (\boldsymbol{\xi}_i^T \gamma f) \right) d\Gamma_c(\mathbf{x}) = 0, \quad (4.31)$$

here we have included a transpose on $\boldsymbol{\mu}_c$ for convenience of notation. It is again possible to bring the constraints inside the derivatives, and to change variables with an orthogonal transformation. We will also want to bring the dipole term inside of

the derivatives, which gives

$$\frac{\partial}{\partial t} \langle \boldsymbol{\mu}_c \rangle_{\mathbf{x}} + M^{-1} \nabla \cdot \langle \mathbf{p}_c^T \boldsymbol{\mu}_c \rangle_{\mathbf{x}} + \frac{\partial}{\partial \mathbf{p}} \cdot \langle \mathbf{F}_c^T \boldsymbol{\mu}_c \rangle_{\mathbf{x}} - \langle \dot{\boldsymbol{\mu}}_c \rangle_{\mathbf{x}} = 0. \quad (4.32)$$

In order to simplify this equation further, it is possible to follow a similar approach as before. Integrating over \mathbf{p} yields a continuity type equation

$$\frac{\partial}{\partial t} \langle \boldsymbol{\mu}_c \rangle_{\mathbf{r}} = -\nabla \cdot \left\langle \frac{\mathbf{p}_c^T}{M} \boldsymbol{\mu}_c \right\rangle_{\mathbf{r}} + \langle \dot{\boldsymbol{\mu}}_c \rangle_{\mathbf{r}}. \quad (4.33)$$

On the right hand side of this equation, the first term is akin to the usual gradient of the flux density, which in this case can be thought of as a dipole flux density. The second term reflects the contribution from the rotation of the molecule. It is also possible to derive a second order equation of this type, but we will leave this for future investigation.

These equations form the basis of an application of the force balance approach to LMF theory. The difficulties with nonlinearities in the equations has made it difficult to implement this in practice, and further research will be required to realize the goal of using force balance approaches in LMF theory. One promising avenue of investigation is to consider the equations of fluctuating hydrodynamics to linearize the equations [55]. This will also be left for future work.

Chapter 5: Stochastic sampling for nonequilibrium LMF theory

5.1 Introduction

The PPPM Ewald algorithm relies on fast Fourier transforms to solve the Poisson equation rapidly [56]. Although this method is fast and robust, there has been some interest in the use of real space solvers such as multi-grid methods to replace it, which could improve both the speed and parallelizability of the calculation. Right now, however, these algorithms are less competitive for the accuracy and system size required of many biological applications [57][58]. The potential advantages, however, make this an interesting avenue for investigation. In this chapter, we argue that a non-equilibrium generalization of LMF theory coupled with a real space solver could lead to improvements in these real space solvers, making them more competitive with PPPM Ewald.

For both real and Fourier space methods, the main bottleneck in computing long range Coulomb forces is the interpolation of the smooth charge density to the grid, and the inverse interpolation required to calculate the resulting force [57]. This issue has an elegant solution within the context of LMF theory, which only requires an average solution to Poisson's equation to define a mimic system with accurate structural behavior. Indeed, in this context it is natural to leverage a separation of

time-scales in the system to interpolate this charge density stochastically, effectively performing a local time average of the statistical fluctuations in the field. As in the original LMF argument, these statistical fluctuations can be safely ignored, assuming that no other degrees of freedom are fast on the time scale of averaging.

This method of interpolation is only possible when an iterative algorithm is used for the solution of Poisson’s equation. For this purpose we introduce a variant of the multigrid method, using a multiple length scale splitting of the Coulomb potential that can be solved on grids with increasingly large spacing. This approach embodies many of the advantages of standard multigrid methods with the added advantage that it is physically meaningful, and leads to a natural set of tools for analyzing the non-equilibrium statistical mechanics of the system. In particular, we investigate the autocorrelation functions for the forces on the different length scales, which gives some guidance on the choice of time scale over which the statistical averaging should occur. We then investigate this method with a series of model systems. As in previous papers, we thoroughly investigate the slab geometry configuration in both equilibrium and non-equilibrium settings.

5.2 Stochastic local molecular field theory

From a practical perspective, it is not always desirable to simulate an ensemble of systems evolving under a time varying external field, especially in systems where the “external field” comes from another slowly varying component of the system. This problem naturally leads to the leveraging of a separation of time scales in a

system to compute a “local time average” of the long range forces in the simulation, which effectively averages over the local fluctuations in the fast components (the solvent), while dynamically capturing the varying field produced by the slow components in the system. This approach to the problem also lends itself to the consideration of practical methods for implementation, and the potential computational advantages that could be gained relative to the more standard PPPM algorithm. These investigations are what led to the Stochastic Local Molecular Field (SLMF) approach to the computation of the long range Coulomb forces.

The SLMF approach consists of two main ideas, which are complementary. The first idea is the stochastic interpolation of the smooth charge density to the grid, which is arguably the most important aspect in terms of computational saving. The second aspect is a modification of the multigrid approach to the solution of Poisson’s equation, which gives a more physical picture for the multigrid method, and is more amenable to the techniques of statistical mechanics. Even without the added savings proposed here, multigrid methods are some of the fastest methods for biomolecular simulations, and have already attracted attention for computational savings versus Ewald methods [59]. An iterative relaxation Poisson solver is necessary to make the stochastic interpolation work, so these two ideas are well suited as a combined whole.

Stochastic interpolation is a way to approximately compute the smoothed charge density without calculating the contribution on every grid point. To illustrate

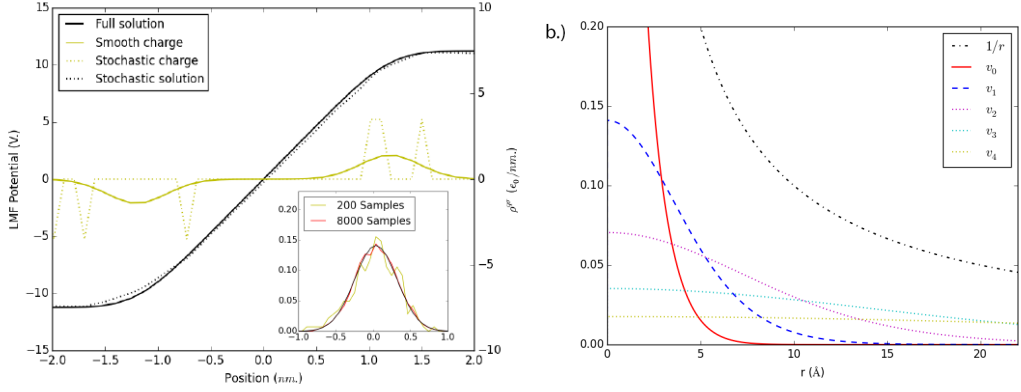


Figure 5.1: Illustration of some of the important concepts behind the SLMF method. In (a) the asymptotic solution to the inhomogeneous heat equation sourced by a stochastic charge density is shown, with an example of Gaussian convolution shown in the inset for two sample sizes. In (b) the splitting of the Coulomb force defined in equation (5.3) is shown for $\sigma_0 = 4\text{\AA}$ and each successive σ multiplied by two.

this idea, consider Poisson's equation for the smooth charge density

$$\vec{\nabla}^2 V(\mathbf{r}) = -\frac{4\pi}{\epsilon} \rho_{tot}^{q\sigma}(\mathbf{r}), \quad (5.1)$$

where $\rho_{tot}^{q\sigma}(\mathbf{r})$ denotes the smooth charge density. By the associativity of convolution, this equation is the relevant equation for both Ewald summation and the LMF equation. The smooth charge density is the convolution $\rho_{tot}^q \star \rho_G(\mathbf{r}; \sigma)$, which is interpolated to a mesh, representing one of the largest computational bottlenecks in the Ewald algorithm. To compute this stochastically, one can sample from a Gaussian distribution centered at each charge in the simulation, adding an appropriately weighted charge for each sample. As the number of samples goes to infinity, this will approach the desired Gaussian convolution, as illustrated in the inset of figure 5.1a.

This stochastic interpolation is not exact, and introduces significant error for

small sample sizes. To effectively average over some of this noise in time, we will consider Poisson's equation as the asymptotic solution of the inhomogeneous heat equation

$$\frac{\partial}{\partial t}V(\mathbf{r}, t) = \alpha \left(\vec{\nabla}^2 V(\mathbf{r}, t) + \frac{4\pi}{\epsilon} \rho_{tot}^{q\sigma}(\mathbf{r}) \right), \quad (5.2)$$

where here $\rho_{tot}^{q\sigma}(\mathbf{r})$ is treated as fixed in time, and α is akin to the thermal diffusivity. We can now compute the convolution $\rho_{tot}^q \star \rho_G(\mathbf{r}; \sigma)$ stochastically in time, and the heat equation will effectively average over the noise in time. For α relatively small, even a small number of samples per unit time for the stochastic convolution will lead to accurate asymptotic behavior for $V(\mathbf{r}, t)$. This behavior is shown for a simple one dimensional example with two charges in the supplementary material, a snapshot of which is shown in figure 5.1a. The heat equation is the simplest example of an iterative Poisson solver, and in fact these ideas can be generalized to many other iterative Poisson solvers, such as a multigrid method, or the multiscale approach described below.

The multiscale method introduced here is inspired by the multigrid approach to solving differential equations. The first step in defining this method is to split the Coulomb potential into a series of potentials that are slowly varying on different length scales. These splittings are a natural generalization of the splitting (2.10), and can be written

$$\frac{1}{r} = \sum_{i=0}^n v_i(r), \quad (5.3)$$

where v_i is defined as

$$v_i(r) = \frac{\text{erf}(r/\sigma_i) - \text{erf}(r/\sigma_{i+1})}{r}, \quad (5.4)$$

for some increasing sequence of positive numbers σ_i , and where $\sigma_0 = 0$ and $\sigma_{n+1} = \infty$, so that $v_0(r) = \frac{1 - \text{erf}(r/\sigma_1)}{r}$ and $v_n(r) = \frac{\text{erf}(r/\sigma_n)}{r}$. These potentials come from the difference of two Gaussian charge densities, and form a telescoping series. From a mathematical perspective, it is interesting to take the continuum limit where σ_i and σ_{i+1} become infinitely close together, which leads to an integral transform

$$\frac{1}{r} = \frac{2}{\sqrt{\pi}} \int_0^\infty \frac{e^{-r^2/\sigma^2}}{\sigma^2} d\sigma. \quad (5.5)$$

Equation (5.3) can then be recovered by splitting this integral into pieces defined by the sequence of numbers σ_i .

An example of the potentials resulting from this procedure is shown in figure 5.1b. Here the splitting is defined by $\sigma_0 = 4 \text{ \AA}$ and $\sigma_i = 2^i \sigma_0$. This splitting leads to a generalized multigrid method, by solving for each potential on a different grid, with increasingly large grid spacing. In this case, the length scale is increased by two on every successive potential, so naturally the grid spacing of each grid would also increase by two. The goal is to then solve Poisson's equation for the smooth charge density on each grid

$$\vec{\nabla}^2 V_i(\mathbf{r}) = -\frac{4\pi}{\epsilon} \left(\rho_{tot}^{q\sigma_i}(\mathbf{r}) - \rho_{tot}^{q\sigma_{i+1}}(\mathbf{r}) \right), \quad (5.6)$$

where the total force from the Coulomb potential is then given by the sum $V_{tot} = \sum_i V_i$. As in the case with multigrid, the motivation for the increased grid spacing is that iterative Poisson solvers are only efficient for length scales that are comparable

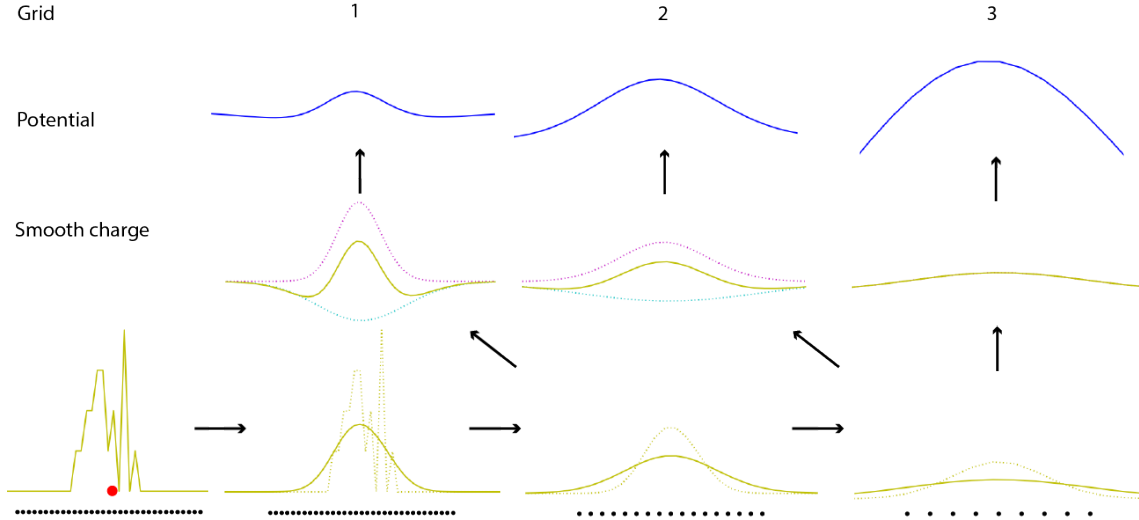


Figure 5.2: Illustration of the SLMF method for a one dimensional system. The horizontal arrows correspond to charge spreading through Gaussian convolution, the diagonal arrows correspond to subtracting the resulting spread density, and the vertical arrows correspond to solving Poisson’s equation. In practice the solution of Poisson’s equation is iterative, but for the purposes of illustration it is shown as a single step. The grid spacing is shown at the bottom of each column.

to the grid spacing, and converge very slowly for longer length scales [60]. This method ensures that each grid is in some sense suited for the potential it is solving for. For the SLMF method, only the initial smooth charge density is computed stochastically, and each successive one is computed through convolution on the grid, which can be performed very quickly using either a diffusion equation approach [61], or a series of one dimensional convolutions in each dimension [57]. Also, as done in the Gauss split method [57], we will include an initial smoothing step as well, to improve the initial Gaussian convolution.

With these ingredients, the overall SLMF method can be described as follows:

1. Stochastically interpolate the charges in the simulation to the first grid, using an initial smoothing length σ_{init} .

2. Convolve with a Gaussian of width $\sqrt{\sigma_0^2 - \sigma_{init}^2}$ to obtain an approximation of the smooth charge density $\rho_{tot}^{q\sigma_0}(\mathbf{r})$.
3. Interpolate this smooth charge density to the next (coarser) grid, and convolve with another Gaussian to approximately obtain $\rho_{tot}^{q\sigma_1}(\mathbf{r})$, then subtract this Gaussian from the original charge density on the first grid, requiring an additional reverse interpolation.
4. Continue this procedure until all charge densities are computed according to equation (5.6), and then iterate the Poisson solver on each grid.

This procedure is illustrated graphically in figure 5.2 for a one dimensional system. We note that the potentials created for this system are very different from those shown in figure 5.1b because the one dimensional Green's function is $-\text{abs}(r)/2$ instead of $(4\pi r)^{-1}$, where we use the Green's function for Poisson's equation. This illustration only shows one timestep of the procedure, but this procedure would be iterated at every time step.

Although this method seems complicated at first glance, each step in this method corresponds to a fast computational algorithm, and these algorithms are performed on increasingly coarse grids, which improves computational efficiency. Furthermore, the initial use of stochastic convolution should lead to a relatively large overall speedup in computation time.

5.3 Dielectric response

To understand the ideas behind the SLMF method in more depth, we will apply the theory of dielectric response, following Bopp et. al. [38] and Netz et. al. [39]. For small perturbations, the response of a medium to an electric field takes a linear form

$$P_\alpha(\mathbf{r}, t) = \frac{1}{4\pi} \int_V \int_{-\infty}^t d\mathbf{r}' dt' \chi_{\alpha\beta}(\mathbf{r}, \mathbf{r}', t - t') D_\beta(\mathbf{r}', t'), \quad (5.7)$$

where \mathbf{P} is the polarization of the medium, \mathbf{D} is the electric displacement field, and $\chi_{\alpha\beta}$ is the dielectric response tensor. In a homogeneous medium, $\chi_{\alpha\beta}(\mathbf{r}, \mathbf{r}', t - t')$ depends only on the relative distance $\mathbf{r} - \mathbf{r}'$. In addition, for isotropic, nonmagnetic, quasi-static fluids, only the longitudinal part of the response tensor need be considered, $\tilde{\chi}(\mathbf{k}, \omega) = \frac{k_\alpha k_\beta}{k^2} \tilde{\chi}_{\alpha\beta}(\mathbf{k}, \omega)$, where we have taken a Fourier transform in space and time. In this context, the fluctuation dissipation theorem relates the imaginary part of the response function to the dynamic structure factor by

$$\text{Im}\{\chi(\mathbf{k}, \omega)\} = 2\pi\beta\omega S(k, \omega), \quad (5.8)$$

where the dynamic structure factor can be written

$$\begin{aligned} S(k, \omega) &= \frac{k_\alpha k_\beta}{k^2} \int_V \int_{-\infty}^{\infty} d\mathbf{r} dt \langle P_\alpha(\mathbf{r}, t) P_\beta(\mathbf{0}, 0) \rangle e^{-i(\mathbf{k}\mathbf{r} - \omega t)} \\ &= \frac{2\pi\beta\omega}{k^2} \langle \rho_b(\mathbf{k}, \omega) \rho_b^*(\mathbf{k}, \omega) \rangle, \end{aligned} \quad (5.9)$$

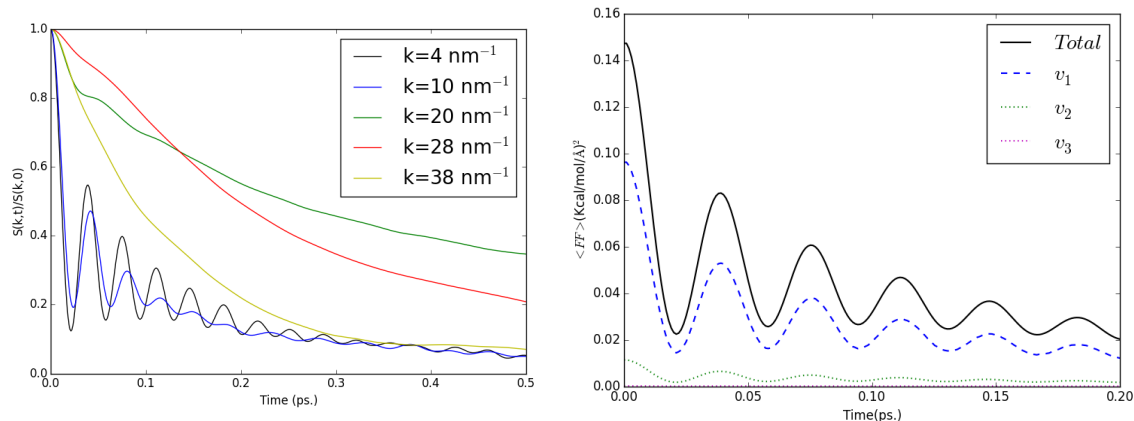


Figure 5.3: Relevant autocorrelation functions for the study of the SLMF method, shown for bulk water evolving under Ewald forces. In (a) the normalized charge-charge autocorrelation function is shown as a function of wave vector, and (b) shows the force-force autocorrelation function for the forces defined by the V_i in the previous section.

and ρ_b is the bound charge density. The charge-charge autocorrelation functions have been studied for multiple water models in different contexts[39]. In addition to the charge-charge autocorrelation function, we will also consider the force-force autocorrelation function, which is related to the friction coefficient [62]. In our case, we will consider the function

$$D_i(t) = \langle F_i(\mathbf{r}, t_0) \cdot F_i(\mathbf{r}, t_0 + t) \rangle, \quad (5.10)$$

where $F_i(\mathbf{r}, t)$ is the force from the potential $V_i(\mathbf{r}, t)$. We will study these functions for bulk water, and so these averages should be independent of the initial time t_0 .

These charge-charge and force-force autocorrelation functions are shown in figure 5.3. The oscillations at low frequencies, and for the long range forces, are attributed to the librational modes of the water molecules [39]. These librational

modes represent the fastest time scales of the solvent dynamics, and are responsible for the rapid relaxation of the solvent to equilibrium. Much of these rapid movements, however, happen on short length scales, and are not significantly affected by the long range forces in the system. The basic idea behind LMF theory, and by extension the SLMF method, is to average out these rapid fluctuations in the long range forces while retaining the physically important short range interactions. In the non-equilibrium ensemble LMF theory investigated previously, this approximation is rigorously valid in a large variety of systems. For SLMF theory, this approximation becomes more complicated because of the need for local time averaging, as opposed to ensemble averaging, requires a separation of time scales between the solvent dynamics and any other degrees of freedom in the system. This will be discussed in the context of bulk water autocorrelation functions, in addition to explicit nonequilibrium systems in the next section.

To get some intuition for how the SLMF method changes the dynamics, we will study the autocorrelation functions defined above using the SLMF approximation. There are many parameters that need to be chosen correctly in order for this method to work, which are outlined below

- The smoothing length σ_0 must be chosen to include the physically important short range interactions in the system. For water, we have found that the dynamics are qualitatively incorrect for $\sigma_0 < 4.5\text{\AA}$, which is consistent with previous results on equilibrium LMF theory.
- The number of stochastically generated samples per charge, N_s , should be

optimized relative to the initial smoothing length σ_{init} and the relaxation rate of the Poisson solver. The effect of changing this parameter at fixed relaxation rate will be investigated.

- The rate of relaxation of the Poisson solver is determined by the number of iterations performed on each grid for each time step, and the relaxation rate of one iterative sweep. In the case of the SOR multiscale Poisson solver considered in this paper, the relevant parameters are the relaxation factors ω_i , and the number of iterative sweeps n_i . The choice of these parameters will be optimized according to the separation of time scales present in the system.
- The grid spacing of the system is chosen to minimize computation time while retaining the desired level of accuracy for the forces. This is analogous to the choice of k_{max} for Ewald simulations, and is also a parameter present in any real space Poisson solver.

In this section, we will focus on the effect of the parameters N_s and ω_i on the dynamics, because the other parameters have analogues in Ewald calculations, and are thus well understood. In this section, σ_0 is held at 4 Å, because for bulk water this value still retains the structure, even though it fails for inhomogeneous simulations. The value of σ_{init} is chosen to be 2 Å, and the smallest grid spacing is 1 Å. The number of iterations per timestep n_i is chosen to be one for each grid, so that the rate of relaxation is determined solely by ω_i . The ratio between successive grid spacings is again chosen to be two.

The parameters ω_i and N_s are in some sense complementary to each other.

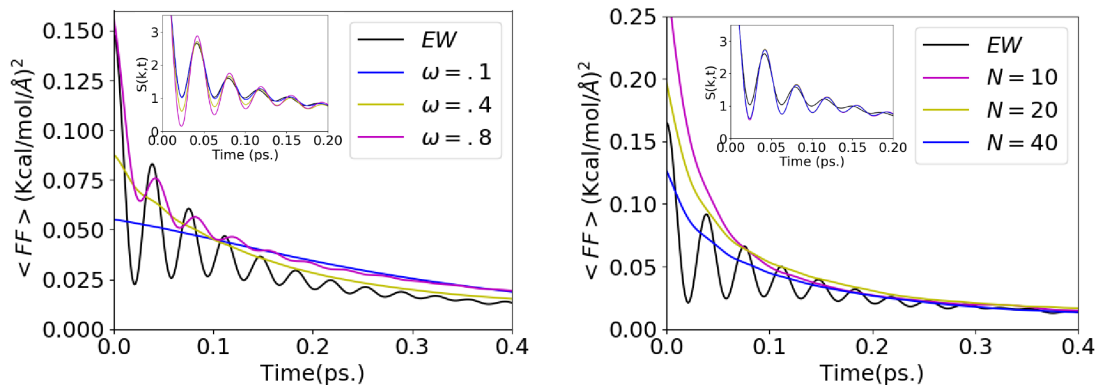


Figure 5.4: Illustration of the effect of the parameters ω and N_s on the force-force and charge-charge autocorrelation functions. In figure a, the parameter ω is varied for $N_s = 100$, and in b the value of N_s is varied for $\omega = .4$. In both figures, the force-force autocorrelation function is shown for the total long range force, and the inset shows the charge-charge autocorrelation function for $k = 10nm^{-1}$.

Intuitively, this comes about because the longer it takes for the Poisson solver to relax to the correct solution, the more statistical fluctuations it averages over as a function of time. If a large separation of time scales exists in the system, then a smaller value of ω_i can be chosen, resulting in slower relaxation. In turn, this allows for a lower value of N_s , because more statistics can be gathered in a larger amount of time. This lower value of N_s is the main source of computational saving from the algorithm, and is therefore how the algorithm takes advantage of a separation of time scales to speed up the simulation.

To begin, we consider the effect of varying ω_i while fixing the value of N_s at a relatively high value of 100, in order to avoid any complications due to inadequate statistics. These results are shown in figure 5.4a. For simplicity, the value of ω_i is held constant for each grid. The SOR method is known to converge for values of ω between 0 and 2, with larger values generally leading to higher rates of convergence.

From the figure, the effects of this slow convergence is clear. The slow dynamics effectively averages over the librational modes in the system, leading to a slower response to time dependent perturbations in the system. Surprisingly, the charge-charge autocorrelation function shows larger oscillations for larger values of ω , which requires more analysis to be understood. This is the parameter that determines how quickly the field will respond to the slow dynamics in the system, and must thus be chosen based on the separation of time scales present in the system, as will be illustrated with some specific examples.

In figure 5.4b, the effect of N_s is considered at fixed $\omega = .4$. It is clear from the force-force autocorrelation function that the values get closer to a smoothed version of the Ewald curve as N_s increases, eventually converging. We interpret this to mean that for fixed ω , a certain minimum number of samples must be collected at each time step in order to obtain enough statistics to get an accurate estimation of the charge density. Once the correct amount of statistics has been achieved, there is no large improvement from increasing the value of N_s , which is why the curve eventually converges. As discussed previously, the minimum value of N_s should increase with the rate of convergence, and therefore slow dynamics should require a lower value of N_s , improving the computational speed. The effect of N_s on the charge-charge autocorrelation function, however, does not seem to be very large.

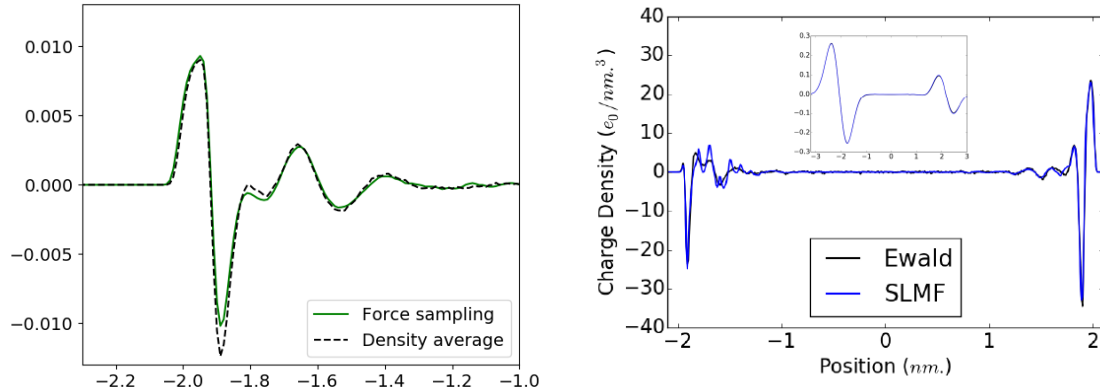


Figure 5.5: Comparison of SLMF results against Ewald summation for equilibrium simulations in the slab geometry. Figure (a.) shows the charge density in the absence of an applied field, and (b.) shows the charge density in the presence of a static field of $10 V/nm.$. The insets show the smooth charge densities.

5.4 Slab geometry

We will now apply this method to the study of the slab geometry, which is a model system that has been important for the study of LMF theory. To begin, we will consider an equilibrium system subject to a static electric field, in order to ensure that the method works in equilibrium. In this section, σ_0 will be chosen to be $.45 nm.$, because lower values do not adequately capture the short range physics, and lead to incorrect results. For the equilibrium simulations, ω will be $.4$ for four grids, with one iteration per timestep.

The results of the equilibrium simulation are shown in figure 5.5. It is clear that the equilibrium charge density does not agree completely with the charge density of the Ewald simulation, but is very close. Furthermore, the smooth charge densities agree very well, which is likely because of the general theory behind the LMF approximation. This suggests that the SLMF approximation is not quite as

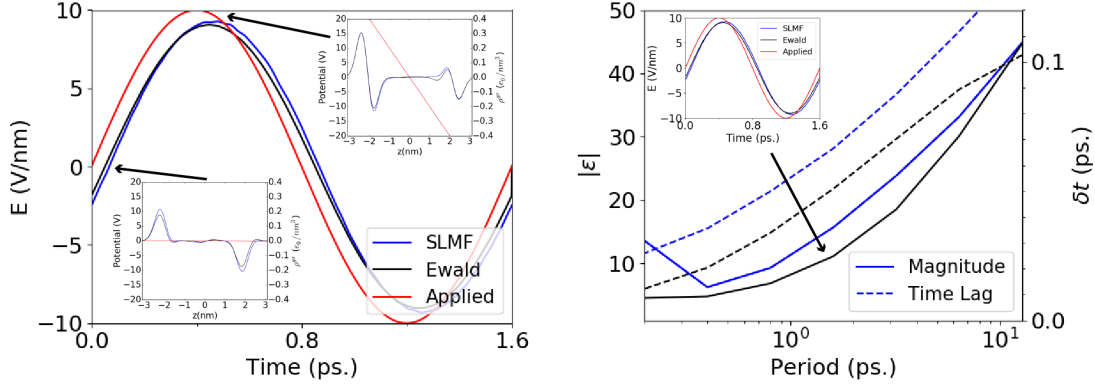


Figure 5.6: Comparison of SLMF results against Ewald summation for the slab geometry in a sinusoidally oscillating field. Figure (a.) shows slope of the response field as a function of time for an applied field with period 1600 fs., and (b.) shows the complex dielectric constant as a function of period.

good as the equilibrium LMF approximation, but is more practical for implementation in many cases of interest.

In addition to the equilibrium case, we tested the SLMF method for a time varying field. To this end, a simulation was performed in the presence of a spatially uniform field varying sinusoidally in time. The applied field has a magnitude of 10 V/nm. , and a varying period. In this case, in order for the response field to respond more quickly to the applied field, the value of ω was increased for the larger grid spacings. This is because the larger grids are sourced by a charge density that is increasingly smoothed, and so are less sensitive to the noise introduced by the stochastic convolution. For this reason, the longer wavelengths will converge faster, which is necessary in the nonequilibrium setting.

For a sinusoidally varying field, the static dielectric response shows a time lag due to the finite time it takes for the dielectric medium to respond to the changing field. This can be expressed using a complex dielectric function, where

the magnitude determines the ratio of the amplitudes of the displacement field and total electric field, and the phase determines the temporal offset of the two fields. This function is defined by the equation

$$D_0 e^{i\omega(t-\delta t)} = |\varepsilon(\omega)| E_0 e^{i\omega t}, \quad (5.11)$$

where we have split the complex dielectric constant into a phase, given by the time offset, and a magnitude.

These two quantities are plotted in figure 5.6. From this figure, it is clear that SLMF does not reproduce the Ewald results exactly, but is very close. This is to be expected due to the local time averaging. It is also clear that the approximation breaks down at small periods, where there is a large divergence between the Ewald and SLMF results. This corroborates the intuition that the local time averaging relies on a separation of time scales in order to achieve accurate results, because if the frequency is too high then the SLMF dynamics do not have time to respond to the change in the field. Also, it is clear that the time offset shows a consistent difference for all frequencies of approximately 20 *fs.*, which we interpret as the approximate response time of the local time averaging. For applications, it will be important to tailor the values of ω_i to the time scales relevant for the simulation being performed.

5.5 Conclusion

In this chapter we have developed a separate approach to non equilibrium LMF theory that goes deeper into the algorithmic side of the long range Poisson solvers. These practical considerations could be combined with the force sampling method developed in the previous section to create a very competitive implementation of LMF theory that would provide significant computational savings relative to the PPPM Ewald algorithm.

To study this method, we considered the theory of dielectric response, and used it to probe the response functions for the simulations evolving under different variants of SLMF Ewald. This was used to probe the relevant ranges where the parameters would be accurate enough to reproduce the results of Ewald summation. Also, these techniques help yield some insight into the underlying dynamics of the method. In principle, this type of analysis could be applied to any statistical alternative to Ewald summation. Finally, the method was applied to the slab geometry.

Chapter 6: Approximate thermofield dynamics of interacting fermions

6.1 Introduction

This chapter is devoted to a new idea related to quantum chemistry and density functional theory. Although it is not directly related to LMF theory, it is similar in spirit and deals with related problems. In particular, many body quantum physics is in many ways complementary to the study of classical statistical systems, and therefore forms a useful class of problems to investigate, in order to lead to greater understanding of statistical physics as a whole. For large systems, the intractable complexity of an exact solution to the many body problem is well known[63], specifically for systems of interacting fermions, which suffer from the so-called sign problem[64]. There are many approaches to finding approximate solutions in different contexts, and for a variety of systems[65][66]. In condensed matter theory, an important general strategy is to search for an effective description of the interacting theory in terms of weakly interacting quasi-particles[67][68]. This approach has had success for a large variety of systems, including superconductors[69], low temperature liquids[70], crystal lattices[71] and plasmas[72]. There are also important examples of strongly correlated systems that are not as amenable to a description in terms of quasi-particles, for which a variety of techniques are be-

ing actively investigated, and have led to some exciting new approaches to the problem[73][74][75].

In the field of quantum chemistry, there are a number of computational approaches with a long history[76][77], generally leading to a tradeoff between accuracy and scalability. Density functional theory (DFT) is perhaps the most scalable method for large systems of interacting particles, and gives high accuracy in many cases[78][79]. However, DFT must approximate the exchange-correlation energy of the system, which is generally uncontrolled and difficult to quantify, and is known to give inaccurate results for a number of systems[80]. Ab initio methods are generally more accurate and complete descriptions of the system[81][82], but are usually too computationally expensive for large numbers of particles. In particular, the coupled cluster method is one of the most scalable ab initio techniques[83], and is similar in form to the approach taken in this paper. A set of alternative approaches known collectively as Quantum Monte Carlo methods are generally more scalable than ab initio methods but less than DFT, thus allowing for more accurate calculations for reasonably large systems [84][85][86].

Here we introduce a technique that is an amalgamation of some of the approaches discussed above, but does not fit neatly into any individual category. Our method will use the thermofield formalism, which is an equivalent alternative to the usual density matrix description of quantum statistical ensembles[87][88]. We first show that in a non-interacting theory, the equilibrium in a grand canonical ensemble always takes the form of a thermal coherent state, which is closely related to the usual definition of a Fermionic coherent state. We then introduce a general

expansion whose first term is this coherent state, and formally solve this expansion in terms of solutions of the many-body Schrodinger equation. The expansion converges poorly for an interacting system, but the introduction of a transformed basis allows for weak effective interactions, in addition to exponential suppression of the excited states at low temperatures. This leads to the possibility of a rapidly converging series if the basis is chosen well, and we develop a method for dynamically optimizing the basis by cooling the system from infinite temperature, using the imaginary time formalism[89].

Our approach is similar in spirit to the coupled cluster method, expanding the wavefunction as an operator exponential which is formally equivalent to a cumulant expansion[90]. However, the use of the thermofield formalism makes all of the operators in the exponential commute, which is a useful simplification. Additionally, this approach is inherently intended for thermal ensembles, incorporating some of the advantages of quantum Monte Carlo techniques, in addition to providing a more general class of calculations than usually possible for ground state methods.

The method is then applied by truncating the series at the first term, and allowing unitary transformations that mix the two Hilbert spaces, bearing some resemblance to the Hartree-Fock-Bogoliubov method[91]. It is shown that the symmetries of the problem allow for the choice of a linear combination of operators in the thermofield double, for which the wavefunction is the vacuum of the system. This leads to simplifications in the calculation, from which an explicit set of differential equations for the dynamics is derived. In the last section, we apply the results to the homogeneous electron gas, deriving a generalization of a familiar result from

the Hartree-Fock analysis of this problem. This technique can be generalized in a number of ways, providing an interesting avenue for future investigation.

6.2 Thermal coherent states

We will begin by reviewing the thermofield formalism, which will be used to define a thermal coherent state. We will then show that these states arise naturally as the equilibrium configuration for a non-interacting system in the grand canonical ensemble.

Thermofield theory is a way of describing mixed states that is different from the density matrix formalism, but yields equivalent results. Consider a quantum mechanical system defined on a Hilbert space \mathfrak{H} with a fixed number of particles N , and Hamiltonian \hat{H} at temperature $T = k_B/\beta$. The density matrix for the equilibrium configuration of this system is given by

$$\hat{\rho}_\beta = \frac{1}{Z} e^{-\beta \hat{H}}, \quad (6.1)$$

where Z is the partition function for this system. Operator expectation values in this ensemble are given by

$$\langle \mathcal{O} \rangle_\beta = \text{Tr}(\mathcal{O} \hat{\rho}_\beta). \quad (6.2)$$

In the thermofield formalism, one introduces a fictitious system that includes two copies of the initial Hilbert space $\mathfrak{H}_{tf} = \mathfrak{H}_1 \otimes \mathfrak{H}_2$, called the thermofield double. Operators acting in the first system are of the form $\mathcal{A}_1 \otimes I_2$ and will be referred

to as \mathcal{A}_1 , and on the second Hilbert space are defined by the Hermitian conjugate, $\mathcal{A}_2 \equiv I_1 \otimes \mathcal{A}_2^\dagger$. In the energy eigenbasis, we can define the entangled state

$$|\psi_\beta\rangle = \frac{1}{Z^{\frac{1}{2}}} \sum_i e^{-\frac{1}{2}\beta E_i} |E_i, E_i\rangle, \quad (6.3)$$

where the state $|E_i, E_j\rangle$ is an energy eigenvector with eigenvalue E_i and E_j in the separate Hilbert spaces. A short calculation shows that the operator expectation value in equation (6.2) is given by

$$\langle \mathcal{O} \rangle_\beta = \langle \psi_\beta | \mathcal{O}_1 | \psi_\beta \rangle, \quad (6.4)$$

which shows the equivalence of this formalism with the usual density matrix approach[87].

We now restrict ourselves to a system of fermions in the grand canonical ensemble, with chemical potential μ . In this case, the Hilbert space \mathfrak{H} includes states with an arbitrary number of particles, and the relevant density matrix is given by

$$\hat{\rho}_{\mu,\beta} = \frac{1}{\mathcal{Z}} e^{-\beta(\hat{H} - \mu\hat{N})}, \quad (6.5)$$

where \mathcal{Z} is the grand partition function. The expectation value of an operator in this ensemble is again given by $\text{Tr}(\mathcal{O}\hat{\rho}_{\mu,\beta})$. Let us introduce a complete set of creation operators \hat{a}_α^\dagger acting on \mathfrak{H}_1 that satisfy canonical anti-commutation relations

$$\{\hat{a}_\alpha, \hat{a}_\beta^\dagger\} = \delta_{\alpha\beta}, \quad \{\hat{a}_\alpha, \hat{a}_\beta\} = 0, \quad \{\hat{a}_\alpha^\dagger, \hat{a}_\beta^\dagger\} = 0. \quad (6.6)$$

We also introduce a set of corresponding creation operators \hat{b}_α acting on \mathfrak{H}_2 , where Hermitian conjugation is included, switching the notation for creation and annihilation operators. Define the state

$$|\psi_{\mu,\beta}\rangle = \frac{1}{\mathcal{Z}^{\frac{1}{2}}} e^{-\frac{1}{2}\beta(\hat{H}_1 - \mu\hat{N}_1)} e^{\sum_\alpha \hat{a}_\alpha^\dagger \hat{b}_\alpha} |0\rangle, \quad (6.7)$$

where $|0\rangle$ is the vacuum of the full Hilbert space, and \hat{N} is the number operator. For an observable \mathcal{O}_1 that commutes with all operators \hat{b}_α , we find the relation

$$\langle \mathcal{O} \rangle_{\mu,\beta} = \langle \psi_{\mu,\beta} | \mathcal{O}_1 | \psi_{\mu,\beta} \rangle, \quad (6.8)$$

which shows that the state (6.7) is the equivalent of (6.3) for the grand canonical ensemble.

There is a close analogy between equation (6.8) and the Grassmann resolution of the identity used in Fermionic path integrals[68][92]

$$I = \int \prod_\alpha d\xi_\alpha^* d\xi_\alpha e^{\sum_\alpha \xi_\alpha \xi_\alpha^*} |\xi\rangle \langle \xi|, \quad (6.9)$$

where $|\xi\rangle$ is a Fermionic coherent state

$$|\xi\rangle = e^{\sum_\alpha \hat{a}_\alpha^\dagger \xi_\alpha} |0\rangle. \quad (6.10)$$

First we note that equation (6.5) can be written in the form

$$\hat{\rho}_{\mu,\beta} = \frac{1}{\mathcal{Z}} e^{-\frac{1}{2}\beta(\hat{H}-\mu\hat{N})} I e^{-\frac{1}{2}\beta(\hat{H}-\mu\hat{N})}. \quad (6.11)$$

Inserting the resolution of the identity (6.9) into this expression, and taking an operator expectation value yields an inner product with the Grassmann valued wavefunction

$$|\tilde{\psi}_{\mu,\beta}\rangle = \frac{1}{\mathcal{Z}^{\frac{1}{2}}} e^{-\frac{1}{2}\beta(\hat{H}-\mu\hat{N})} e^{\sum_{\alpha} \hat{a}_{\alpha}^{\dagger} \xi_{\alpha}} |0\rangle, \quad (6.12)$$

where the inner product includes the Grassmann integrals. This state is manifestly similar to equation (6.7), with the Grassmann numbers ξ_{α} replacing the operators \hat{b}_{α} . In this case, the Grassmann integrals in equation (6.9) impose similar delta functions to the canonical anti-commutation relations of the operators \hat{b}_{α} , and one can readily verify that they yield the same results.

This analogy motivates us to define a thermal coherent state

$$|b\rangle = e^{\sum_{\alpha} \hat{a}_{\alpha}^{\dagger} \hat{b}_{\alpha}} |0\rangle, \quad (6.13)$$

which satisfies the formal eigenvalue equation

$$\hat{a}_{\alpha} |b\rangle = \hat{b}_{\alpha} |b\rangle. \quad (6.14)$$

Let us consider how the state (6.7) evolves in imaginary time $\tau = \frac{1}{2}\beta$ for a non-

interacting Hamiltonian

$$\hat{H}^{(0)} = \sum_{\alpha\beta} H_{\alpha\beta}^{(0)} \hat{a}_\alpha^\dagger \hat{a}_\beta, \quad (6.15)$$

where we will set $\hbar = 1$. Assume that the state is of the form (6.13) at time τ , and consider an infinitesimal evolution of the system to time $\tau + \delta\tau$, where the operators $\hat{b}_\alpha(\tau)$ are now taken to be time dependent. Acting with an annihilation operator, we find

$$\hat{a}_\alpha |b(\tau + \delta\tau)\rangle = \left(\hat{b}_\alpha(\tau) - \delta\tau \left[\hat{a}_\alpha, (\hat{H}^{(0)} - \mu\hat{N}) \right] \right) |b(\tau + \delta\tau)\rangle + O(\delta\tau^2). \quad (6.16)$$

Because the Hamiltonian is non-interacting, the commutator gives only annihilation operators, which also yield eigenvalues up to order $(\delta\tau)^2$. So we see that the state remains in a coherent state whose eigenvalues satisfy the differential equation

$$\partial_\tau \hat{b}_\alpha(\tau) = \mu \hat{b}_\alpha(\tau) - \sum_\beta H_{\alpha\beta}^{(0)} \hat{b}_\beta(\tau). \quad (6.17)$$

This shows that in a non-interacting system, the thermal wave function in the grand canonical ensemble (6.7) is given by a thermal coherent state whose eigenvalues satisfy the above differential equation.

Let us choose the operators \hat{a}_α^\dagger to be eigenfunctions of the non-interacting Hamiltonian

$$[\hat{H}^{(0)}, \hat{a}_\alpha^\dagger] = E_\alpha^0 \hat{a}_\alpha^\dagger, \quad (6.18)$$

In this case, the eigenvalues $\hat{b}_\alpha(\tau)$ are given by

$$\hat{b}_\alpha(\tau) = e^{-\tau(E_\alpha^0 - \mu)} \hat{b}_\alpha(0). \quad (6.19)$$

The occupation number of the state α is then given by

$$n_\alpha \equiv \langle \hat{a}_\alpha^\dagger \hat{a}_\alpha \rangle_{\mu, \beta} = \frac{1}{1 + e^{\beta(E_\alpha^0 - \mu)}}, \quad (6.20)$$

which is the Fermi-Dirac distribution, as would be expected. The average number of particles and variance are given by

$$\begin{aligned} \langle \hat{N} \rangle_{\mu, \beta} &= \sum_\alpha n_\alpha, \\ \langle (\Delta \hat{N})^2 \rangle_{\mu, \beta} &= \sum_\alpha n_\alpha (1 - n_\alpha), \end{aligned} \quad (6.21)$$

which are also as expected.

6.3 Interacting dynamics

We will now consider how a two-body interaction changes the results derived above. We introduce a Hamiltonian of the form

$$\hat{H} = \hat{H}^{(0)} + \hat{H}^{(1)}, \quad (6.22)$$

where $\hat{H}^{(1)}$ is a two-body potential

$$\hat{H}^{(1)} = \sum_{\alpha\beta\gamma\delta} w_{\alpha\beta\gamma\delta} \hat{a}_{\alpha}^{\dagger} \hat{a}_{\beta}^{\dagger} \hat{a}_{\gamma} \hat{a}_{\delta}, \quad (6.23)$$

and $\hat{H}^{(0)}$ is given by equation (6.15). In this case, the commutator $[\hat{a}_{\alpha}, \hat{H}]$ does not consist of terms that only contain annihilation operators. Based on equation (6.16) we can no longer conclude that coherent states are preserved by the dynamics. This is similar to the situation for Slater determinants, stemming from the intrinsic complexity of interacting systems.

To proceed, we will introduce an operator expansion to include the effects of correlation in a systematic way. First, we introduce some terminology. We say that an operator is *thermofield (tf) normal of order n*, if it is of the form

$$\hat{\psi}^{(n)} = \frac{1}{(n!)^2} \sum_{\alpha, \beta} t_{\alpha\beta} \prod_{i=1}^n \hat{a}_{\alpha_i}^{\dagger} \hat{b}_{\beta_i}. \quad (6.24)$$

where α and β are multi-indices of order n, and $t_{\alpha\beta}$ is a complex valued function of these indices. These are similar in form to excitation operators in the coupled cluster or configuration interaction expansions, with n-excitation operators corresponding to tf normal operators of order n. In this case, however, the creation and annihilation operators act in different Hilbert spaces. We say that a wavefunction is tf normal if it can be written

$$|\psi\rangle = \left(1 + \sum_{n=1}^{\infty} \hat{\psi}^{(n)} \right) |\Omega\rangle, \quad (6.25)$$

where $\hat{\psi}^{(n)}$ are tf normal of order n, and $|\Omega\rangle$ is a reference wavefunction in the full

Hilbert space.

We now rewrite equation (6.25) as an exponential

$$|\psi\rangle = \exp\left(\sum_{n=1}^{\infty} \hat{T}^{(n)}\right) |\Omega\rangle, \quad (6.26)$$

where the operators $\hat{T}^{(n)}$ are also normal of order n , and the notation is the same as the coupled cluster method. This will be called a thermal cumulant expansion. Assuming everything converges properly, we can relate the operators in equation (6.26) to those in (6.25) through the relation

$$\hat{T}^{(n)} = \hat{\psi}^{(n)} - \sum_{p \in \mathcal{P}_n} \prod_{m=1}^{n-1} \frac{1}{p_m!} \left(\hat{T}^{(m)}\right)^{p_m}, \quad (6.27)$$

where \mathcal{P}_n is the set of multi-indices $\{(p_1, \dots, p_{n-1}) : p_m \geq 0, \sum_{m=1}^{n-1} p_m m = n\}$, and $n > 0$.

As discussed in the introduction, this expansion is closely related to the expansion used in the coupled cluster method, and the interpretation is similar. In particular, the expansion has the property of size extensivity, which is a desirable property for a many body ansatz[90]. The mathematics of this construction is also formally the same as the cumulant expansion, with the corresponding statistical interpretation[93].

To get some intuition for the expansion in this context, consider expanding the wavefunction $|\psi_{\mu,\beta}\rangle$ of equation (6.7) in this way, for the Hamiltonian (6.22). We will again use the imaginary time formalism, setting $\tau = \frac{1}{2}\beta$, and see how the

function $|\psi_\mu(\tau)\rangle$ evolves in imaginary time. The initial conditions are given by

$$\hat{T}^{(1)}(0) = \sum_{\alpha} \hat{a}_{\alpha}^{\dagger} \hat{b}_{\alpha} \quad (6.28)$$

$$\hat{T}^{(n)}(0) = 0, \quad \forall n > 1.$$

Inserting this into equation (6.27) implies the initial conditions

$$\hat{\psi}^{(n)}(0) = \frac{1}{n!} (\psi^{(1)}(0))^n, \quad \forall n > 1, \quad (6.29)$$

in addition to $\hat{\psi}^{(1)}(0) = \hat{T}^{(1)}(0)$. The inverse factors of $n!$ generally account for symmetrization in products of the form $\prod_{i=1}^n \hat{b}_{\alpha_i} \hat{a}_{\alpha_i}^{\dagger}$. Similarly, the inverse factor of $p_m!$ in equation (6.27) is a combinatorial factor that accounts for permutations among groups of the same size. In this case, the operators $\hat{\psi}^{(n)}$ will satisfy the modified Schrodinger equation

$$\partial_{\tau} \hat{\psi}^{(n)}(\tau) = [(\mu \hat{N} - \hat{H}), \hat{\psi}^{(n)}(\tau)]. \quad (6.30)$$

We therefore interpret the operators $\hat{T}^{(n)}$ as probing the n-particle correlation of a group of particles, after subtracting off all possible lower order correlations. For example, the function $\hat{T}^{(2)}$ compares the interacting evolution of two particles $\hat{\psi}^{(2)}$ with the uncorrelated evolution of the product state $(\hat{\psi}^{(1)})^2/2$. In a similar way, equation (6.27) subtracts off all possible lower order correlations from the coherent evolution of n particles, isolating the n-particle correlation, which is similar to the

statistical interpretation of cumulants.

This expansion will only converge rapidly if the theory is weakly interacting, because a strongly interacting theory will make the coherent evolution very different from the independent evolution, so the corrections will be large. To see this more explicitly, we again choose the eigenbasis of the non-interacting Hamiltonian $\hat{H}^{(0)}$, where the functions $\hat{T}^{(1)}(\tau)$ are given by

$$\hat{T}^{(1)}(\tau) = \sum_{\alpha} e^{-\tau(E_{\alpha}^0 - \mu)} \hat{a}_{\alpha}^{\dagger} \hat{b}_{\alpha}, \quad (6.31)$$

as they were in the non-interacting theory. Clearly this term will only be a good approximation for the interacting system if the interactions are weak. This also illustrates why the non-interacting theory only contains the first term in the expansion, because the higher order corrections are identically zero.

6.4 Optimized basis set

In the discussion so far, the basis of operators has been kept general. The only restriction on the basis has been the form of the Hamiltonian (6.22), and the use of the number operator for the grand canonical partition function. If one considers a more general basis, the Hamiltonian and number operator no longer retain their usual form, but the rest of the results remain unchanged as long as the operators form a complete set that satisfy the anti-commutation relations (6.6), and the Hamiltonian acts in \mathfrak{H}_1 . Even more generally, one might consider a basis of operators that have a mixture of Fermionic and Bosonic statistics, similar to the

situation for Cooper pairs, or even anyonic commutation relations. It is also possible to consider basis sets that are not orthonormal in any sense, as in quantum chemistry algorithms that use nonorthogonal basis sets[94]. Finally, in the approach taken here, it will be possible to consider transformations that mix the two Hilbert spaces, which will be further explored. As special cases of transformed basis sets, one could consider Bogoliubov transformations[67][68], local canonical transformations[95][96], or more general nonlinear canonical transformations[97]. Some general results on canonical transformations are reviewed in appendix C.1.

We will develop a method to incrementally optimize the basis set so that the cumulant expansion (6.13) converges as rapidly as possible. Ideally, the full wavefunction could be accurately approximated by the first term in the infinite sum, giving it the general form of a thermal coherent state. To achieve this goal, we must introduce a truncation scheme, and then maximize the overlap of the truncated wavefunction with the “full” wavefunction, over the set of allowed basis transformations. The truncation scheme is a choice of terms to keep in the exponential, as considered in the coupled cluster method. For example, one could keep only operators of first order, conventionally called singles, or also include doubles, or higher order terms.

The following analysis will apply to real or thermal time evolution, so for

convenience we define the modified Hamiltonian

$$\hat{\mathcal{H}} = \begin{cases} \hat{H} & \text{real,} \\ -i(\hat{H} - \mu\hat{N}) & \text{thermal,} \end{cases} \quad (6.32)$$

where we note that the number operator must be defined in the physical basis of particle excitations, and then transformed to whatever basis is being used. Let us assume that the basis has been optimized at time t , and try to optimize it at time $t + \delta t$. At time t , the truncated wavefunction has the form

$$|\psi(t)_s\rangle = e^{\hat{T}_s(t)} |\Omega\rangle, \quad (6.33)$$

where the subscript s denotes a truncated (or short) cumulant expansion. At time $t + \delta t$, the evolved wavefunction will become

$$|\psi(t + \delta t)\rangle = e^{-i\delta t\hat{\mathcal{H}}} e^{\hat{T}_s(t)} |\Omega\rangle. \quad (6.34)$$

After using the Baker-Campbell-Hausdorff formula, it is clear that the state will no longer be truncated, and will in general have terms of all orders in the exponential. We would like to find a truncated wavefunction $|v\rangle$ that maximizes the overlap $|\langle v|\psi(t + \delta t)\rangle|^2$, within a set Υ of wavefunctions that have a constant magnitude, so that

$$|\psi(t + \delta t)_s\rangle = \operatorname{argmax}_{v \in \Upsilon_n} |\langle v|\psi(t + \delta t)\rangle|^2. \quad (6.35)$$

We do not demand the wavefunction to be normalized because we will take advantage of the freedom to simplify the equations.

It is desirable to turn equation (6.35) into a differential equation using the calculus of variations. To do this, one can use Lagrange multipliers, and vary the state $\langle v|$ independently of $|v\rangle$ to obtain

$$\langle \delta v | \psi \rangle \langle \psi | v \rangle = \lambda \langle \delta v | v \rangle, \quad (6.36)$$

where we suppress the time dependence, and the subscript s , for convenience. To obtain a dynamic equation, we take a derivative of this equation, set $|v\rangle = |\psi\rangle$, and divide by $\langle \psi | \psi \rangle$ to get

$$\langle \delta \psi | \mathbb{P}_\perp i \partial_t | \psi \rangle = \langle \delta \psi | (\hat{\mathcal{H}} - \langle \hat{\mathcal{H}}^\dagger \rangle - R) | \psi \rangle, \quad (6.37)$$

where $\mathbb{P}_\perp = (1 - |\psi\rangle \langle \psi | \langle \psi | \psi \rangle^{-1} \langle \psi |)$ is a projector onto the subspace orthogonal to $|\psi\rangle$, and $\langle \hat{\mathcal{H}}^\dagger \rangle$ is the normalized expectation value. The variable R is related to the Lagrange multiplier λ , but will not appear in the final equations. A more detailed derivation of this equation is presented in appendix C.2, which gives more insight into this parameter.

Because of the presence of the projector in equation (6.37), only the perpendicular part of the derivative is constrained by this equation. The parallel part determines the normalization of the wavefunction, which we set by imposing the

condition

$$\frac{\langle \psi | i\partial_t | \psi \rangle}{\langle \psi | \psi \rangle} = \langle \hat{\mathcal{H}}^\dagger \rangle + R, \quad (6.38)$$

which simplifies equation (6.37) to

$$\langle \delta\psi | i\partial_t | \psi \rangle = \langle \delta\psi | \hat{\mathcal{H}} | \psi \rangle. \quad (6.39)$$

This equation is similar to a time-dependent Hartree Fock equation[98], but adapted to the thermofield formalism for a more general ansatz. In order to use this equation, we must demand that the variation $|\delta\psi\rangle$ maintains the form of the ansatz for the wavefunction, and so does the derivative. In the next two sections, we illustrate how this works for a specific choice of truncation and optimization scheme.

6.5 Thermal coherent state evolution

In this section we will develop a specific implementation of the general approach developed previously that might be suitable for quantum chemistry applications. We will make the following choices:

- The cumulant expansion is truncated at the first term, imposing the form of a thermal coherent state.
- The wavefunction will be chosen to be thermofield normal.
- The basis of excitations will be a set of single particle molecular orbitals satisfying canonical anti-commutation relations.

- We will allow arbitrary unitary transformations on the vector space spanned by the operators \hat{a}_α and \hat{b}_α , mixing the two Hilbert spaces.

The reason we choose to retain the thermofield normal form is that it simplifies calculations, which will be demonstrated, in addition to the fact that it is exact in the non-interacting case. We will want to find the differential equations that result from using these choices in the variational equation (6.39). There are two parameters that will be optimized in the variation, changes in the operator \hat{T} and changes in the basis of excitations. In general, changes in the basis of excitations will affect the vacuum $|\Omega\rangle$ in addition to the operator \hat{T} . In order to maintain the thermofield normal form, we demand that when the basis is changed, there is a corresponding change to the wavefunction that leaves the operator \hat{T} form invariant. More explicitly, the combined effect of this transformation on the wavefunction will be

$$e^{\sum_{\alpha\beta} t_{\alpha\beta} \hat{a}_\alpha^\dagger \hat{b}_\beta} |\Omega\rangle \rightarrow e^{\sum_{\alpha\beta} t'_{\alpha\beta} \hat{a}'_\alpha \hat{b}'_\beta} |\Omega'\rangle, \quad (6.40)$$

where the prime indicates the changed basis. Changes in the operator \hat{T} will take the form $t_{\alpha\beta} \rightarrow t'_{\alpha\beta}$, so the two types of transformations are effectively decoupled.

We note that the state remains invariant under the following set of simultaneous transformations

$$\hat{a}^\dagger \rightarrow \hat{a}^\dagger U^\dagger, \quad \hat{b} \rightarrow V \hat{b}, \quad t \rightarrow U t V^\dagger, \quad (6.41)$$

where matrix multiplication is implied, and the matrices are unitary. In the Hartree-

Fock approach this type of freedom is used to diagonalize the matrix of Lagrange multipliers, imposing orthonormality on the basis of excitations[99]. In this case, however, the transformations are infinitesimal so it is possible to directly constrain them to satisfy canonical anti-commutation relations. For this reason, we will use this freedom to perform a singular value decomposition on the matrix $t_{\alpha\beta}$, which means that this matrix can be chosen to be diagonal, with diagonal elements t_α .

The unitary transformations that mix the Hilbert spaces are included to allow for some correlation in the wavefunction. The generators of these transformations take the form

$$\begin{bmatrix} \hat{a} \\ \hat{b} \end{bmatrix} \rightarrow \begin{bmatrix} \hat{a} \\ \hat{b} \end{bmatrix} + i\varepsilon \begin{bmatrix} A & B \\ B^\dagger & C^\dagger \end{bmatrix} \begin{bmatrix} \hat{a} \\ \hat{b} \end{bmatrix} \quad (6.42)$$

where A and C are Hermitian. This is a one parameter group of transformations, whose derivative at $\varepsilon = 0$ gives the Lie derivative, which in this case will be denoted $\mathcal{L}_{A,B,C}$. The vacuum transforms as

$$i\mathcal{L}_{A,B,C} |\Omega\rangle = \hat{a}^\dagger B \hat{b} |\Omega\rangle. \quad (6.43)$$

which can be checked by acting with any annihilation operator. Additionally we find

$$i\mathcal{L}_{A,B,C} |\psi\rangle = \left(\hat{a}^\dagger (A^\dagger t - t C^\dagger + B - t B^\dagger t) \hat{b} + \text{Tr}(B^\dagger t) \right) |\psi\rangle. \quad (6.44)$$

The second term in this equation changes the normalization of $|\psi\rangle$, which will not

be important. Consider the matrix in the first term

$$M = A^\dagger t - tC^\dagger + B - tB^\dagger t. \quad (6.45)$$

We note that the diagonal can be chosen to be anything, which implies that we can absorb a change in the singular values t_α into a change in the matrix M , allowing us to always choose the singular values to be constant. For simplicity, we choose $t_\alpha = 1$, so the wavefunction takes the form of the thermal coherent state

$$|\psi\rangle = e^{\sum_\alpha \hat{a}_\alpha^\dagger \hat{b}_\alpha} |\Omega\rangle. \quad (6.46)$$

The matrix M then becomes

$$M = A^\dagger - C^\dagger + B - B^\dagger. \quad (6.47)$$

With this form, it is clear that the state is invariant under transformations with $A = C$ and $B = B^\dagger$. If we choose $A = -C$ and $B = -B^\dagger$, then this makes the first term Hermitian and the second term anti-Hermitian, which decouples the two transformations. This is interpreted naturally by defining the operators $\hat{a} \pm \hat{b}$, which is developed below.

6.6 Simplified basis

To make better sense of the above results, we define the operators

$$\hat{v}_\alpha = \frac{1}{\sqrt{2}}(\hat{a}_\alpha - \hat{b}_\alpha), \quad \hat{w}_\alpha = \frac{1}{\sqrt{2}}(\hat{a}_\alpha + \hat{b}_\alpha), \quad (6.48)$$

which will eventually be considered an initial condition. These operators satisfy canonical anti-commutation relations, and anti-commute with each other. Also, the state

$$|\Omega\rangle \propto e^{\sum_\alpha \hat{a}_\alpha^\dagger \hat{b}_\alpha} |0\rangle, \quad (6.49)$$

is annihilated by the operators \hat{v}_α and \hat{w}_α^\dagger , so is proportional to the vacuum of this basis. One can readily check that for the choices $A = C$ and $B = B^\dagger$, the transformation (6.42) can be written succinctly as

$$\hat{v} \rightarrow (1 + i\varepsilon X)\hat{v}, \quad \hat{w} \rightarrow (1 + i\varepsilon \tilde{X})\hat{w}, \quad (6.50)$$

where we have defined $X = A - B$ and $\tilde{X} = A + B$, which are both Hermitian.

With this result, it is clear why the vacuum is invariant under these transformations, because they rotate the creation and annihilation operators independently. For the transformations with $A = -C$ and $B = -B^\dagger$, we find

$$\hat{v} \rightarrow \hat{v} + i\varepsilon Y \hat{w}, \quad \hat{w} \rightarrow \hat{w} + i\varepsilon Y^\dagger \hat{v}, \quad (6.51)$$

where $Y = A + B$, but this matrix is not Hermitian unless $B = 0$. Under this change, the vacuum transforms as

$$i\mathcal{L}_Y |\Omega\rangle = \hat{v}^\dagger Y \hat{w} |\Omega\rangle, \quad (6.52)$$

which can be checked by acting with annihilation operators at small ε .

These equations are simplified by defining a Hermitian operator

$$\hat{\mathcal{H}}^c = \hat{v}^\dagger Y \hat{w} + \hat{w}^\dagger Y^\dagger \hat{v} + \hat{v}^\dagger X \hat{v} + \hat{w}^\dagger \tilde{X} \hat{w}. \quad (6.53)$$

The transformations described so far can then be written succinctly as

$$i\mathcal{L}_{\mathcal{H}^c} |\Omega\rangle = \hat{\mathcal{H}}^c |\Omega\rangle, \quad i\mathcal{L}_{\mathcal{H}^c} \hat{A} = [\hat{\mathcal{H}}^c, \hat{A}], \quad (6.54)$$

where \hat{A} refers to \hat{v} or \hat{w} . These equations are naturally interpreted as generating Hamiltonian dynamics in the Schrodinger picture, where the operator $\hat{\mathcal{H}}^c$ can be found from equation (6.39). Before developing these dynamics further, we will use the unitary freedom to relate the defined basis to the original basis of operators \hat{a}_α .

The Hamiltonian $\hat{\mathcal{H}}$ is only a function of the operators in the first copy of the original Hilbert space, denoted \mathfrak{H}_1^0 , so we would like to find a relation between the transformed basis and the original operators. To simplify notation, we will now consider the operators \hat{a} to always lie in \mathfrak{H}_1^0 , taking the operators \hat{v} and \hat{w} to rotate independently of this basis, meaning that relation (6.48) no longer holds for $t > 0$. Denote the initial basis of operators by \hat{a}_0 , and relate the complex basis to the initial

basis by the relation

$$\hat{a}_0 = M\hat{v} + N\hat{w}, \quad (6.55)$$

for some matrices M and N . In appendix C.3 we prove that these matrices have the same left singular vectors, and there is a unitary change of basis that brings this to the form

$$\hat{a} = \tilde{\Lambda}\hat{v} + \Lambda\hat{w}, \quad (6.56)$$

where Λ and $\tilde{\Lambda}$ are real diagonal matrices with eigenvalues in the range $[0, 1]$, related by

$$\tilde{\Lambda}^2 + \Lambda^2 = 1. \quad (6.57)$$

The operators \hat{a} are now a time dependent basis for the first Hilbert space, unitarily related to the initial basis \hat{a}_0 . These relations simplify the calculation of physical correlators, which depend only on operators in \mathfrak{H}_1^0 . As an example, we see that the eigenvalues λ_α are closely related to the occupation number of the state α , as seen by the relation

$$n_\alpha = \langle \hat{a}_\alpha^\dagger \hat{a}_\alpha \rangle = \lambda_\alpha^2. \quad (6.58)$$

In light of equation (6.57), one could also define a mixing angle θ_α for which $\lambda_\alpha = \cos(\theta_\alpha)$ and $\tilde{\lambda}_\alpha = \sin(\theta_\alpha)$, but we will continue to use the defined notation.

6.7 Approximate dynamics

To find the equations of motion, we will demand that $|\Omega_c\rangle$ retains the form of the ansatz, implying that it changes according to (6.52)

$$i\partial_t |\Omega\rangle = \hat{v}^\dagger Y \hat{v} |\Omega\rangle. \quad (6.59)$$

Using this form for the derivative in equation (6.39), and setting the variation to zero gives

$$Y_{\alpha\beta} = \langle \hat{w}_\beta^\dagger \hat{v}_\alpha \hat{H} \rangle. \quad (6.60)$$

We define the matrix $Y_{\alpha\beta}$ for real time evolution, using (6.32) to find the corresponding imaginary time evolution. Consider now a Hamiltonian of the form (6.22). Define time dependent coefficients $H_{\alpha\beta}^{(0)}(t)$ and $w_{\alpha\beta\gamma\delta}(t)$ to expand the Hamiltonian in the basis $\hat{a} = U\hat{a}_0$,

$$H_{\alpha\beta}^{(0)}(t) = \sum_{\gamma\delta} U_{\alpha\gamma} H_{\gamma\delta}^{(0)}(0) U_{\delta\beta}^\dagger, \quad w_{\alpha\beta\gamma\delta}(t) = \sum_{\epsilon\zeta\eta\theta} U_{\alpha\epsilon} U_{\beta\zeta} w_{\epsilon\zeta\eta\theta}(0) U_{\eta\gamma}^\dagger U_{\theta\delta}^\dagger, \quad (6.61)$$

where the time dependence will be suppressed for notational convenience. Equation (6.60) then becomes

$$\frac{Y_{\alpha\beta}}{\tilde{\lambda}_\alpha \lambda_\beta} = H_{\alpha\beta}^{(0)} + \sum_{\gamma} n_\gamma \left(w_{\alpha\gamma\gamma\beta} - w_{\alpha\gamma\beta\gamma} - w_{\gamma\alpha\gamma\beta} + w_{\gamma\alpha\beta\gamma} \right), \quad (6.62)$$

This calculation motivates us to define the matrix

$$H_{\alpha\beta}^c = \frac{Y_{\alpha\beta}}{\tilde{\lambda}_\alpha \lambda_\beta}, \quad (6.63)$$

which is Hermitian. For imaginary time evolution, the operator $\hat{\mathcal{H}}$ becomes anti-Hermitian, but in the following we will use this definition and equation (6.32) to find the dynamics explicitly.

We can also define the effective Hamiltonian to induce the unitary transformation on the bases \hat{a} , \hat{v} , and \hat{w} resulting in equation (6.56). The generators of these unitary transformations are derived in appendix C.3, which can then be used in equation (6.53). The resulting operator is only simplified for real time evolution, given by

$$\hat{\mathcal{H}}^c = \hat{a}^\dagger H^c \hat{a}, \quad \text{real.} \quad (6.64)$$

In imaginary time the resulting operator is complicated, and not particularly enlightening, instead the explicit equations are derived below. For real time evolution, the equations of motion for the vacuum and bases are the same as in equation (6.54), and the occupation numbers are invariant, reflecting the fact that normalization is preserved by unitary time evolution.

In imaginary time, we will again use the parameter $\tau = \beta/2$. Using the

definition (6.32), and changing variables to $n_\alpha = \lambda_\alpha^2$ we find¹

$$\frac{\partial_\tau n_\alpha}{n_\alpha(1-n_\alpha)} = -2 H_{\alpha\alpha}^c, \quad \partial_\tau \hat{a}_\alpha = \sum_{\beta \neq \alpha} \frac{n_\alpha + n_\beta - 2n_\alpha n_\beta}{n_\alpha - n_\beta} H_{\alpha\beta}^c \hat{a}_\beta, \quad (6.65)$$

where the latter equation is only true if the occupancies n_α are non-degenerate. The degenerate case is explained in appendix C.3. These equations can be simplified further by imposing the form of a Fermi-Dirac distribution

$$n_\alpha = \frac{1}{1 + e^{\beta(E_\alpha - \mu)}}, \quad (6.66)$$

which defines an energy E_α . With this definition, equations (6.65) become

$$\tau \frac{dE_\alpha}{d\tau} = H_{\alpha\alpha}^c - E_\alpha \quad (6.67)$$

$$\partial_\tau \hat{a}_\alpha = \sum_{\beta \neq \alpha} \coth\left(\tau(E_\beta - E_\alpha)\right) H_{\alpha\beta}^c \hat{a}_\beta, \quad (6.68)$$

where we have used a total derivative in the first equation to emphasize the dependence on n_α .

These equations give some physical insight into the dynamics. Equation (6.67) shows that the energies are driven towards a self consistent field in which the defined energies E_α are close to the energies $H_{\alpha\alpha}$, which can be considered a mean-field energy for the state. Equation (6.68) imposes a unitary transformation which tends to diagonalize the effective Hamiltonian. In the limit of low-temperature, or large

¹For this derivation we have assumed that the number operator is given by $\hat{N} = \sum_\alpha \hat{a}_\alpha^\dagger \hat{a}_\alpha$, so that these operators are unitarily related to the original creation and annihilation operators.

τ , the system is driven towards an equilibrium configuration which approximately diagonalizes the Hamiltonian and in which the occupation numbers approach those of the self consistent field, as is the case for the Hartree Fock solution. Indeed, as $\beta \rightarrow \infty$, the occupation numbers (6.66) are driven to zero or one, so the state approaches a Slater determinant. In this case, the effective Hamiltonian reduces to the Fock operator, and the dynamics approaches the Hartree-Fock solution.

6.8 Homogeneous electron gas

We now apply these approximate dynamics to the homogeneous electron gas. In this case, the Hamiltonian (6.22) consists of the terms

$$\hat{H}^{(0)} = \sum_{\mathbf{k}\sigma} \frac{k^2}{2m} \hat{a}_{\mathbf{k}\sigma}^\dagger \hat{a}_{\mathbf{k}\sigma}, \quad \hat{H}^{(1)} = \frac{2\pi e^2}{V} \sum_{\mathbf{k}\mathbf{k}'\sigma\sigma'} \sum_{\mathbf{q}\neq 0} \frac{1}{q^2} \hat{a}_{\mathbf{k}-\mathbf{q}\sigma}^\dagger \hat{a}_{\mathbf{k}'+\mathbf{q}\sigma'}^\dagger \hat{a}_{\mathbf{k}'\sigma'} \hat{a}_{\mathbf{k}\sigma}, \quad (6.69)$$

where we use units such that $4\pi\epsilon_0 = 1$, and \mathbf{k} label the wavevectors of a periodic box. For this Hamiltonian, equation (6.62) gives

$$H_{\mathbf{k}\sigma, \mathbf{k}'\sigma'}^c = \delta_{\mathbf{k}\mathbf{k}'} \delta_{\sigma\sigma'} \left(\frac{k^2}{2m} - \frac{4\pi e^2}{V} \sum_{\mathbf{q}\neq 0} \frac{1}{q^2} n_{\mathbf{k}+\mathbf{q}\sigma} \right), \quad (6.70)$$

which shows that the effective Hamiltonian is always diagonal in the Fourier basis, and that the interaction energy is negative due to the exchange energy, as correlation effects are not included well in this approximation. In the limit of low density this should become an unstable fixed point, because of the tendency towards spin-polarization and Wigner crystallization, making equation (6.68) relevant. We define

the occupation energy of interaction by $E_{\mathbf{k}\sigma}^{int} = E_{\mathbf{k}\sigma} - \frac{k^2}{2m}$, which evolves according to

$$-\tau \frac{dE_{\mathbf{k}\sigma}^{int}}{d\tau} = E_{\mathbf{k}\sigma}^{int} + \frac{4\pi e^2}{V} \sum_{\mathbf{q} \neq 0} \frac{1}{q^2} n_{\mathbf{k}+\mathbf{q}\sigma}. \quad (6.71)$$

We now take the infinite volume limit, where \mathbf{k} becomes a continuous variable. We assume that the density only depends on the magnitude $|\mathbf{k}|$, and omit the dependence on σ . The sum in equation (6.71) then approaches an integral, defined by

$$\mathcal{I}_{\beta\mu}(k) = \frac{e^2}{2\pi^2} \int \frac{d^3q}{q^2} n_{\beta\mu}(|\mathbf{k} + \mathbf{q}|), \quad (6.72)$$

In this integral, there are three relevant distances: $|\mathbf{k}|$, $|\mathbf{q}|$, and $|\mathbf{k} + \mathbf{q}|$. This situation lends itself to the two-center bipolar coordinate system, related to the upper half-plane by

$$x = \frac{r_1^2 - r_2^2}{4a}, \quad y = \frac{1}{4a} \sqrt{(4ar_2)^2 - (r_2^2 - r_1^2 + 4a^2)^2}. \quad (6.73)$$

In this case, we rotate this coordinate system around the axis connecting the points defining the coordinate system, which introduces an extra angle ϕ . The volume element is given by

$$dV = \frac{r_1 r_2}{2a} dr_1 dr_2 d\phi. \quad (6.74)$$

Choosing $k = 2a$, $r_1 = q$ and $r_2 = |k + q|$, we find

$$\mathcal{I}_{\beta\mu}(k) = \frac{e^2}{\pi} \int_0^\infty dx \log \left(\frac{k+x}{|k-x|} \right) x n_{\beta\mu}(x). \quad (6.75)$$

In the low temperature limit, when the occupation numbers are filled until the

Fermi level, this reduces to a standard result in the Hartree-Fock analysis of the homogeneous electron gas[100].

6.9 Conclusion

We have found a natural way of using thermofield dynamics for imaginary time evolution in the grand canonical ensemble, showing that the approach works for a non-interacting system. We then applied this analysis to interacting systems, giving rise to a general strategy for approximating the time-dependent Schrodinger equation in a grand canonical ensemble, by introducing an ansatz and optimizing it variationally at every time step to yield approximate equations of motion. We implemented this strategy for a thermal coherent state, which turns out to be a generalization of time dependent Hartree-Fock theory to fractional occupation numbers. It will be useful to consider how to include correlation into this ansatz in future work.

Appendix A: Detailed simulation methods

Most of the simulations in this paper were performed for an ensemble of boxes periodic in the x and y directions with 1024 SPC/E water molecules, with box size approximately 2.8x2.8x4.5 nm, where the width was modified to the bulk density of water in the presence of an electric field. The dynamic simulations were modeled with a z length of 4.3 nm. The number of realization in the ensembles varied from 8 to 16, depending on the context and how much smoothing was required, but the results are not extremely sensitive to this parameter, as long as it is large enough. The LMF procedure developed was implemented with a modified version of the LAMMPS molecular dynamics package, where an algorithm was developed to compute the average long range field from an ensemble of parallel simulations running simultaneously, and replace the long range Ewald potential with this dynamic LMF field. The applied electric field was implemented by including a sheet of closely spaced discretized charges on the wall. If the electric field is imposed externally, there are problems with the Yeh-Berkowitz slab correction [35].

Appendix B: Alternative approaches to non-equilibrium LMF theory

B.1 Introduction

In this appendix we will discuss two alternate approaches to nonequilibrium LMF theory that showed some promise, but which ultimately do not work well. The first approach attempts to give the LMF potential its own Hamiltonian dynamics, which might lead to an effective field averaging due to slowed dynamics. This is an interesting approach, but ultimately would be unlikely to be that useful or computationally efficient. It is worth considering however, because it is hard to know in what context this type of idea could find applications.

The second section describes an attempt to use linear response theory at every time step of a simulation in order to correct the LMF potential for the next time step. Ultimately this approach does not seem to work due to the nature of the linear response technique, but it is still worth presenting in order to show alternate ways of thinking about the problem. Together these are presented in order to illustrate the various ways of thinking about this problem, and possibly to assist others who intend to pursue this problem further.

B.2 Non equilibrium LMF with Hamiltonian LMF dynamics

In this section we will consider a very formal approach to nonequilibrium LMF theory which attempts to give the LMF potential its own dynamics. The LMF potential is denoted $\mathcal{V}_{R1}(\mathbf{r}; t)$, and the procedure will use the techniques of Hamiltonian field theory, which are used for systems that have fields as dynamical degrees of freedom in the theory. These techniques are used extensively in quantum field theory, and can be reviewed for example in Giochetto et. al. [101].

We will want to consider a configuration dependent field $\mathcal{V}_{R1}(\mathbf{r}; t)$ that evolves according to a Hamiltonian $\mathcal{H}(\Gamma)$, where Γ is the configuration space consisting of particle positions and momenta $(\mathbf{r}_i, \mathbf{p}_i)$, in addition to the value of the field $\mathcal{V}_{R1}(\mathbf{r})$ and its conjugate momentum $\Pi_{R1}(\mathbf{r})$, which will also be considered as part of the configuration space of the field. In many cases we will suppress the time dependence of the fields, but include it where appropriate. We will first write down the version of Liouville's equation with this field, which follows from the continuity equation

$$\frac{\partial f}{\partial t} + \sum_{i=1}^N \left(\frac{\partial f}{\partial \mathbf{r}_i} \cdot \dot{\mathbf{r}}_i + \frac{\partial f}{\partial \mathbf{p}_i} \cdot \dot{\mathbf{p}}_i \right) + \int d\mathbf{r} \left(\frac{\delta f}{\delta \mathcal{V}_{R1}(\mathbf{r})} \dot{\mathcal{V}}_{R1}(\mathbf{r}) + \frac{\delta f}{\delta \Pi_{R1}(\mathbf{r})} \dot{\Pi}_{R1}(\mathbf{r}) \right) = 0. \quad (\text{B.1})$$

Using Hamilton's equations of motion, this becomes

$$\frac{\partial f}{\partial t} = -\{f, \mathcal{H}\}_{\mathcal{V}}, \quad (\text{B.2})$$

where we have defined the generalized Poisson bracket

$$\{f, g\}_{\mathcal{V}} = \sum_{i=1}^N \left(\frac{\partial f}{\partial \mathbf{r}_i} \cdot \frac{\partial g}{\partial \mathbf{p}_i} - \frac{\partial f}{\partial \mathbf{p}_i} \cdot \frac{\partial g}{\partial \mathbf{r}_i} \right) + \int d\mathbf{r} \left(\frac{\delta f}{\delta \mathcal{V}_{R1}(\mathbf{r})} \frac{\delta g}{\delta \Pi_{R1}(\mathbf{r})} - \frac{\delta f}{\delta \Pi_{R1}(\mathbf{r})} \frac{\delta g}{\delta \mathcal{V}_{R1}(\mathbf{r})} \right). \quad (\text{B.3})$$

We will be interested in systems interacting under the long range Coulomb potential, which is split according to

$$\frac{1}{r} = v_0(r) + v_1(r), \quad (\text{B.4})$$

where the long range component $v_1(r)$ is defined through convolution of the Coulomb potential with a unit Gaussian of width σ , denoted $\rho_G(\mathbf{r})$. For the long range field, we introduce the potential \mathcal{V}_1 , so that the Hamiltonian takes the form

$$\mathcal{H}_1 = \int d\mathbf{r} \left(\frac{\epsilon_0 \mathbf{E}_1(\mathbf{r})^2}{2} + 4\pi \rho^{q\sigma}(\mathbf{r}) \mathcal{V}_1(\mathbf{r}) \right). \quad (\text{B.5})$$

Here $\rho^{q\sigma}(\mathbf{r}, t)$ is the smooth charge density, and $\mathbf{E}_1(\mathbf{r}, t) = -\nabla \mathcal{V}_1(\mathbf{r}, t)$ is the long range electric field in the mimic system. In fact, this is a Hamiltonian for an LMF potential that is smoothed by a Gaussian of width $\sqrt{2}\sigma$. To see this, we note that the Euler-Lagrange equation for the field $\mathcal{V}_1(\mathbf{r})$ is

$$\nabla^2 \mathcal{V}_1(\mathbf{r}) = -\frac{4\pi}{\epsilon_0} \rho^{q\sigma}(\mathbf{r}), \quad (\text{B.6})$$

which gives the long range force with a smoothing length σ . Using the definition of

the smooth charge density, however, the interaction Hamiltonian can be rewritten

$$\mathcal{H}_1 = 4\pi \int d\mathbf{r} \int d\mathbf{r}' \rho^q(\mathbf{r}') \rho_G(|\mathbf{r} - \mathbf{r}'|) \mathcal{V}_1(\mathbf{r}) = \sum_i q_i \mathcal{V}_1^\sigma(\mathbf{r}_i), \quad (\text{B.7})$$

where $\mathcal{V}_1^\sigma(\mathbf{r}) = \int d\mathbf{r}' \rho_G(|\mathbf{r} - \mathbf{r}'|) \mathcal{V}_1(\mathbf{r}')$. So we have an additional convolution of width σ , yielding a total smoothing length of $\sqrt{2}\sigma$.

In the spirit of LMF theory, we will want to consider dynamics for a mimic system evolving under a potential $\mathcal{V}_{R1}(\mathbf{r})$ that effectively averages over statistical fluctuations. One natural way of achieving this with a Hamiltonian system is by adding a “kinetic” term to the field $\mathcal{V}_{R1}(\mathbf{r})$,

$$\mathcal{H}_{R1} = \int d\mathbf{r} \left(\frac{\Pi_{R1}(\mathbf{r})^2}{2\nu} + \frac{\epsilon_0 \mathbf{E}_{R1}(\mathbf{r})^2}{2} + 4\pi \rho^{q\sigma}(\mathbf{r}, t) \mathcal{V}_{R1}(\mathbf{r}) \right). \quad (\text{B.8})$$

Here ν is a parameter that acts analogously to a mass term, which can be seen from Hamilton’s equations

$$\begin{aligned} \Pi_{R1}(\mathbf{r}) &= \nu \dot{\mathcal{V}}_{R1}(\mathbf{r}), \\ \dot{\Pi}_{R1}(\mathbf{r}) &= \epsilon_0 \nabla^2 \mathcal{V}_{R1}(\mathbf{r}) + 4\pi \rho^{q\sigma}(\mathbf{r}, t), \end{aligned} \quad (\text{B.9})$$

which is an inhomogeneous wave equation with speed $c_l^2 = \epsilon_0/\nu$.

If the smooth charge density is linear in time, these equations can be solved by introducing a modified potential

$$\tilde{\mathcal{V}}_{R1}(\mathbf{r}, t) = \mathcal{V}_{R1}(\mathbf{r}, t) - \mathcal{V}_e(\mathbf{r}, t), \quad (\text{B.10})$$

where $\mathcal{V}_e(\mathbf{r}, t)$ is the solution of Poisson's equation

$$\nabla^2 \mathcal{V}_e(\mathbf{r}, t) = -\frac{4\pi}{\epsilon_0} \rho^{q\sigma}(\mathbf{r}, t). \quad (\text{B.11})$$

In this case, because the second derivative of $\mathcal{V}_e(\mathbf{r}, t)$ vanishes, $\tilde{\mathcal{V}}_{R1}(\mathbf{r}, t)$ satisfies a homogeneous wave equation with speed c_l

$$\frac{\partial^2 \tilde{\mathcal{V}}_{R1}(\mathbf{r}, t)}{\partial t^2} = c_l^2 \nabla^2 \tilde{\mathcal{V}}_{R1}(\mathbf{r}, t), \quad (\text{B.12})$$

which is the solution of Poisson's equation superposed with homogeneous wave solutions. If the charge density is not linear this solution is still approximately correct if the field is slowly varying. This is an important feature of these differential equations.

For the full LMF Hamiltonian we include an index α for the different particle species, and a pair potential $u_0^{\alpha\beta}(|\mathbf{r}_i - \mathbf{r}_j|)$ between species α and β , which includes the short range Coulomb interaction and the Lennard-Jones interaction, and an external field $\phi(\mathbf{r}, t)$. Using this full Hamiltonian in equation (B.2) then yields a generalized Liouville equation

$$\begin{aligned} \frac{\partial f_\alpha}{\partial t} + \sum_i \left[\frac{\mathbf{p}_i}{m_\alpha} \cdot \frac{\partial f_\alpha}{\partial \mathbf{r}_i} - \frac{\partial f_\alpha}{\partial \mathbf{p}_i} \cdot \frac{\partial}{\partial \mathbf{r}_i} \left(\phi(\mathbf{r}, t) + q_\alpha \mathcal{V}_{R1}^\sigma(\mathbf{r}, t) + \sum_{\beta, j} u_0^{\alpha\beta}(|\mathbf{r}_i - \mathbf{r}_j|) \right) \right] \\ + \int d\mathbf{r} \left(\frac{\Pi_{R1}(\mathbf{r})}{\nu} \frac{\delta f_\alpha}{\delta \mathcal{V}_{R1}(\mathbf{r})} + (\epsilon_0 \nabla^2 \mathcal{V}_{R1}(\mathbf{r}) + 4\pi \rho^{q\sigma}(\mathbf{r}, t)) \frac{\delta f_\alpha}{\delta \Pi_{R1}(\mathbf{r})} \right) = 0, \quad (\text{B.13}) \end{aligned}$$

where i sums over all particles of type α , and j over particles of type β . The terms

in the first line of this equation are recognizable as the usual Liouville equation, whereas the terms in the second equation arise due to the introduction of extra phase space degrees of freedom.

The extra terms in equation (B.13) may seem to complicate the equation, but they can be integrated out in order to derive a generalized BBGKY hierarchy. In particular, we can perform a functional integration of this equation over all of the field configuration degrees of freedom, and all of the extra terms vanish, because the integral of a total functional derivative vanishes, where we assume that the phase space density vanishes at infinite field strength. We note the importance of using a Hamiltonian system to achieve this cancellation, in addition to the fact that $\frac{\delta \mathcal{H}}{\delta \mathcal{V}_{R1}}$ must not depend on \mathcal{V}_{R1} , and similarly for Π_{R1} . After the integration, equation (B.13) becomes

$$\begin{aligned} \frac{\partial f_{r,\alpha}}{\partial t} + \sum_i \left(\frac{\mathbf{p}_i}{m_\alpha} \cdot \frac{\partial f_{r,\alpha}}{\partial \mathbf{r}_i} - \frac{\partial f_{r,\alpha}}{\partial \mathbf{p}_i} \cdot \frac{\partial}{\partial \mathbf{r}_i} \left(\phi(\mathbf{r}, t) + \sum_{\beta,j} u_0^{\alpha\beta}(|\mathbf{r}_i - \mathbf{r}_j|) \right) \right) \\ = \sum_i q_\alpha \left\langle \frac{\partial f_\alpha}{\partial \mathbf{p}_i} \cdot \frac{\partial}{\partial \mathbf{r}_i} \mathcal{V}_{R1}^\sigma(\mathbf{r}, t) \right\rangle_{\mathcal{V}}. \end{aligned} \quad (\text{B.14})$$

where we have defined the total phase space average,

$$\langle A(\Gamma) \rangle = \int \int [D\mathcal{V}_{R1}] [D\Pi_{R1}] A(\Gamma), \quad (\text{B.15})$$

and we have defined a reduced phase space density $f_{r,\alpha}(\mathbf{r}^N, \mathbf{p}^N) = \langle f_\alpha(\Gamma) \rangle_{\mathcal{V}}$. The notation $\int [DF]$ for a field F denotes the functional integration, which we will assume is well defined.

Equation (B.14) is very similar to the Liouville equation, differing only in the average over the field phase space. The same manipulations that lead to the BBGKY hierarchy can be used to simplify this equation, and the first equation in the hierarchy is

$$\begin{aligned} & \left(\frac{\partial}{\partial t} + \frac{\mathbf{p}}{m_\alpha} \cdot \nabla - \nabla \phi(\mathbf{r}, t) \cdot \frac{\partial}{\partial \mathbf{p}} \right) f_{r,\alpha}^{(1)}(\mathbf{r}, \mathbf{p}; t) - q_\alpha \left\langle \frac{\partial f_\alpha^{(1)}(\mathbf{r}, \mathbf{p}; t, \Gamma_\nu)}{\partial \mathbf{p}} \cdot \frac{\partial}{\partial \mathbf{r}} \mathcal{V}_{R1}^\sigma(\mathbf{r}, t) \right\rangle_\nu \\ & = \sum_\beta \int \int \nabla u_0^{\alpha\beta}(|\mathbf{r} - \mathbf{r}'|) \cdot \frac{\partial}{\partial \mathbf{p}} f_{r,\alpha\beta}^{(2)}(\mathbf{r}, \mathbf{p}, \mathbf{r}', \mathbf{p}'; t) d\mathbf{r}' d\mathbf{p}'. \end{aligned} \quad (\text{B.16})$$

Again, this equation is exactly analogous to the usual BBGKY hierarchy, with an additional phase space average. We can use the same manipulations as in chapter 3 to find

$$\begin{aligned} m_\alpha \left(\frac{\partial}{\partial t} \mathbf{j}_{r,\alpha}(\mathbf{r}; t) + \nabla \cdot \tilde{Q}_{r,\alpha}(\mathbf{r}; t) \right) & = \rho_{r,\alpha}(\mathbf{r}, t) \nabla \phi(\mathbf{r}, t) + \frac{1}{\beta} \nabla \rho_{r,\alpha}(\mathbf{r}; t) \\ & + \langle \rho_\alpha(\mathbf{r}; t, \Gamma_\nu) \nabla \mathcal{V}_{R1}^\sigma(\mathbf{r}; t) \rangle_\nu + \rho_{r,\alpha}(\mathbf{r}; t) \sum_\beta \int \nabla u_0^{\alpha\beta}(|\mathbf{r} - \mathbf{r}'|) \rho_{r,\alpha\beta}(\mathbf{r}|\mathbf{r}'; t) d\mathbf{r}', \end{aligned} \quad (\text{B.17})$$

where the definitions are the same as before. Here again, the only difference from the equation derived previously is the presence of the phase space average.

Given that all the terms in equation (B.17) are the same as they were in the chapter 3, besides the field average of the term $\langle \rho_\alpha(\mathbf{r}; t) \nabla \mathcal{V}_R(\mathbf{r}; t) \rangle_\nu$, the arguments leading to LMF theory go through exactly the same way as in the previous paper, and the generalized LMF equation takes the form

$$\langle \rho^q(\mathbf{r}; t, \Gamma_\nu) \nabla \mathcal{V}_{R1}^\sigma(\mathbf{r}; t) \rangle_\nu = \rho_r^q(\mathbf{r}; t) \nabla \left(\phi(\mathbf{r}; t) + \int \rho_r^q(\mathbf{r}'; t) v_1^\sigma(|\mathbf{r} - \mathbf{r}'|) d\mathbf{r}' \right). \quad (\text{B.18})$$

Here the gradient cannot be taken out of the average, because then it would also act on $\rho(\mathbf{r}; t)$, which is why it is included here in the LMF equation. This modified LMF equation is different in character than the original LMF equation, because the average over field configurations cannot be chosen, and instead it takes a value that is determined by the dynamics. In other words, the equation must be proved. In the following, we will argue that in certain circumstances the Hamiltonian (B.8) will give rise to dynamics that approximately satisfy this equation.

The argument that equation (B.18) holds approximately requires a separation of time scales. We have in mind a solvent, like water, with a timescale τ_f of interaction that is much faster than other time scales in the system, denoted τ_s . The parameter ν is then chosen to effectively average over time scales longer than the time scale of the solvent, but shorter than all other relevant time scales. This will allow us to assume that the fluctuations in the charge density are approximately uncorrelated with the fluctuations in the long range forces, or

$$\langle \delta\rho^q(\mathbf{r}; t, \Gamma_\nu) \delta\nabla\mathcal{V}_{Rl}^\sigma(\mathbf{r}; t) \rangle_\nu \approx 0, \quad (\text{B.19})$$

where here we use the notation

$$\delta A(\Gamma) = A(\Gamma) - \langle A(\Gamma) \rangle_\nu. \quad (\text{B.20})$$

This will be approximately true when the time scale of averaging is longer than the time scale of fluctuations, because the instantaneous fluctuations in the charge

density will not dramatically affect the long range forces, which reflect the dynamics on a longer time scale.

If we can make the approximation (B.19), then equation (B.18) can be rewritten

$$\langle \mathcal{V}_{R1}^\sigma(\mathbf{r}; t) \rangle = \phi(\mathbf{r}; t) + \int \langle \rho^q(\mathbf{r}'; t) \rangle v_1^\sigma(|\mathbf{r} - \mathbf{r}'|) d\mathbf{r}' + C, \quad (\text{B.21})$$

where the average is now independent of $\rho^q(\mathbf{r}; t, \Gamma_\nu)$, and so can be taken over the entire phase space. This is closer to the familiar form of the LMF equation. To show that this equation holds approximately, we multiply equation (B.13) separately by $\mathcal{V}_{R1}(\mathbf{r})$ and $\Pi_{R1}(\mathbf{r})$, then integrate over all phase space to obtain

$$\begin{aligned} \langle \Pi(\mathbf{r}) \rangle &= \nu \langle \dot{\mathcal{V}}(\mathbf{r}) \rangle, \\ \langle \dot{\Pi}(\mathbf{r}) \rangle &= \epsilon_0 \langle \nabla^2 \mathcal{V}_{R1}(\mathbf{r}) \rangle + 4\pi \langle \rho^{q\sigma}(\mathbf{r}, t) \rangle, \end{aligned} \quad (\text{B.22})$$

which is the ensemble averaged version of Hamilton's equations. As argued previously, in the presence of a separation of time scales, characterized by the inequality $\nu \frac{\partial^2}{\partial t^2} \mathcal{V}_e(\mathbf{r}, t) \ll 4\pi \rho^{q\sigma}(\mathbf{r}, t)$, the solution to these equations are the solution to Poisson's equation superposed with wave solutions. This separation of time scales is exactly the opposite as that used previously, because it requires that the field dynamics are faster than the slow dynamics of the system. The field effectively averages over the fast degrees of freedom, but is faster than the slow degrees of freedom, which is the situation we wish to describe with LMF theory. If this approximation is accurate, then equation (B.21) approximately holds.

In the case of a time independent charge density $\rho^{q\sigma}(\mathbf{r})$ we can again subtract the time independent solution of Poisson's equation and define

$$\tilde{\mathcal{V}}_{R1}(\mathbf{r}, t) = \mathcal{V}_{R1}(\mathbf{r}, t) - \mathcal{V}_e(\mathbf{r}, t), \quad (\text{B.23})$$

so that $\tilde{\mathcal{V}}_{R1}$ satisfies the equation

$$\frac{\partial^2}{\partial t^2} \tilde{\mathcal{V}}_{R1}(\mathbf{r}, t) + \frac{1}{\tau_0} \frac{\partial}{\partial t} \tilde{\mathcal{V}}_{R1}(\mathbf{r}, t) = c_l^2 \nabla^2 \tilde{\mathcal{V}}_{R1}(\mathbf{r}, t). \quad (\text{B.24})$$

After a Fourier transform, we find

$$\frac{\partial^2}{\partial t^2} \tilde{\mathcal{V}}_{R1}(\mathbf{k}, t) + \frac{1}{\tau_0} \frac{\partial}{\partial t} \tilde{\mathcal{V}}_{R1}(\mathbf{k}, t) + c_l^2 k^2 \tilde{\mathcal{V}}_{R1}(\mathbf{k}, t) = 0, \quad (\text{B.25})$$

where no extra tilde is included for the Fourier transform. This is the equation of a damped harmonic oscillator with frequency $\omega_0^2 = c_l^2 k^2$ and damping ratio $\zeta = (2kc_l\tau_0)^{-1}$. We therefore find that the system becomes overdamped for fourier modes for which $2kc_l < \tau_0^{-1}$.

Although this approach to the problem is theoretically and practically complicated, it could in principle lead to an interesting alternative approach to non-equilibrium LMF theory. In the next section, we consider another alternative approach.

B.3 Generalized linear response approach to non-equilibrium LMF theory

The non-equilibrium form of the linear response equation is usually stated in frequency space, for a uniform fluid in the presence of an oscillating field

$$\langle \Delta \rho_{\mathbf{k}}(t) \rangle \approx \chi_{\rho\rho}(k, \omega) \phi_{\mathbf{k}} \exp(-i\omega t). \quad (\text{B.26})$$

The derivation of this equation uses the Liouville equation, which is split into an equilibrium component \mathcal{L}_0 and a perturbation, and then solved for the perturbation. We will proceed with a similar derivation, modifying some of the details. For the non-equilibrium linear response derivation, we will loosely follow Hansen and McDonald [23].

To begin, as in the derivation of Hu and Weeks, let us assume that we have a “trial” solution for the LMF potential as a function of time, which we denote $\tilde{\phi}_0(\mathbf{r}; t)$. The correction to this potential, which we will treat as a perturbation, will be denoted $\tilde{\phi}_{R1}(\mathbf{r}; t)$. Consider the full phase space distribution $f^{[N]}(\mathbf{r}^N, \mathbf{p}^N, t)$, which will be denoted $f^{[N]}(\Gamma, t)$ for the configuration dependence. This function satisfies the Liouville equation

$$\frac{\partial f^{[N]}(\Gamma, t)}{\partial t} = -i\mathcal{L}(\Gamma, t)f^{[N]}(\Gamma, t), \quad (\text{B.27})$$

where $\mathcal{L}(\Gamma, t) = i\{\mathcal{H}(\Gamma, t), \cdot\}$ represents the Liouville operator, $\{\cdot, \cdot\}$ is the Poisson

bracket, and we explicitly include the time dependence to contrast this from the case where the reference system is stationary. In this case, the Hamiltonian is given by

$$\mathcal{H}(\Gamma, t) = \mathcal{H}_0(\Gamma, t) + \mathcal{H}_1(\Gamma, t), \quad (\text{B.28})$$

where we defined the trial Hamiltonian $\mathcal{H}_0 = U_0 + \Phi_0$. The Liouville equation then becomes

$$\frac{\partial f^{[N]}(\Gamma, t)}{\partial t} = -i\mathcal{L}_0(\Gamma, t)f^{[N]}(\Gamma, t) + \{\mathcal{H}_1(\Gamma, t), f^{[N]}(\Gamma, t)\}. \quad (\text{B.29})$$

We will be interested in the response of the density to the change in the potential relative to the trial system. For this reason, we write

$$f^{[N]}(\Gamma, t) = f_0^{[N]}(\Gamma, t) + \Delta f^{[N]}(\Gamma, t), \quad (\text{B.30})$$

where $f_0^{[N]}(\Gamma, t)$ is the phase space density of an ensemble evolving under the reference Hamiltonian. To first order in the perturbation, we find

$$\frac{\partial \Delta f^{[N]}(\Gamma, t)}{\partial t} = -i\mathcal{L}_0(\Gamma, t)f^{[N]}(\Gamma, t) + \{\mathcal{H}_1(\Gamma, t), f_0^{[N]}(\Gamma, t)\}. \quad (\text{B.31})$$

The solution to this equation is

$$\Delta f^{[N]}(\Gamma, t) = \int_{-\infty}^t ds \mathcal{T} \left(e^{-i \int_s^t \mathcal{L}_0(\Gamma, \tau) d\tau} \right) \{ \mathcal{H}_1(\Gamma, s), f_0^{[N]}(\Gamma, s) \}, \quad (\text{B.32})$$

where we have introduced the time ordering operator \mathcal{T} , which is necessary when the reference system depends on time.

In order to simplify the Poisson bracket appearing in the above equation, we will introduce the assumption of local equilibrium, which asserts that the function $f_0^{[N]}(\Gamma, t)$ takes the form

$$f^{[N]}(\mathbf{r}^N, \mathbf{p}^N; t) = \prod_{i=1}^N e^{-\frac{1}{2}\beta(\mathbf{p}_i - m\mathbf{v}(\mathbf{r}_i, t))^2} g^{[N]}(\mathbf{r}^{[N]}, t). \quad (\text{B.33})$$

In this equation, the function $\mathbf{v}(\mathbf{r}; t)$ is the average velocity of the system $\langle \mathbf{p}(\mathbf{r}; t)/m \rangle$. This hypothesis should be valid for systems that have a separation of time scales. We have in mind the case of a relatively slowly varying external field with quickly equilibrating particles responding to the changes in this field. An important example of such a system would be a large protein in the presence of water, where the time scale of relaxation for the water molecules is much faster than that of the protein. In this case, the water should satisfy the local equilibrium hypothesis to a good approximation, and the following analysis will approximate the dynamics accurately.

Given the local equilibrium hypothesis, the Poisson bracket can be simplified as follows

$$\begin{aligned} \{\mathcal{H}_1(\Gamma, s), f_0^{[N]}(\Gamma, s)\} &= \sum_{i=1}^N \nabla \tilde{\Phi}(\mathbf{r}_i, s) \cdot \frac{\partial f_0^{[N]}(\Gamma, s)}{\partial \mathbf{p}_i} \\ &= \beta \sum_{i=1}^N \mathbf{F}_{R1}(\mathbf{r}_i, s) \cdot (\mathbf{v}_i - \mathbf{v}(\mathbf{r}_i, t)) f_0^{[N]}(\Gamma, s), \end{aligned} \quad (\text{B.34})$$

where $\mathbf{F}_{R1}(\mathbf{r}_i, s) = -\nabla \tilde{\Phi}_{R1}(\mathbf{r}_i, s)$ is the force from the modified potential. To simplify

this equation, we define the total power of the system at time s

$$P(\Gamma, s) = \sum_{i=1}^N \mathbf{F}_{R1}(\mathbf{r}_i, s) \cdot \mathbf{v}(\mathbf{r}_i, s), \quad (\text{B.35})$$

so that equation (B.34) becomes

$$\{\mathcal{H}_1(\Gamma, s), f_0^{[N]}(\Gamma, s)\} = \beta \delta P(\Gamma, s) f_0^{[N]}(\Gamma, s),$$

where $\delta P(\Gamma, s) = P(\Gamma, s) - \langle P(s) \rangle$. Using this formula, equation (B.32) becomes

$$\Delta f^{[N]}(\Gamma, t) = \beta \int_{-\infty}^t ds \int d\Gamma' K_0(\Gamma, t | \Gamma', s) P(\Gamma', s) f_0^{[N]}(\Gamma', s),$$

where $K_0(\Gamma, t | \Gamma', s) = \mathcal{T} \left(e^{-i \int_s^t \mathcal{L}_0(\Gamma, \tau) d\tau} \right) \delta(\Gamma - \Gamma')$ is the propagator of the reference system.

We now consider the expectation value of an observable $A(\Gamma, t)$

$$\langle A(t) \rangle = \frac{\int d\Gamma A(\Gamma, t) f^{[N]}(\Gamma, t)}{\int d\Gamma f^{[N]}(\Gamma, t)}.$$

Linearizing this equation to first order in $\langle \Delta A(t) \rangle$ and $\Delta f^{[N]}(\Gamma, t)$, we find

$$\langle A(t) \rangle \approx \langle A(t) \rangle_{ref} + \beta \int_{-\infty}^t ds \langle \delta A(t) \delta P(s) \rangle_{ref}, \quad (\text{B.36})$$

where $\delta A(\Gamma, s) = A(\Gamma, s) - \langle A(s) \rangle_{ref}$.

We will be interested in deriving a differential equation for the expectation

value $\langle A(t) \rangle$. For this purpose, we will consider an unusual reference system. We will assume that our reference system is correct at times $s < t$, and consider this equation at times t and $t + \delta t$. The perturbation of the Hamiltonian will only be turned on at times $s = t + \delta t$ for small δt , so that equation (B.28) becomes

$$\mathcal{H}(\Gamma, s) = \begin{cases} \mathcal{H}_0(\Gamma, s), & s < t \\ \mathcal{H}_0(\Gamma, t) + \delta t \frac{\partial}{\partial t} \phi(\Gamma, t), & s = t + \delta t. \end{cases} \quad (\text{B.37})$$

For this particular choice of reference system, the perturbation vanishes for times $s < t$, so $P(s)$ also vanishes for times $s < t$. Subtracting equation (B.36) at times t and $t + \delta t$, and using the vanishing of $P(s)$ for $s < t$, we find

$$\langle A(t + \delta t) - A(t) \rangle \approx \langle A(t + \delta t) - A(t) \rangle_{ref} + \beta \int_t^{t+\delta t} ds \langle \delta A(t + \delta t) \delta P(s) \rangle_{ref}.$$

Dividing by δt and taking the limit as $\delta t \rightarrow 0$, we find

$$\frac{\partial \langle A(t) \rangle}{\partial t} = \frac{\partial \langle A(t) \rangle_{ref}}{\partial t} + \beta \langle \delta A(t) \delta P(t) \rangle_{ref}. \quad (\text{B.38})$$

In the context of LMF theory, this will give a self consistent for the change in the LMF potential.

It was shown previously that the non-equilibrium generalization of the LMF equation is given by

$$\phi_R(\mathbf{r}; t) = \phi(\mathbf{r}, t) + \int \rho_R(\mathbf{r}', t) u_1(|\mathbf{r} - \mathbf{r}'|) d\mathbf{r}' + C, \quad (\text{B.39})$$

where here $\rho_R(\mathbf{r}', t)$ refers to the ensemble averaged singlet density, $\phi(\mathbf{r}, t)$ is the external field, and $u_1(|\mathbf{r} - \mathbf{r}'|)$ is the long range component of the interaction under consideration. In the case of the Coulomb interaction, the LMF equation can be written in differential form as

$$\vec{\nabla}^2 \mathcal{V}_{R1}(\mathbf{r}, t) = -\frac{4\pi}{\epsilon} \langle \rho_{R,tot}^{q\sigma}(\mathbf{r}, t) \rangle,$$

where we have defined the instantaneous smooth charge density, which is the convolution of the charge density with a unit Gaussian charge distribution of width σ . We include the ensemble average here because we will also consider the smooth charge density of individual realizations of the ensemble.

The idea behind the linear response approach is to use equation (B.38), in conjunction with the differential form of the LMF equation, to correct the LMF potential at every timestep. This approach was not implemented, but the theoretical work does show some promise, and therefore could be worth pursuing in future work.

Appendix C: Thermofield dynamics background and calculations

C.1 Canonical transformations

The most general canonical transformation that retains the type of statistics can formally be written as a unitary transformation on the many-particle Hilbert space [95][96]. For a system of N particle excitations, the many particle Hilbert space is spanned by 2^N basis functions, which are labeled χ_i , where we take χ_0 to be the vacuum. The group $SU(2^N)$ acts on this basis, whose action can be written as a polynomial of Fermi operators. To do this, define Wenger's matrix, which satisfies $m_{ij}\chi_k = \chi_i\delta_{jk}$. This can be generated by explicitly constructing m_{0j} , then using the relations $m_{i,0} = m_{0,i}^\dagger$ and $m_{i,j} = m_{i,0}m_{0,j}$. Given a matrix $x \in SU(2^N)$, define the polynomial

$$P(x) = Tr(xm). \quad (\text{C.1})$$

When acting on the Hilbert space in the usual way, this polynomial induces the unitary transformation x . Also, these polynomials satisfy $P(x)P(y) = P(xy)$ and $P(x^\dagger) = P(x)^\dagger$. The most general canonical transformation of operators can then be written

$$\hat{a}_\alpha \rightarrow P(x)^\dagger \hat{a}_\alpha P(x). \quad (\text{C.2})$$

These transformations are probably too general for practical calculation, but this construction shows how large the space of canonical transformations is for a given Hilbert space.

We can also consider canonical transformations from an infinitesimal point of view

$$\hat{a}_\alpha \rightarrow \hat{a}_\alpha + \delta\hat{a}_\alpha, \quad (\text{C.3})$$

For this transformation to be canonical, the variation must satisfy

$$[\hat{a}_\alpha, \delta\hat{a}_\beta]_\zeta = -[\delta\hat{a}_\alpha, \hat{a}_\beta]_\zeta, \quad [\hat{a}_\alpha, \delta\hat{a}_\beta^\dagger]_\zeta = -[\delta\hat{a}_\alpha, \hat{a}_\beta^\dagger]_\zeta, \quad (\text{C.4})$$

where we include excitations with Fermionic or Bosonic statistics, defined by $[\hat{a}_\alpha, \hat{a}_\beta]_\zeta = \hat{a}_\alpha\hat{a}_\beta - \zeta\hat{a}_\beta\hat{a}_\alpha$. By inserting the resolution of the identity, we find the variation of the vacuum

$$|\Omega\rangle \rightarrow \left(1 - \sum_\alpha \hat{a}_\alpha^\dagger \frac{1}{\hat{N}_\alpha + 1} \delta\hat{a}_\alpha\right) |\Omega\rangle, \quad (\text{C.5})$$

where $\hat{N}_\alpha = \sum_\alpha \hat{a}_\alpha^\dagger \hat{a}_\alpha$ is the number operator in this basis. This can also be checked by acting with the transformed annihilation operators.

C.2 Incremental optimization

Here we derive equation (6.37) in a more rigorous way. First, we define $|\psi_0\rangle = |\psi(t)\rangle$ and $|\psi\rangle = |\psi(t + \delta t)\rangle = (1 - i\delta t\hat{\mathcal{H}})|\psi_0\rangle$. Assume that $\langle\psi_0|\psi_0\rangle = 1$, which can always be chosen. Define $|v\rangle = |\psi_0\rangle + |\epsilon\rangle$, where $|\epsilon\rangle$ is small, and similarly $\lambda = 1 + \epsilon$. With these definitions, and keeping only terms of at most second order in small

quantities, equation (6.36) becomes

$$\langle \delta\psi_0 | \left(1 - |\psi_0\rangle\langle\psi_0|\right) i |\epsilon\rangle = \delta t \langle \delta\psi_0 | \left(\hat{\mathcal{H}} - \langle\hat{\mathcal{H}}\rangle - \frac{\epsilon}{\delta t}\right) |\psi_0\rangle. \quad (\text{C.6})$$

If we define $\partial_t |\psi\rangle = \lim_{\delta t \rightarrow 0} \frac{|\epsilon\rangle}{\delta t}$ and $R = \lim_{\delta t \rightarrow 0} \frac{\epsilon}{\delta t}$, this gives equation (6.37).

C.3 Relations between unitary transformations

To prove equation (6.56), we first note that

$$\hat{a}_0 = \frac{1}{\sqrt{2}}(\hat{v}_0 + \hat{w}_0). \quad (\text{C.7})$$

The basis at time t is related to the original basis by a unitary transformation of the form

$$\begin{bmatrix} \hat{v}_0 \\ \hat{w}_0 \end{bmatrix} = \begin{bmatrix} A & B \\ C & D \end{bmatrix} \begin{bmatrix} \hat{v} \\ \hat{w} \end{bmatrix}. \quad (\text{C.8})$$

Using this in equation (C.7) yields

$$\hat{a}_0 = \frac{1}{\sqrt{2}}\left((A + C)\hat{v} + (B + D)\hat{w}\right). \quad (\text{C.9})$$

from which one can read off $M = \frac{1}{\sqrt{2}}(A + C)$ and $N = \frac{1}{\sqrt{2}}(B + D)$. Because the matrix is unitary, the blocks satisfy the constraints

$$AA^\dagger + BB^\dagger = I, \quad CC^\dagger + DD^\dagger = I, \quad AC^\dagger + BD^\dagger = 0. \quad (\text{C.10})$$

The left singular vectors of a matrix M are the eigenvectors of MM^\dagger . Using equations (C.10) we find the relation

$$MM^\dagger = I - NN^\dagger, \quad (\text{C.11})$$

which shows that the matrices M and N have the same left singular vectors. Therefore, there exist unitary matrices U , V , and W and diagonal matrices Λ and $\tilde{\Lambda}$ that satisfy

$$U\hat{a}_0 = \tilde{\Lambda}V\hat{v} + \Lambda W\hat{w}, \quad (\text{C.12})$$

where U^\dagger is the matrix of left singular vectors for M and N . Diagonalizing equation (C.11) with this matrix, we find the relation

$$\tilde{\Lambda}^2 = 1 - \Lambda^2. \quad (\text{C.13})$$

Because the singular values can always be chosen to be real, this also implies that they lie in the interval $[0, 1]$.

It is useful to obtain differential equations relating the various matrices defined above. The change in the operators v and w are given by

$$\partial_t \hat{v} = iY\hat{w} + iX\hat{v}, \quad \partial_t \hat{w} = iY^\dagger \hat{v} + i\tilde{X}\hat{w}. \quad (\text{C.14})$$

The unitary transformations implemented above are obtained infinitesimally from equation (6.50). Define the generator of the unitary transformation on the basis \hat{a}

by J so that

$$\partial_t \hat{a} = iJ\hat{a}. \quad (\text{C.15})$$

where J , X , and \tilde{X} are Hermitian. Taking a derivative of equation (6.56) we find

$$(\tilde{\Lambda}X - J\tilde{\Lambda} + \Lambda Y^\dagger - i\partial_t \tilde{\Lambda})\hat{v} + (\Lambda\tilde{X} - J\Lambda + \tilde{\Lambda}Y - i\partial_t \Lambda)\hat{w} = 0. \quad (\text{C.16})$$

If the eigenvalues of Λ are non-degenerate, this equation can be solved by choosing

$$J_{\alpha\beta} = \frac{[\Lambda Y^\dagger \tilde{\Lambda} - \tilde{\Lambda} Y \Lambda]_{\alpha\beta}}{\lambda_\alpha^2 - \lambda_\beta^2}, \quad X_{\alpha\beta} = \frac{[\tilde{\Lambda} \Lambda Y^\dagger - Y \Lambda \tilde{\Lambda}]_{\alpha\beta}}{\lambda_\alpha^2 - \lambda_\beta^2}, \quad \tilde{X}_{\alpha\beta} = \frac{[Y^\dagger \Lambda \tilde{\Lambda} - \Lambda \tilde{\Lambda} Y]_{\alpha\beta}}{\lambda_\alpha^2 - \lambda_\beta^2} \quad (\text{C.17})$$

for $\alpha \neq \beta$. For the diagonal elements, the real part can also be canceled by the unitary transformations, and the imaginary part gives

$$\partial_t \tilde{\lambda}_\alpha = -\text{Im}(Y_{\alpha\alpha})\lambda_\alpha, \quad \partial_t \lambda_\alpha = \text{Im}(Y_{\alpha\alpha})\tilde{\lambda}_\alpha. \quad (\text{C.18})$$

These equations can also be derived from first order perturbation theory on the matrix MM^\dagger under a small transformation (6.51) to find J , and similarly for X and \tilde{X} . Under a small transformation, $MM^\dagger = (\tilde{\Lambda} + i\varepsilon\Lambda Y^\dagger)(\tilde{\Lambda} - i\varepsilon Y \Lambda)$. In the case of degeneracies one must use degenerate perturbation theory, first diagonalize the perturbing matrix in the degenerate subspace. In the case of J , for example,

this means first solving the eigenvalue problem

$$i\varepsilon(\Lambda Y^\dagger \tilde{\Lambda} - \tilde{\Lambda} Y \Lambda)_{\alpha\beta} u_\beta = (\delta\tilde{\lambda}_\alpha^2) u_\alpha \quad (\text{C.19})$$

in this subspace.

Bibliography

- [1] X. Wu, B. R. Brooks, *The Journal of Chemical Physics* **129**, 154115 (2008).
- [2] C. J. Fennell, J. D. Gezelter, *The Journal of Chemical Physics* **124**, 234104 (2006).
- [3] S. Izvekov, J. M. J. Swanson, G. A. Voth, *The Journal of Physical Chemistry B* **112**, 4711 (2008). PMID: 18366209.
- [4] M. Deserno, C. Holm, *The Journal of Chemical Physics* **109**, 7694 (1998).
- [5] J. de Joannis, A. Arnold, C. Holm, *The Journal of Chemical Physics* **117**, 2503 (2002).
- [6] P. Hunenberger, J. McCammon, *Biophysical Chemistry* **78**, 69 (1999).
- [7] I. Nezbeda, *Molecular Physics* **103**, 59 (2005).
- [8] R. C. Remsing, J. M. Rodgers, J. D. Weeks, *Journal of Statistical Physics* **145**, 313 (2011).
- [9] F. Figueirido, G. S. Del Buono, R. M. Levy, *The Journal of Chemical Physics* **103**, 6133 (1995).
- [10] J. M. Rodgers, J. D. Weeks, *Journal of Physics: Condensed Matter* **20**, 494206 (2008).
- [11] Y.-g. Chen, C. Kaur, J. D. Weeks, *The Journal of Physical Chemistry B* **108**, 19874 (2004).
- [12] Y.-G. Chen, J. D. Weeks, *Proceedings of the National Academy of Sciences* **103**, 7560 (2006).
- [13] J. M. Rodgers, J. D. Weeks, *Proceedings of the National Academy of Sciences* **105**, 19136 (2008).

- [14] Z. Hu, J. D. Weeks, *Phys. Rev. Lett.* **105**, 140602 (2010).
- [15] B. Widom, *Science* **157**, 375 (1967).
- [16] J. D. Weeks, D. Chandler, H. C. Andersen, *The Journal of Chemical Physics* **54**, 5237 (1971).
- [17] H. C. Andersen, J. D. Weeks, D. Chandler, *Phys. Rev. A* **4**, 1597 (1971).
- [18] R. C. Remsing III, From structure to thermodynamics with local molecular field theory, Ph.D. thesis, Institute for Physical Science and Technology, UMCP (2013).
- [19] R. Evans, *Density Functionals in the Theory of Non-Uniform Fluids* (Marcel Dekker, 1992), pp. 85 – 175.
- [20] A. Gao, Manipulating and simplifying the intermolecular interactions in liquid mixtures, Ph.D. thesis, Institute for Physical Science and Technology, UMCP (2017).
- [21] J. Rodgers, Z. Hu, J. Weeks, *Molecular Physics* **109** (2010).
- [22] J. M. Rodgers, J. D. Weeks, *The Journal of Chemical Physics* **131**, 244108 (2009).
- [23] J. Hansen, I. McDonald, *Theory of Simple Liquids* (Elsevier Science, 1990).
- [24] S. Harris, *An Introduction to the Theory of the Boltzmann Equation*, Dover books on physics (Dover Publications, 2004).
- [25] L. Landau, E. Lifshitz, *Statistical Physics*, no. v. 5 (Elsevier Science, 2013).
- [26] L. Landau, E. Lifshitz, *Fluid Mechanics*, no. v. 6 (Elsevier Science, 2013).
- [27] C. Jarzynski, *Phys. Rev. Lett.* **78**, 2690 (1997).
- [28] J. M. Rodgers, J. D. Weeks, *Journal of Physics: Condensed Matter* **20**, 494206 (2008).
- [29] Y.-g. Chen, C. Kaur, J. D. Weeks, *The Journal of Physical Chemistry B* **108**, 19874 (2004).
- [30] J. M. Rodgers, J. D. Weeks, *Proceedings of the National Academy of Sciences* **105**, 19136 (2008).
- [31] J. Hansen, I. McDonald, *Theory of Simple Liquids* (Elsevier Science, 2006).
- [32] S. Wang, J. A. Krumhansl, *The Journal of Chemical Physics* **56**, 4287 (1972).
- [33] S. E. Feller, *et al.*, *The Journal of Physical Chemistry* **100**, 17011 (1996).

- [34] C. Lee, J. A. McCammon, P. J. Rossky, *The Journal of Chemical Physics* **80**, 4448 (1984).
- [35] I.-C. Yeh, M. L. Berkowitz, *The Journal of Chemical Physics* **110**, 7935 (1999).
- [36] Z. Zhao, D. M. Rogers, T. L. Beck, *The Journal of Chemical Physics* **132** (2010).
- [37] A. J. Lee, S. W. Rick, *The Journal of Chemical Physics* **134** (2011).
- [38] P. A. Bopp, A. A. Kornyshev, G. Sutmann, *The Journal of Chemical Physics* **109**, 1939 (1998).
- [39] F. Sedlmeier, S. Shadkhoo, R. Bruinsma, R. R. Netz, *The Journal of Chemical Physics* **140** (2014).
- [40] P. W. Rosenkranz, *IEEE Transactions on Geoscience and Remote Sensing* **53**, 1387 (2015).
- [41] J. T. Kindt, , C. A. Schmuttenmaer, *The Journal of Physical Chemistry* **100**, 10373 (1996).
- [42] D. Borgis, R. Assaraf, B. Rotenberg, R. Vuilleumier, *Molecular Physics* **111**, 3486 (2013).
- [43] D. de las Heras, M. Schmidt, *Phys. Rev. Lett.* **120**, 218001 (2018).
- [44] J. Comer, *et al.*, *The Journal of Physical Chemistry B* **119**, 1129 (2015). PMID: 25247823.
- [45] Y. wu, H. L. Tepper, G. A. Voth **124**, 024503 (2006).
- [46] S. W. Coles, D. Borgis, R. Vuilleumier, B. Rotenberg, *The Journal of Chemical Physics* **151**, 064124 (2019).
- [47] J. Liouville, *Journal de mathématiques pures et appliquées* (1838).
- [48] G. S. Ezra, *Journal of Mathematical Chemistry* **32**, 339 (2002).
- [49] G. S. Ezra, *Journal of Mathematical Chemistry* **35**, 29 (2004).
- [50] W.-H. Steeb, *Physica A: Statistical Mechanics and its Applications* **95**, 181 (1979).
- [51] J.-P. Ryckaert, G. Ciccotti, H. J. Berendsen, *Journal of Computational Physics* **23**, 327 (1977).
- [52] G. Ciccotti, M. Ferrario, *Computation* **6** (2018).
- [53] J. H. R. Clarke, W. Smith, L. V. Woodcock, *The Journal of Chemical Physics* **84**, 2290 (1986).

- [54] Z. Shi, P. G. Debenedetti, F. H. Stillinger, P. Ginart, *The Journal of Chemical Physics* **135**, 084513 (2011).
- [55] G. de Fabritiis, M. Serrano, R. Delgado-Buscalioni, P. V. Coveney, *Physical review. E, Statistical, nonlinear, and soft matter physics* **75 2 Pt 2**, 026307 (2007).
- [56] U. Essmann, *et al.*, *The Journal of Chemical Physics* **103**, 8577 (1995).
- [57] Y. Shan, J. L. Klepeis, M. P. Eastwood, R. O. Dror, D. E. Shaw, *The Journal of Chemical Physics* **122**, (2005).
- [58] P. Koehl, *Current Opinion in Structural Biology* **16**, 142 (2006).
- [59] C. Sagui, T. Darden, *jcp* **114**, 6578 (2001).
- [60] W. Briggs, V. Henson, S. McCormick, *A Multigrid Tutorial, Second Edition* (Society for Industrial and Applied Mathematics, 2000), second edn.
- [61] J. V. L. Beckers, C. P. Lowe, S. W. D. Leeuw, *Molecular Simulation* **20**, 369 (1998).
- [62] R. Vogelsang, C. Hoheisel, *Journal of Statistical Physics* **47**, 193 (1987).
- [63] M. Troyer, U.-J. Wiese, *Phys. Rev. Lett.* **94**, 170201 (2005).
- [64] E. Y. Loh, *et al.*, *Phys. Rev. B* **41**, 9301 (1990).
- [65] A. Fetter, J. Walecka, *Quantum Theory of Many-Particle Systems*, Dover Books on Physics (Dover Publications, 2012).
- [66] C. Cramer, *Essentials of Computational Chemistry: Theories and Models* (Wiley, 2005).
- [67] A. Altland, B. Simons, *Condensed Matter Field Theory* (Cambridge University Press, 2006).
- [68] J. Negele, H. Orland, *Quantum Many-Particle Systems*, Frontiers in Physics: Lecture Note Series (Addison-Wesley, 1995).
- [69] J. Bardeen, L. N. Cooper, J. R. Schrieffer, *Phys. Rev.* **108**, 1175 (1957).
- [70] P. Nozieres, D. Pines, *Theory Of Quantum Liquids*, Advanced Books Classics Series (Westview Press, 1999).
- [71] B. Donovan, j. a. Angress, J. F, *Lattice vibrations* (London : Chapman and Hall, 1971). Distributed in the U.S.A. by Barnes & Noble.
- [72] B. Vanderheyden, G. Baym, *Journal of Statistical Physics* **93**, 843 (1998).
- [73] Y. Yanase, *et al.*, *Physics Reports* **387**, 1 (2003).

- [74] V. Murg, F. Verstraete, R. Schneider, P. R. Nagy, O. Legeza, *Journal of Chemical Theory and Computation* **11**, 1027 (2015). PMID: 25844072.
- [75] K. Held, I. A. Nekrasov, N. Blumer, V. I. Anisimov, D. Vollhardt, *International Journal of Modern Physics B* **15**, 2611 (2001).
- [76] M. Head-Gordon, E. Artacho, *Phys Today* **61**, 58 (2008).
- [77] P. Geerlings, F. D. Proft, W. Langenaeker, *Chemical Reviews* **103**, 1793 (2003). PMID: 12744694.
- [78] M. Orio, D. A. Pantazis, F. Neese, *Photosynthesis research* **102**, 443 (2009).
- [79] R. M. Dreizler, E. K. Gross, *Density functional theory: an approach to the quantum many-body problem* (Springer Science & Business Media, 2012).
- [80] A. J. Cohen, P. Mori-Sánchez, W. Yang, *Science* **321**, 792 (2008).
- [81] F. Jensen, *Introduction to Computational Chemistry* (Wiley, 2007).
- [82] R. J. Bartlett, J. F. Stanton, *Applications of Post-Hartree-Fock Methods: A Tutorial* (John Wiley & Sons, Inc., 2007), pp. 65–169.
- [83] R. J. Bartlett, M. Musiał, *Rev. Mod. Phys.* **79**, 291 (2007).
- [84] M. Nightingale, C. Umrigar, *Quantum Monte Carlo Methods in Physics and Chemistry, C*: [Nato ASI series (Springer Netherlands, 1999)].
- [85] R. E. Thomas, Q. Sun, A. Alavi, G. H. Booth, *Journal of Chemical Theory and Computation* **11**, 5316 (2015).
- [86] R. C. Clay, M. A. Morales, *The Journal of Chemical Physics* **142** (2015).
- [87] N. Goheer, M. Kleban, L. Susskind, *JHEP* 0307:056,2003 (2003).
- [88] Y. Takahashi, H. Umezawa, *Int. J. Mod. Phys* **2**, 55 (1975).
- [89] J. B. Anderson, *The Journal of Chemical Physics* **63**, 1499 (1975).
- [90] I. Shavitt, R. Bartlett, *Many-Body Methods in Chemistry and Physics: MBPT and Coupled-Cluster Theory*, Cambridge Molecular Science (Cambridge University Press, 2009).
- [91] A. Goodman, *Adv. Nucl. Phys.; (United States)* **11:1** (1979).
- [92] M. E. Peskin, D. V. Schroeder, *An introduction to quantum field theory*, Advanced book program (Westview Press Reading (Mass.), Boulder (Col.), 1995). Autre tirage : 1997.
- [93] R. Kubo, *Journal of the Physical Society of Japan* **17**, 1100 (1962).

- [94] K. Koepernik, H. Eschrig, *Phys. Rev. B* **59**, 1743 (1999).
- [95] S. Östlund, E. Mele, *Phys. Rev. B* **44**, 12413 (1991).
- [96] M. Bazzanella, J. Nilsson, *Non-Linear Methods in Strongly Correlated Electron Systems* (2014).
- [97] J.-W. v. H. K. Scharnhorst, *Nonlinear Bogolyubov-Valatin transformations: 2 modes* (2011).
- [98] X. Li, *et al.*, *Physical Chemistry Chemical Physics* **7**, 233 (2005).
- [99] P. Echenique, J. L. Alonso, *Molecular Physics* **105**, 3057 (2007).
- [100] N. Ashcroft, N. Mermin, *Solid State Physics* (Saunders College, Philadelphia, 1976).
- [101] G. Giachetta, L. Mangiarotti, G. Sardanashvily, *Advanced Classical Field Theory* (WORLD SCIENTIFIC, 2009).